Integrated Hazard and Risk Maps Using Analytical Hierarchy Process Considering Land Use and Climate Change Issues in Lao PDR

Doctoral Dissertation

Dissertation Title

Integrated Hazard and Risk Maps Using Analytical Hierarchy Process Considering Land Use and Climate Change Issues in Lao PDR

PHRAKONKHAM SENGPHRACHANH

Department Civil and Environmental Engineering

Graduate School of Engineering

TOHOKU UNIVERSITY

(ID No. B7TD6013)

ACKNOWLEFGEMENTS

First and foremost, I am grateful to my advisor Professor So Kazama and Assoc. Prof. Dr. Daisuke Komori, for their supervision on our research, gave me the guidance and opportunity to be part of his research group in Hydro-Environmental System Laboratory and an excellent chance for the financial support under Japanese Government Scholarship (Monbukagakusho) from Ministry of Education, Culture, Sports, Science and Technology, The Environment Research and Technology Development Fund of the Ministry of the Environment, Japan, Advancing Co-design of Integrated Strategies with Adaptation to Climate Change (ADAP-T) of JST/JICA, SATREPS, which sustained my cost of living during the Doctoral degree fulfillment at the Graduate School of Civil Engineering, Tohoku University.

I would like to express my sincere and appreciation to the other member of the examination committee, Professor Hitoshi Tanaka and Associate Professor Makoto Umeda who evaluated my work and given many comments to improve the dissertation..

I am extremely grateful to all member in Hydro-Environmental System Laboratory, Department of Civil Engineering, Tohoku University, who helped and supported me during my stay in Japan. They had spent time to bring me to places in Japan and given me a valuable experience with Japanese language and culture.

Lastly, I would like to express my gratitude to my family, who gave me the great chance to study in Japan, funding support, merciful guidance and the best encouragement. I also would like to express my gratefulness to my wife (Soliya Sopha) and my un-born daughter for their support and understanding during my pursuit of Ph.D degree

Integrated Hazard and Risk Maps Using Analytical Hierarchy Process Considering Land Use and Climate Change Issues in Lao PDR

ABSTRACT:

In recent decades, many floods have occurred in Laos. To reduce the impacts and losses from flood events, it is important to understand the magnitude of each flood and the area it could potentially impact. Land use change and climate change have played significant roles, and it is important to understand the impacts of flooding. Landslides are another hazard that can occur after flooding. Therefore, flood hazard mapping serves as an important tool for decision-makers to identify sensitive areas. We have developed an integrated hazard map based on a combination of five hazard maps, including flood, land use change, landslide climate change impact to flood and climate change impact to landslide hazard maps. The analytical hierarchy process (AHP) is a tool for multi-criteria decision making. This method used the AHP as a tool to combine the different hazard maps into an integrated hazard map. The AHP is used to provide the relative weights of each hazard map. It is necessary to understand the relative importance of each hazard map, and this can be done by using the pairwise comparison matrix to compare their significance. The value of each row in a pairwise comparison was determined based on the judgment of experts. The result shows that the areas around southern and northern Laos have a high hazard value. Then, we compared our result with the historical record to validate our study.

Risk mapping serves as an important tool for decision-makers to identify sensitive areas. We propose integrated risk maps based on integrated hazard maps and land use categories. The integrated hazard maps consist of five hazard maps, i.e., flood, land use change, landslide, climate change leading to floods and climate change leading to landslides.. The vulnerabilities are discussed based on each hazard and the land use data, which are classified into 3 categories: urban areas, agricultural areas and paddy fields. The results show that the areas in the southern (12 billion USD) and central regions (16 billion USD) of Lao PDR sustain the highest damage cost in the 2100s under representative concentration pathway (RCP) 8.5.

Contents

List of Figure

List of Table

LIST OF ABBREVIATIONS

AHP	Analytical Hierarchy Process
CDF	Cumulative Distribution Function
DEM	Digital Elevation Map
GCMs	General Circulation Models
GHG	Green House Gas
GIS	Geographic Information System
GoL	Government of Laos
HWSD	Harmonized World Soil Database
IDW	Inverse Disctince Weight
RCP	Representative Concentration Pathway
SU	Soil Unit

List of variable

ΔH	variation of depth (m)
Δt	time interval of flow direction (d)
Δx	mash interval of flow direction (m)
r_e	precipitation (m/d)
B	width of flow path (m)
Q	flow rate (m^3/d)
h	water depth (m)
I	gradient slope
n	manning roughness coefficient ($d/m^{1/3}$)
R_{in}	amount of infiltration (m/d)
k_a	infiltration coefficient (d^{-1})
s	apparent storage level (m)
q	outflow level of base flow (m/d)
L_p	probability of a landslide
$hydro$	hydraulic gradient
$relief$	relative relief (m)
θ	water volume content
V_x	velocity in the horizontal (m/d)
V_z	velocity in vertical direction (m/d)
K	unsaturated hydraulic conductivity (m/d)
hh	total hydraulic head (m)
ψ	hydraulic pressure head (m)
α	Slope angle (degree)
L_x	grid size in horizontal (m)
L_z	grid size in vertical (m)
C	specific moisture capacity
Ks	saturated hydraulic conductivity (m/d)
β	soil characteristic value
θ_r	residual water volume content
θ_s	saturation water volume content
ψ_0	initial pressure (m)
ψ'	saturated pressure (m)
z_{cor}	precipitation after correcting the bias (m/d)

z_{gcm}	precipitation from GCMs before bias correction (m/d)
CDF_{gcm}	Cumulative Distribution Function (CDF) of z_{gcm}
CDF_0^{-1}	inverse CDF of observed rainfall
Rel_j	relative important of pairwise jth (j =1, 2, …10)
$A_{m,j}$	element response from questionnaire from option A (j =1, 2, …10)
$B_{m,j}$	element response from questionnaire from option B (j =1, 2, …10)
$\boldsymbol{w}_i$	weight priority of each criteria (i = 1, 2,…., N)
m	Number of samples from questionnaire
CR	consistency ratio
CI	consistency index
Ri	random index
λ_{max}	maximum eigenvalue
$\boldsymbol{D}_{i,k}$	a pair-wise comparison matrix ($k = 1, 2, \ldots, N$), ($i = 1, 2, \ldots, N$)
N	number of criteria
$AHP_{\bar{x},\bar{z}} hazard\ index$	hazard index value in each grid after integrated
$HI_{\bar{x},\bar{z},flood}$	hazard index value of coordination of $\bar{x}$ (vertical) and $\bar{z}$ (horizontal) from $flood$ hazard map ($\bar{x}$ = 1, 2,…..,$\overline{xx}$; $\bar{z} = 1, 2, \ldots, \overline{zz}$)
$HI_{\bar{x},\bar{z},land\ use\ change}$	azard index value of coordination of $\bar{x}$ (vertical) and $\bar{z}$ (horizontal) from $land\ use\ change$ hazard map ($\bar{x}$ = 1, 2,…..,$\overline{xx}$; $\bar{z} = 1, 2, \ldots, \overline{zz}$)
$HI_{\bar{x},\bar{z},landslide}$	azard index value of coordination of $\bar{x}$ (vertical) and $\bar{z}$ (horizontal) from $landslide$ hazard map ($\bar{x}$ = 1, 2,…..,$\overline{xx}$; $\bar{z} = 1, 2, \ldots, \overline{zz}$)
$HI_{\bar{x},\bar{z},climate\ change\ to\ flood}$	azard index value of coordination of $\bar{x}$ (vertical) and $\bar{z}$ (horizontal) from $climate\ change\ to\ flood$ hazard map ($\bar{x}$ = 1, 2,…..,$\overline{xx}$; $\bar{z} = 1, 2, \ldots, \overline{zz}$)

$HI_{\bar{x},\bar{z},climate\ change\ to\ landslide}$	azard index value of coordination of $\bar{x}$ (vertical) and $\bar{z}$ (horizontal) from $climate\ change\ to\ landslide$ hazard map ($\bar{x}$ = 1, 2,…..,$\overline{xx}$; $\bar{z} = 1, 2, \ldots\ldots, \overline{zz}$)
$\overline{xx}$	number of grid in vertical of hazard map (all of hazard map have equal number of grid in vertical)
zz	number of grid in horizontal of hazard map (all of hazard map have equal number of grid in horizontal)
DC_x	damage cost in x area (USD/km^2), x is either agricultural or paddy field,
DC_{urban}	damage cost in an urban area (USD/km^2)
HC	asset value of house content (USD/km^2)
GDP	total gross domestic product (billions USD)
Pop	population in millions
T	period over the project is analyzed (year)
r	discount rate
TB	total benefits from the project from start of project until end (USD)
$benefit$	project benefit (USD/year)
TC	total costs of project (USD)
$Costs\ of\ adaptation\ measure$	cost for adaptation (USD/year)
B/C	ratio of costs and benefits
R^2	coefficient of determination
O_{ia}	ia^{th} observed data for the element being evaluated (ia = 1, 2,…., nn)
$\bar{O}$	mean value of observed data
y_{ia}	ia^{th} simulated data for the element being evaluated (ia = 1, 2,…., nn)
$\bar{y}$	mean value of simulated data
nn	number of evaluated data
E	Nash-Sutcliffe efficiency
Z_p	estimation value for location p
Z_{ib}	value at ib^{th} sample point (ib = 1, 2,….., M)

d_{ib}	Euclidean distance between estimated location to ib^{th} sample point location (ib = 1, 2,….., M)
M	the number of sample points
pw	distant exponent power
$F_{Tr,Cs}$	logarithm of predicted input data at return period Tr
$\bar{F}$	average of input data logarithms
$K_{Tr,Cs}$	function of the skew coefficient (Cs) and return period Tr
Cs	skew coefficient
Tr	return period (year)
S_F	standard deviation of input data logarithms
F_{ic}	logarithm of input data (ic =1, 2, 3…., f)
f	number of input data
X_{id}	(id = 1, 2, 3…., tg) is id^{th} probability grid data of land slide hazard map (from smallest to largest probability)
tg	total number of grid from hazard map
X_{mean}	mean of probability grid data
$X_{id1}, X_{id2}, X_{id3}$ and X_{id4}	$(id1 = 1,2,3, \dots cl1)$, $id2 = cl1 + 1, cl1 + 2, \dots\dots, cl2)$, $(id3 = cl2 + 1, cl2 + 2, \dots, cl3)$, $(id4 = cl3 + 1, cl3 + 2, \dots\dots, tg)$ Group 1, 2, 3 and 4 data, respectively which divided from X_{id} data
$cl1, cl2$ and $cl3$	Break point in X_{id} data
$X_{class1}, X_{class2}, X_{class3}$ and X_{class4}	mean of probability grid data from group 1,2 3 and 4, respectively

CHAPTER 1: INTRODUCTION

1.1. Research context

1.1.1. Flood and landslide situation in Laos

The Mekong River is the largest river basin in the Southeast Asia, and is shared by the six countries of China, Myanmar, Thailand, Cambodia, Vietnam and Laos. In the last decade a lot of researches have been done research in Mekong River especially its flood component are expected to have significant impacts on several keys functions of the river but none of those researches are focus on the flood risk index in Laos.

Floods are among the most dangerous natural hazards. Flooding can happen anywhere, and sometimes, it is unavoidable. The economy, people's livelihood and the infrastructure of many countries around the world have been affected by flooding (Golian et al., 2010). Lao People's Democratic Republic (or Lao PDR) suffers from flooding every year. Lao PDR is a developing country located in Southeast Asia. The country's people depend heavily on agriculture and natural resources for their livelihood. Currently, the water supply system in the country is not well distributed, particularly in rural areas. Therefore, most people living in rural areas are resettled downstream of dams and irrigation areas (Baird and Shoemaker, 2007). Changes in land use, such as decreases in forest density, can lead to increases in flood magnitude (Jongman et al., 2012; Winsemius et al., 2016). The Laos PDR have experienced a range of floods of different magnitudes and duration. Particularly in three consecutive years from 1994 to 1996, the flood were large and disastrous. In the last decade flood have occurred on greater scale and more

frequently, leading to an increasing number of casualties and further compromising flood security and livelihood in rural area. According to Government of Laos (GoL) since 2000, large scale flooding has occurred in Laos PDR in 2000, 2002, 2005, 2008, 2009 and 20011. While in previous years a single major food event could be identified, in 2013 the country experienced continuous heavy rain affecting villages and crops at various levels, and this year was marked by a series of flood events affecting people across country. The rain led to floods and landslide, those disasters destroyed and severely damaged to village infrastructures such as road, irrigation systems the flood events were caused by different weather systems, occurred in different location at different time (starting in July and end in October), in total 12 out of 17 provinces, and 52 out of 145 districts, it also impact to huge area of agriculture land, paddy field which is the most is directly impact to the standard living for a majority of Laos people living in agriculture sector and its significant resource for our economic growth and for sustainable development.

1.1.2. Impact of land use change

Forest also has a significant role on the water resource, it can store water in rainy season and delay water discharge from upper basin to reach lower basin. As a landlocked country, the Laos is endowed with abundant natural resources, relative to many other Asian countries, especially water, forests, and minerals. However, the forest cover has declined from 70 percent of the total land area in 1940 to 41.5 % in 2002. The most basic factors for decline of forest are widespread poverty and rapid population increase amongst the rural population; as a results, obliges to practice forms of cropping resulting in destruction of forest. The government has been engaged in systematic campaigns to

reduce and eventually eradicate swidden cultivation and opium cultivation though poverty eradication. Therefore, it is important to understand the impact from deforestation to the flooding, which that we can identify regions that will have significant effect to the flood.

1.1.3. Impact of climate change

Climate change increases the intensity of rainfall and more rainfall events happen, it is means for the risk of flooding. However, it is varied widely from location to location depend on the studied hydrological climatic area. In this study, we focus on the hydrological system in Laos. Now a days, the hydrological regime of the country change significantly, seasonal changes of precipitation considerably affect the hydrological regime and induce important impact on the water resource, and this could have a significant impact to the hydropower production, irrigation and also increase water related risks for instance flood; many of researchers believe that increasing in a number of hydrological extreme events such as flood, landslide and so on are happened because of climate change (Hirabayashi et al., 2008; IPCC, 2007). River flood are generated differently in different geographic environmental. They may be generated by intense rainfall exceeding the infiltration capacity of soil, or by rain falling on saturated ground; when floods area largely generated by intense rainfall and antecedent conditions area not relevant then changes in flood characteristics area strongly influenced by changes in the frequency of intense rainfall. However floods may be generated by the melting of snow; since, no snow fall in Laos, this study will not include snow factor in climate change factor. Therefore, by knowing how change in extreme rainfall affect the distribution of

water at a regional scale is significant to the impact from climate change to flooding, which was one major objective of this study.

In recent years, many researchers have conducted global studies on the impact of climate change on the water cycle and its effect on people's livelihood (Adeloye et al., 2013; Parmesan and Yohe, 2003a; Westra et al., 2014). However, there have been only a few assessments and analyses for predictions on the country's environmental impacts when considering possible climate changes. According to the Intergovernmental Panel on Climate Change (IPCC) report, Southeast Asia will suffer from increasing flood frequency in the future (IPCC, 2007). General Circulation Models (GCMs) have been developed to study future climate scenarios and the associated impacts, and they help support strategies and mitigation plans to address the effect of climate change

1.2. Objective of study

The effects of hazards on an area could be in either a single or multiple forms. In the last decade, the uses of multi-hazard assessment focusing on all scales have been considered in several studies (Cutter et al., 2000; Marzocchi et al., 2012; Sendai Framework, 2015; Sullivan-Wiley and Short Gianotti, 2017). However, exhaustive data are required in most assessments. Recently, geographic information systems (GIS) have been used as a tool for such assessment. This is an effective tool for handling large amounts of spatial data, assimilating data from several sources and undertaking analyses (Fernández and Lutz, 2010; Kazakis et al., 2015). In contrast, the tool is ineffective in performing multi-criteria analyses, and hence, it is not appropriate for executive or managerial purposes. For multi-criteria supervision, a combination of GIS and multi-

criteria decision analysis (MCDA) is essential. Many studies have indicated the applicability of GIS for MCDA flood hazard maps. One of the most common MCDA methods is the analytic hierarchy process. This approach is appropriate because it offers precise results, and it is used for studying hazards in several studies (Kazakis et al., 2015; Stefanidis and Stathis, 2013). In recent development, flow accumulation, slope, elevation, land use, and rainfall intensity have been used as GIS-based map information to map flood hazards using AHP and GIS (Gigović et al., 2017). According to the Sendai Framework (2015), it is important to pay more attention to risk analysis. Single risk analysis addressing single hazards provides information about only an individual risk in a specific location; however, in a specific location, more than a single hazard can occur. For example, in mountainous areas, landslides and floods can occur together. Therefore, the integration of the risk assessment of these hazards is necessary. Phrakonkham (2019) estimated the hazards in Lao PDR due to landslides, floods, land use change to floods, climate change leading to floods and landslides, and integrated hazard maps; the results were used in the analysis of the negative consequences of these hazards in this article.

The main objective of this study was to propose a new approach to integrated risk maps to detect subtle areas on the national scale, for which there are limited data available. This modelling method combined several maps of hazards, i.e., land use change, climate change and flooding. As a priority weighting function for the maps, AHP was deployed. Furthermore, analyzing the distribution pattern of hazard and risk for both individual and integrated maps. Both individual and integrated risk maps were used to provide the damage costs from the risk to the land use area (urban, paddy, and agriculture). The integrated risk maps can be apply in adaptation measure for risk reduction or combine with future development plan to identify suitable location for development.

1.3. Organization of dissertation

This dissertation is consist with seven chapters. Chapter 1 provides the overview of this thesis. Current situation of flooding, what is happened in recent decade. Following it, the impact of climate change and deforestation to the hydrological cycle in Lao PDR. The objective to solve the encountered problem statements. The research frameworks used to achieve the prescribed objective in this study. Chapter 2 presents the report of the former researches in flood, landslide, land use change, climate change and risk. Chapter 3 provide the fundamental details of the study area beginning with the location, topography and continue to forest and climate change situation. All necessary required data for input, such as land use, soil types, hydrological, meteorological and GIS data as well as the data sources are described in this chapter. Chapter 4 consists of a set of mathematical models and conceptual of hydrological distributed model for simulate runoff are given in this chapter. Following it, calibration and validation of the model and its applications to the study area were clearly explain. Chapter 5 focus on the analysis of individual hazard maps such as flood, land use change, land slide and climate change leading to flood and landslide. In addition, decision making method for integrated those hazard maps together and explain the methodology to validation of the hazard maps. Chapter 6 focuses on analysis of risk and cost from multi hazard impact in Lao PDR for both present condition and future impact from climate change. Additionally, an adaptation measure to reduce damage cost from integrated risk map had been analysis. Chapter 7, summary of the main finding, scientific contribution and their practical implications are discussed as well as the recommendations for the further research (Figure 1-1).

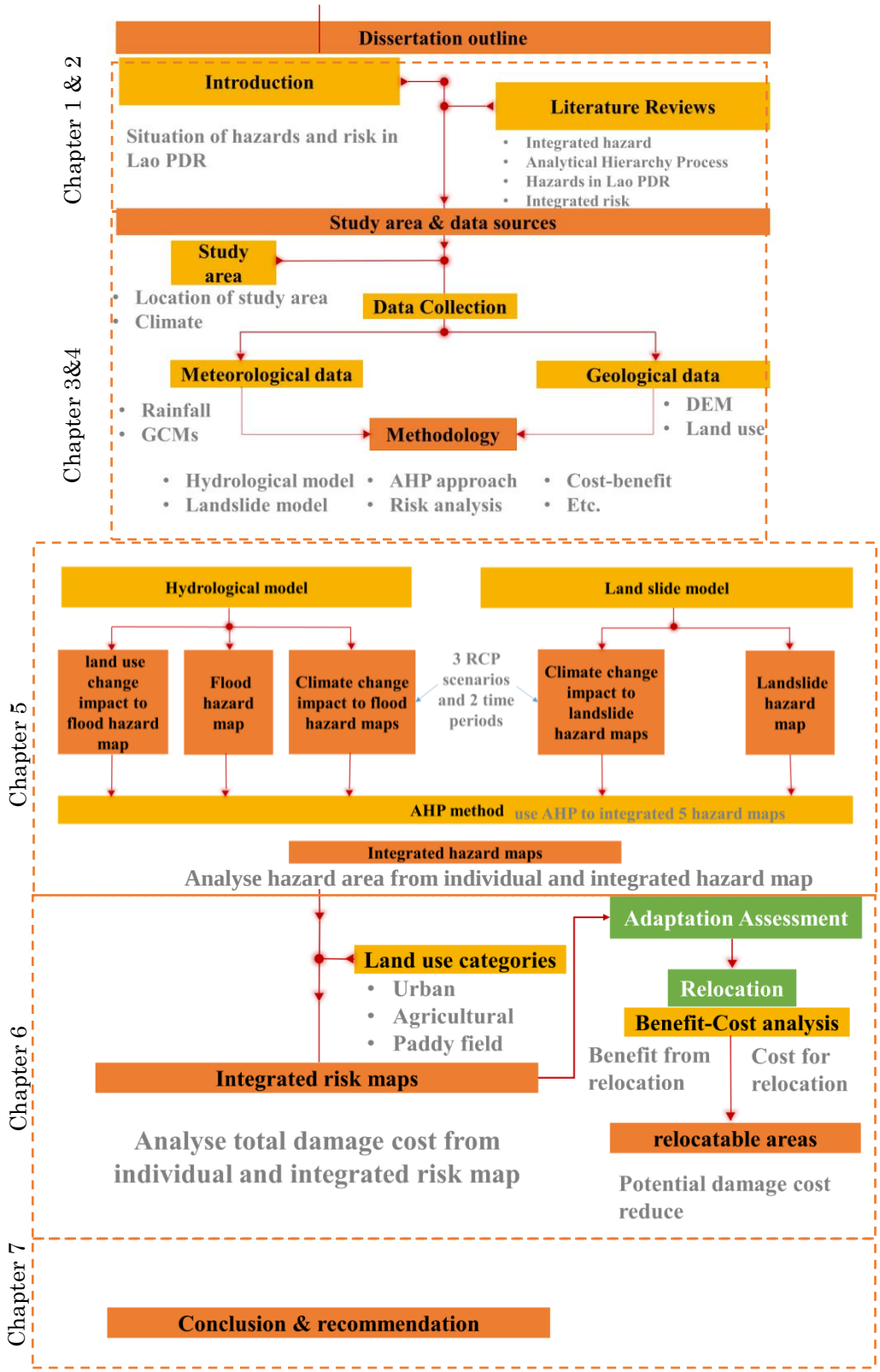

Figure 1-1 Schematic of the dissertation context

CHAPTER 2: LITERATURE REVIEW

2.1 Concept of integrated hazard and hazards in study area

2.1.1 Integrated hazard

Generally, integrated hazard is mean that we integration multi-hazards into a single system for joint evaluation (Carpignano et al., 2009; Marzocchi et al., 2009). Basically, it considering the characteristic of each hazard such as probability, magnitude and frequency. The challenge for integrated hazard or multi-hazard is that each hazard have their own characteristic and different method to analyse them and their magnitude also measured in different way and using different units (Carpignano et al., 2009). Accordingly, reference unit of each hazard become a problem for comparison of multi-hazard.

Moran et al (2004) presented the methodology for integrated multi hazard namely avalanches and rock falls. The aim of this study is to assessment the risk potential of natural hazard in lacking of hazard zoning. The study used a worst case scenario as the common basis of hazards, therefore the potential impact areas of each hazard can be compared and jointly. The classification was scale in 4 classes as low, moderate, high and extra high. Instead of used maximum of overlap classes, they used mean of overlap classes to represent the classification of integrated hazard for example in one area avalanches have high hazard and rock falls have low hazard the integrated map will classification that area as moderate hazard area.

Another type of method is present in Zine El Abidine et al (2007), this study aim to

identify potential affected areas from multi-hazard in the same time. The potential affected area cover all high population areas that can be exposed to multi-hazard. Instead of used classification scheme, they proposed hazard weight method for integration of multi-hazard. The hazard weights were determine by their impact on humans and economic.

Phrakonkham (2017) used the equal weight method to integrated multi-hazard. The study aim to provide integrated map that consist with flood, land slide, land use change and climate change to flood. The results shown good correlation between the simulation map and historical events. Using equal weight for integration is possible but basically all hazard not equally importance. The weight of each hazard have a significant impact on the integrated hazard map. Moreover, damage from individual hazard and integrated hazard map to economic have not discuss in the study yet. Therefore, methodology for integration multi hazard risk map is necessary.

2.1.2 Analytical Hierarchy Process

Previous studies have presented many methodologies to integrate multi-hazard such as using classification scheme or provide weighting for each hazard. However, none of the studies have taken consideration of natural abilities of human to sense, adapt, or modify their environment to avoid danger which is the human perception of risk as individual and the public perception of risk as communities or group. A stakeholder involvement in the study will provide advantages to both researchers and stakeholders. The stakeholders will have opportunities to share their vision, needs and knowledge on the hazards. They could also assist in reducing conflicts and increasing the cooperation

in the future. The objective of this study is to provide the integrated hazard risk map in using stakeholder's judgement to retrieve weighting of each hazard. There are several multi criteria decision making methods to solve multiple conflicts among independent criteria when evaluating multi hazard risk map. For instance, Multi Attribute Utility Theory (MAUT) (Keeney and Raiffa, 1993) is an expected utility theory that can decide the best course of action in a giving problem by assigning a utility to every possible consequence and calculating the best possible utility. The drawback of this method is the requirement of huge amount of input in every step of procedure (Konidari and Mavrakis, 2007). Simple Additive Weight (SAW) (Fishburn, 1967) is established based on a simple addition of scores that represent the goal achievement under each criteria, multiplied by the particular weight. The disadvantage of SAW is the estimation weight does not always reflect the real situation, (Qin et al., 2008). Technique for Order Preference by Similarity to Ideal Solutions (TOSIS) (Hwang and Yoon, 1981) is an approach to identify an alternative which is closed to ideal solution and farthest to negative ideal solution in a multi-dimensional space. The drawback of this method is the difficulty to weight criteria and keep consistency of judgement, especially with additional criteria (Behzadian et al., 2012). Analytical Hierarchy Process (AHP) (Saaty, 1994) uses a pairwise comparison to compare the relative significance between criteria designed from the stakeholder's judgement. The disadvantage of this method is the expert knowledge dependency. Although, AHP requires data to properly perform pairwise comparisons, but it is not nearly as data intensive as MAUT. Among various multi criteria decision making methods, AHP's property is in line with our study objective. Furthermore, AHP is recognized as a multi-criteria method that is incorporated into GIS-based procedures for determining suitability (Parry et al., 2018; Prakash, 2003). Pourkhabbaz et al (2014) used AHP in GIS

environment with the aim of choosing the suitable location for agriculture land use. Gigović et al (2017) presented a reliable GIS-AHP methodology for hazard zone mapping of flood prone area in urban areas. In the study, firstly six factors that reverent to hazard of flood in urban area were considered. Then, the hazard zone mapping was compared with historical flood events for validation. From the results, the GIS-AHP hazard map proves a good correlation between high hazard area of the map and historical event of flood. The results of this study provided a good basis for developing a system for hazard management. Ramya et al (2019) analysed suitable location for industrial development by using GIS, AHP and Technique for Order Preference by Similarity to Ideal Solution (TOSIP). In this study, various type of criteria, for example near major road, far from agriculture, paddy field, river (flood prevention) etc, were used. As a result, most suitable locations for industrial can be highlighted. Based on research studies mentioned above, it could be concluded that AHP is an effective and powerful tool to analyze, structure and prioritize complex problems considering expert judgment on various aspects. Therefore, the AHP is chosen for the studies of the integration multi hazard risk mapping.

2.1.3 Hazards in Lao PDR

2.1.3.1 Flood

Flood is one of the most dangerous hazard in the world. Major of flood events in Asia and Pacific region are cause by the heavy rainfall from Monson (Mikkelsen et al., 1999). According to Westra (2014), Pattern of rainfall over space and time. Moreover, the pattern of rainfall is changing due to the climate change and the rating of changing is

varied depending on the geographic location (Trenberth et al., 2003).

Mostly, flood can be classified to 4 types by location of occurrence and what cause flood to happen. River flood occurs when the amount of water flow are exceed the capacity of river channel. It is usually happen in rainy season. Coastal flood occurs in coastal area when the ocean water flow are strong and the water surge over coastal areas. Normally it is happen because of storm, offshore low pressure, sea wave that occurs because of earthquake or underwater volcanic. Urban flood occurs from heavy rainfall and runoff water in urban area exceed discharge capacity. Urban flood can be more serious than river flood in term of flood depth. Mostly, paved road in urban area is the main factor that cause the high flood depth. Runoff water cannot infiltrate to underground or discharge channel because of the paved road have less absorbing ability. Flash floods occur when a large amount of water flood within short period of time. Normally it occurs locally and suddenly without or with little warning. Flash floods could happen due to immoderate rainfall or a sudden release of water from a dam. Flood mapping is a tool for risk management. It is use to defined concern areas which are risk to flooding. Flood maps are powerful tool for support flood hazard management. The map can provided several of flood attributes such as flood velocity and flood depth. The flood hazard map can adjust its requirement and classification depends on the purpose of the study.

Many researches have been study about the flood hazard, they want to understand the behaviour, magnitude and occurrence of flood (Di Baldassarre and Montanari, 2009; Crispino et al., 2015; Horritt and Bates, 2001; Patro et al., 2009; Poretti and De Amicis, 2011). Even thought, flood hazard map can provide useful information on the potential inundation area, many uncertainties still remain in flood hazard map. Mostly of uncertainties in flood hazard map come from accuracy of data for example

rainfall data, geological data and model parameter. In recent decade, numerous studies has been discuss and identified the source of uncertainties from flood hazard map (Bales and Wagner, 2009; Domeneghetti et al., 2013; Dottori et al., 2016; Jung et al., 2013). Nevertheless, it is still impossible to remove all of the uncertainties due to the lack of many factor such as knowledge, technology, times and cost. Rainfall runoff model are classified as lumped and distributed model based on the model parameters. According to Devia et al (2015) lumped model, the entire river catchment is considering as a single unit where spatial variability is neglect and the output are generated without considering the spatial process; distributed model is divide the entire catchment into small unit, therefore the parameter, input and output data can vary spatially. In this study, we used distributed hydrological model proposed by Kashiwa et al (2010) and adapted to use in Lao PDR by Phrakonkham (2017). Phrakonkham (2017) assessed the flood hazard map in Lao PDR by using distributed hydrological model, the hazard map can illustrated distribution of potential flood hazard area throughout whole country.

2.1.3.2 Land slide

Landslide is one kind of natural disaster, it is occurs because of the mass movement of debris flow or rock and sliding under the influence of gravity. Additional, landslide usually occurs when rainfall around steep slope area such as mountainous area. Hence, rainfall and slope gradient can be consider as significant factor for occurrence of landslide. In Lao PDR many ethnic groups are living in mountainous area. Their livelihood is depend on agriculture and livestock. When landslide occurs, their productivity is greatly damaged which create huge economic loss to them. Therefore, we consider landslide

hazard into our study, in order to analyse potential impact area and damage cost from landslide. Based on Shirole et al (2017), the impact of landslide can be very serious including the loss of people live, destruction to household and income resource of people who live near those area such as agriculture, pond, paddy field and forest. Based on Orlowsky et al (2012) stability of slope can be influence by different phenomena. When the slope is unstable is lead to the landslide. The influence that cause unstable slope including precipitation, change of temperature, earthquake and actions of human such as construction. Collison et al (2000) proposed coupling methodology between GIS and slope stability model to investigate the impact of rainfall on landslide frequency and evaluate factor safety in hillslope area. In addition, according to White and Singham (2012) have analyse sensitivity of slope failure model to various rainfall pattern. According to results, average rainfall is the significant indicator to trigger landslide. Based on those studies clearly shown that rainfall is a significant factor to trigger landslide. Furthermore, in shallow slope rainfall can cause delay of slope failure (Zhang et al., 2019).

In order to evaluate landslide hazard, they are mainly two approach deterministic and statistical approach. Many studies aim to compare and evaluated the assessment of land slide hazard from both mentioned approach (Aleotti and Chowdhury, 1999; Calcaterra et al., 1998; Lee et al., 2008). Deterministic approaches are based on analysis of slope stability and the drawback of this method are ground conditions need to be uniform for the whole study area and the land slide type that occurred in the study area need to be known (Dai et al., 2001). For the statistical approach, it is consider as indirect hazard mapping method. The statistical approach used statistical determination of various variables that have triggered landslide hazard event in the past and this approach is possible to use for large area (Refice and Capolongo, 2002). Ono (2011) have studies

about rainfall-induced landslide by used Shallow landslide instability model. The model consider rainfall as a triggering factor of landslide. The studied have consider two events of landslide events in Thailand as a case study. The model shows the good accuracy of safety factor in those areas with it can explain the high potential of shallow landslide in each area. Kawagoe (2010) used probabilistic model based on multiple logistic regression analysis to evaluate the frequency of landslide hazard in Japan. From the results of this study shows some significant physical parameters such as hydraulic gradient, relieve energy and geological parameters which these parameters are considered to be influent to the occurrence of landslide. Therefore, in this study we use statistical approach to evaluate landslide hazard probability in our study area.

2.1.3.3 Land use change

According to many studies (Huntington, 2006; Li et al., 2009) land cover variability have influent to hydrological flow which has effect to the fluctuation of surface stream flow. The fluctuation of surface stream flow can lead to natural disaster such as flood. In order to prevent and avoid damage from natural disaster to our human community, it is necessary to examine the impact of land use change such as forest area and expand of urban on natural disaster. Based on Macklin and Lewin (2003) magnitude and frequent of flooding may be increase due to the land use change. In small-medium scale river basin, land use is play a significant role in either of reducing or amplifying the serve of flooding. In Lao PDR the decreasing of forest become serious problem in nation scale. Deforestation results from clearing forestland for shifting cultivation and removing logs for industrial use and fuel. The volume of logs removed for industrial purposes increased

by around 70 percent between 1975-1977 and 1985-1987, to about 330,000 m^3. Between 1980 and 1989, the volume of logs removed for fuel to about 3.7 million m^3 and only about 100,000 m^3 were removed for industrial purposes. By 1991 these volumes had increased to approximately 3.9 million m^3 and 106,000 m^3, respectively. Following the introduction of the New Economic Mechanism in 1994, decentralization of forest management to autonomous forest enterprises at the provincial level encouraged increased exploitation of forests. At the central and provincial levels, autonomous forest enterprises area responsible for forest management. Timber resource has been commercially exploited on a small scale since the colonial period and are an important source of foreign exchange. In 1988 wood products accounted for more than half of all export earnings. In 1992 timber and wood products were almost one-third of the total principle exports. Another reason for the decreasing of forest density is swidden agriculture, most farmers employ one of two cultivation systems: wet field paddy system, practices primarily in the plains and valleys, or the swidden cultivation system, practiced primarily in the hills. These systems are not mutually exclusive among Laotian in areas remote from major river valleys, swidden cultivation was practiced by approximately one million farmers in 1990, who grew mostly rice on about 40 percent of the total land area planted to rice.

2.1.3.4 Climate change

Based on Intergovernmental Panel on Climate Change (IPCC, 2007), recently many greenhouse gases such as carbon-di-oxide, methane and nitrous oxide have been increased. In addition, the growth rate of these greenhouse gases are increase every year which is influent to pattern of precipitation around the world. Climate change has potential impact to natural disaster frequency such as flood, landslide, drought and etc. In order to understand potential changing of climate pattern, climate data from Global Climate Models (GCMs) were used. These models provides future projection of future climatic conditions such as rainfall intensity, wind velocity and greenhouse gases concentration. GCMs data is provided in big spatial resolution (80-300 km grid size). Therefore, it is required a preparation (downscale) before it can be used for smaller scale such as regional or catchment scale. Downscaling is a method for get better spatial resolution of GCM output. Methodology for downscale GCM data can be classify into two methods. First method is dynamic downscaling, it is use high resolution regional simulations for reanalysis data to produce regionalised climate information. Second method is statistical downscaling. It is based on relationships between local climate factor such as rainfall, temperature, wind velocity and large scale predictors.

Dankers and Feyen (2008) assess influent of climate change to future flood hazard in Europe. They have concluded, by the end of this century discharge level from many rivers in European will increase for both of magnitude and frequency. However, few rivers will have decrease of discharge level such as rivers of northeast Europe region. Mirza et al (2011) indicated as it is highly that climate change will influent to monsoon precipitation and it is lead to increase of frequency, magnitude and extend of flood hazard

in south Asia such as Bangladesh, India and Pakistan. Also the damage to agriculture, human live and infrastructure will increase in the future. Bouwer (2010) investigate change of flood risk due to climate change and its damage cost. Change of future precipitation and socioeconomic change such as land use change and increase of value asset were consider for assess the damage cost from future flood risk. They concluded that the climate change will increase the damage cost from flood risk around 35 – 170 % by 2040 in Netherland. Sidle and Ochiai (2006) evaluation climate change variables that will triggering landslide hazard. They concluded that increasing of air temperature and precipitation in seasonal were the most interrelated climate variables that will triggering landslide hazard. Ciabatta (2016) investigated the impact of climate change to occurrence of landslide in Italy by using PRESSA model develop by Central Italy. The model based on relationship between rainfall and soil moisture condition (Ponziani et al., 2012). They concluded that the increase in the occurrence of landslide hazard is related to increase of rainfall intensity.

2.2. Integrated risk

Integrated risk or multi-hazard risk is a result from integrated hazard combine with vulnerability. Integrated risk is a development of integrated hazard. Integrated hazard map is focuses on potential impact areas from serval hazards. It is can use for decrease the probability of occurrence and intensity of hazards. Integrated risk map is emphasizes on risk, risk is the combination of the probability of occurrence of a hazard and its negative consequences or vulnerability (UNISDR, 2009). The aim of integrated risk is to have a holistic view of the total impact by mapping and assessing the expected loss from the

occurrence of various hazards on social, economic and human life (Komendantova et al., 2014). Grieving et al (2006) presents indices-based integrated hazard combine with vulnerability index to calculate integrated risk. Delphi process method was used to obtain weight of all hazards. The Delphi process is based on a structured process for obtain and synthesizing knowledge from people in study area by questionnaire. The vulnerability is generate from two indicator hazard exposure and coping capacity, equally weight were used for integrated two indicator into vulnerability. Both of integrated hazard and vulnerability were subdivides into five classes. Subsequently, integrated hazard and vulnerability's classes were summed up to generate integrated risk. Tate, Cutter and Berry (2010) develop a GIS based integrated risk methodology. The objective of this study is to presents GIS based technique that simple for generate mapping of hazard risk. The map is applicable in a screening process to identification of highly risk area. The GIS based technique implemented are not complex and the required input data publicly available. Many studies have used GIS based to calculate integrated risk by aggregating many hazard risk together for instance Wipulanusa et al (2009) discusses aggregation of drought risk and flood risk by overlapping each integrated risk map. Bell and Glade (2004) presents the integrated risk from snow avalanche debris flow and rock fall by created overlaying each integrated risk map with equal weight. Based on previous study, most of method for integrated risk is calculated by aggregating each risk map with equal weight.

2.3. Significance of this study

The existing studies on multi hazard risk mapping are mainly focus on aggregating all individual hazard risk with equal weight, sum of hazard index from individual hazard or using frequency of occurrence for each hazard to decide the weigh, which does not sufficiently reflect the various impacts of different hazards present in the same area. In addition, those studies have not consider participation of stakeholders. In this study, we take into account the stakeholders opinion by comparison of each individual hazard to find the importance of each hazard. The importance of each individual hazard was determined by AHP method. Future more, AHP is a method that attempts to imitate human rationality for decision making by using the experiences and perception from the stakeholders and experts. It offers organization of knowledge, simplifies structures for understanding the issue and consistency, and involves human logic and intuition as well as experiences. In addition, the pairwise comparisons help stakeholders and expert to focus their judgment on each comparison criteria. Each criterion has a certain value that represents a judgment of the likelihood of its scale of importance to others. The integrated hazard risk map based on AHP can identify potential distributed of hazard and risk areas across the country. In addition, the integrated map can provide the preliminary results for distribution pattern of hazard and risk areas, also the damage cost from the potential risk area can be estimated. Moreover, the integrated map can use as support tool for mitigation strategies, future development planning or adaptation measure for decrease hazard area or reduce damage cost of hazard risk.

CHAPTER 3: STUDY AREA AND DATA SOURCES

3.1 Study area

3.1.1 Location and topography

3.1.1.1 Location

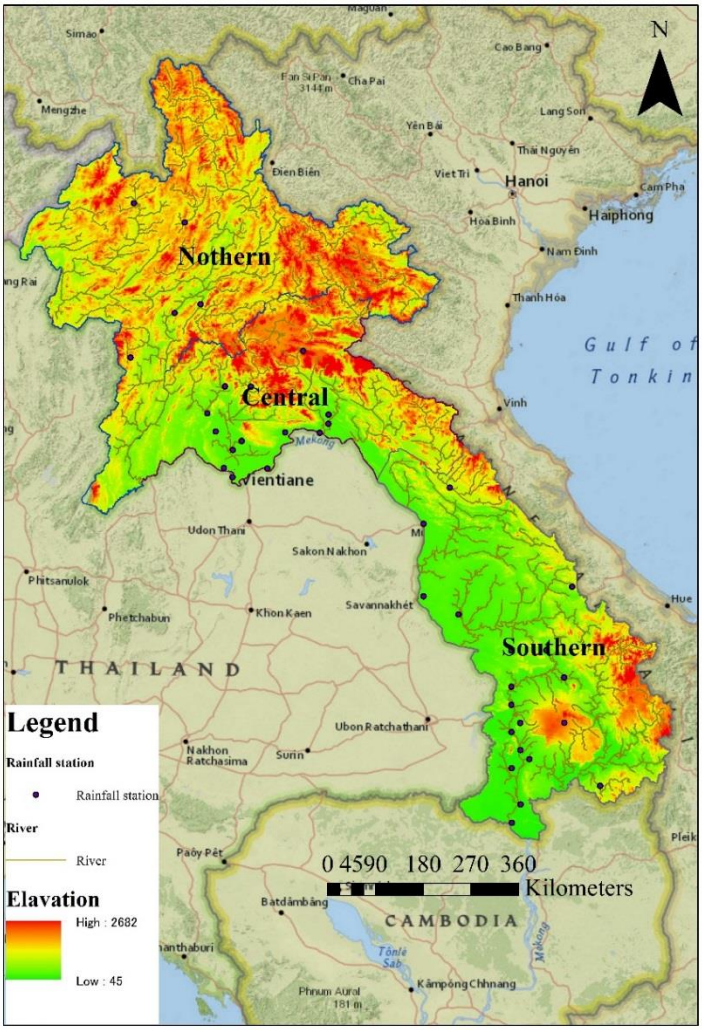

Figure 3-1 Location and Topography of Laos

Figure 3-2 Lao PDR's Provinces map

The Laos PDR, or Laos, is situated in the middle of South East Asia. The country is landlocked, so it has no direct access to the sea and has common borders with China, Vietnam, Cambodia, Thailand and Myanmar. The country is located in the Center of the Indochinese peninsula, located between Longitude 100 to 108 degree East and latitude 14 to 23 degree North, with a total area of 236,800 km^2 with Mekong river flows through almost 1,900 km of Lao territory from the North to the south and it's form a natural border with Thailand on over 800 km. In addition, Laos PDR can divide into 3 regions. These regions are determined by the Lao government, namely, southern, central and northern (Figure 3-1). Future more, Lao PDR is divided into 16 provinces and one capital Vientiane Capital city as shown in Figure3-2

3.1.1.2 Topography

The country is dived into three distinct regions – mountains, plateaus and plains along the Mekong region. The mountain and plateaus make up three quarter of the total area especially in the area of the North and South-East. Northern Laos is dominated by rough mountain, jungle and agricultural areas. The plain region is located along the Mekong River and forms the other quarter of the country. Most of the western boarder of Laos is demarcated by the Mekong River, which is an important mainstream for transportation. The Mekong fall at the end of southern part of Laos prevent access to the sea, but cargo boats still can travel along the entire length of the Mekong in Laos during the most of the years. Smaller power boats and pirogues provide an important role for transportation on many of the tributaries of the Mekong.

The Mekong has thus not been obstacle but a facilitator for communication within

country and the similarities of Laos and northeast Thai society from people to local language, which reflect the close contact that has existed across the river for centuries. Prior to the twentieth century, Laotian kingdoms and principalities encompassed areas on both sides of the Mekong, and Thai control in the late nineteenth century extended to the left bank. Although the Mekong was established as a boarder by French colonial forces, travel from one side to the other side has been significantly limited only since the establishment of the Laos in 1975.

The eastern border with Vietnam extends for 2,130 km mostly along the crest of the Annamite Chain, and serves as physical barrier between the Chinese-influenced culture of Vietnam and the Indianized states of Laos and Thailand. These mountains areas sparsely populated by tribal minorities who traditionally have not acknowledged the border with Vietnam any more than lowland Laotian have been constrained by the Mekong river border with Thailand. Thus ethnic minority populations are found on both Laotian and Vietnamese side of the frontier. Because of their relative isolation, contact between these groups and lowland Lao has been mostly confined to trade. Laos shares its short border of southern with Cambodia and ancient Khmer ruin at What Pho other southern locations attest to the long history of contact between the Laos and the Khmer, in the north, Laos is bounded by a mountainous border with china and shares long Mekong river boarder with Myanmar.

3.1.2 Climate

3.1.2.1 Temperature

Lao PDR is a tropical country and it have a tropical monsoon climate. Lao PDR have two season year as rainy season start from May through October and dry season from November to April. The highest temperature in Lao PDR is close to 40 degree C in April. The lowest temperature is around 10 degree C from December to January. In the Northern sky is often cloudy so the sunshine is very low lead to the temperature in this area is lowest when compare to central and southern area. In the central-southern area the temperature slightly higher than northern during December to January.

3.1.2.2 Rainfall

Rainfall in Lao PDR is influents by the monsoon winds that have a seasonal character. Normally, annual rainfall in Lao PDR is around 1200 to 2200 mm/year in plain area and in mountainous area of northern and southern region annual rainfall can exceed 3000 mm/year. The rainy season in Laos start from May through October, rainfall peak happen in August to September (Figure 3-3). During this time flood events occurs in many areas.

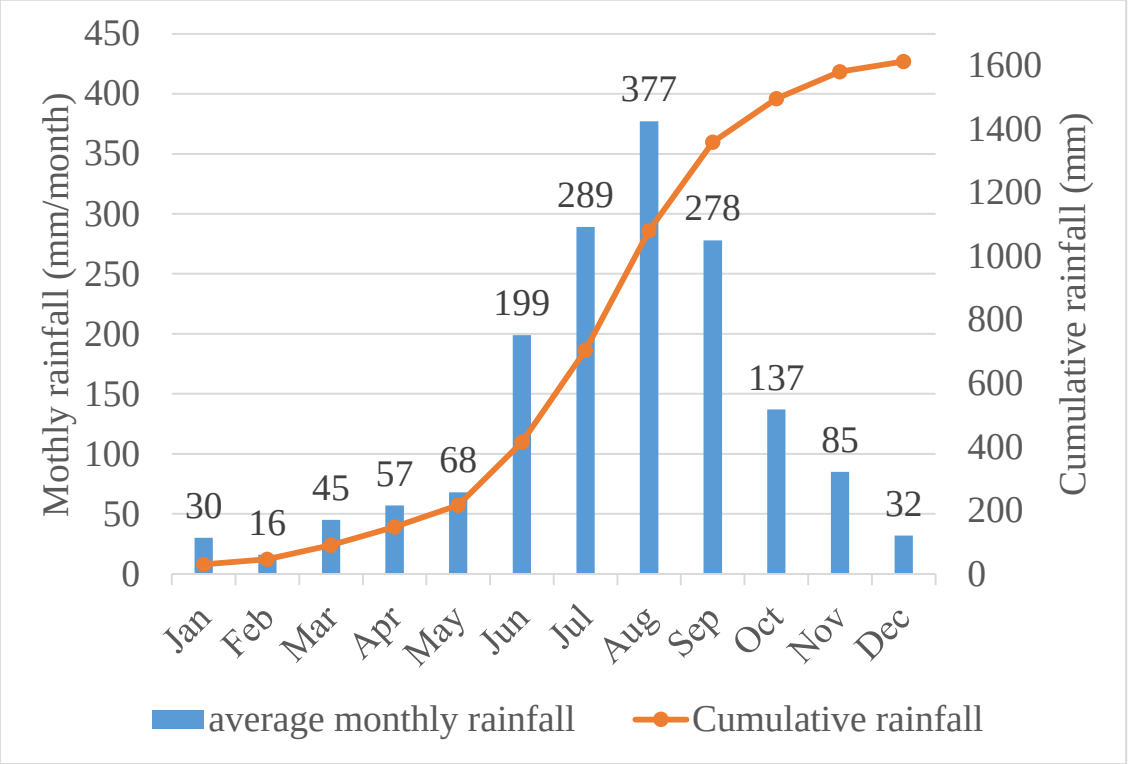

Figure 3-3 Annual rainfall of Lao PDR

3.1.3 Land use

The land use of Laos classified the total area into forest, paddy field, agriculture area, water body and urban. Almost of the agriculture area is paddy field. In recently decade, forest area have been decrease. The reason for the decreasing of forest density is farmers employ one of two cultivation systems: wet field paddy system, practices primarily in the plains and valleys, or the swidden cultivation system, practiced primarily in the hills. Land use type is use as one of factor in infiltration for both hydrological model and probability of landslide model. Land use data can classified into 5 classes, it is consist of agricultural, paddy field, urban, water and forest area (Figure 3-4). Price of agricultural and paddy field data were collected by the Ministry of Agriculture and Forestry of Laos (Ministry of agriculture and Forestry, 2018) (Figure 3-5 and 3-6).

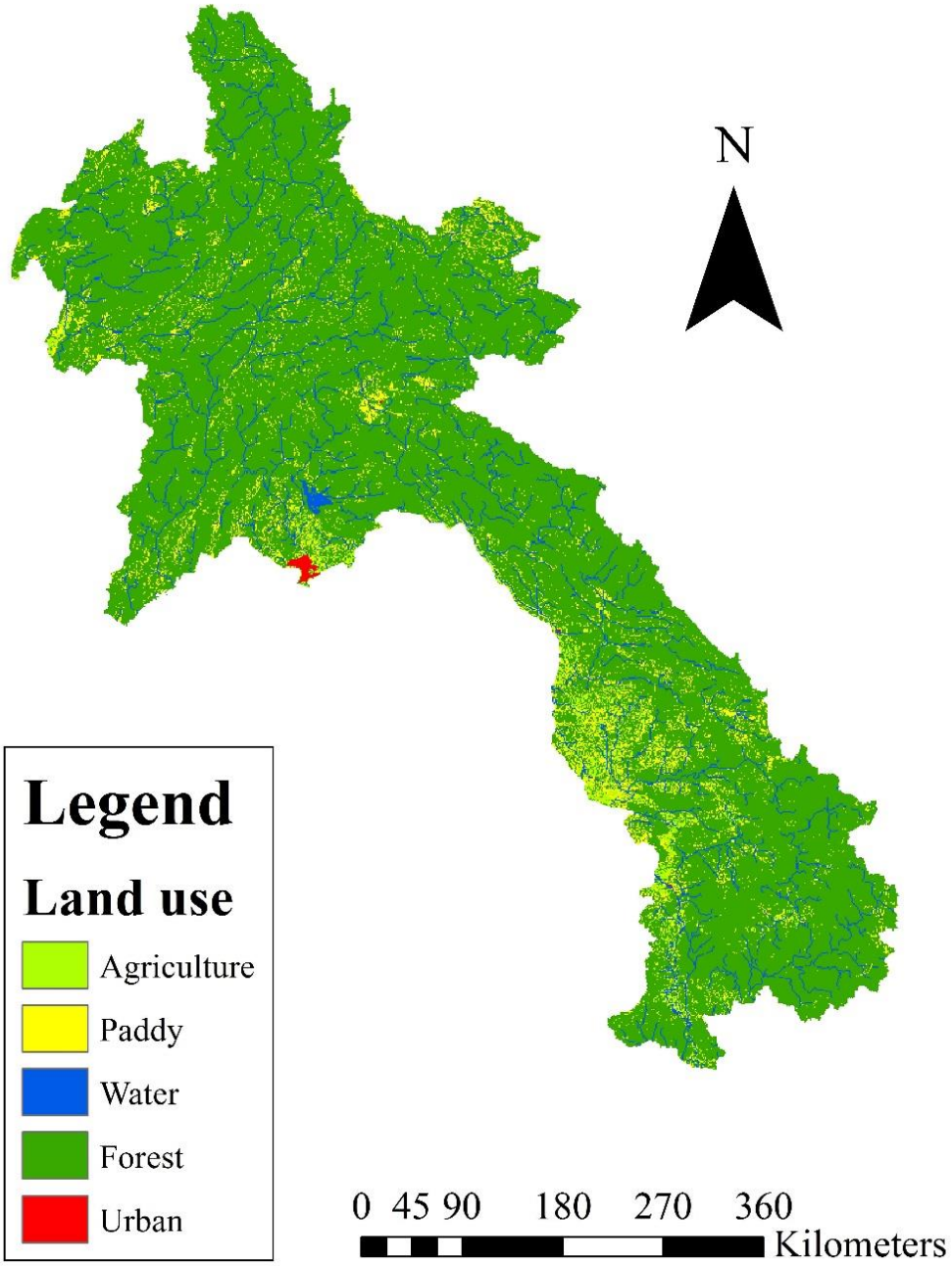

Figure 3-4 Land use type of Lao PDR

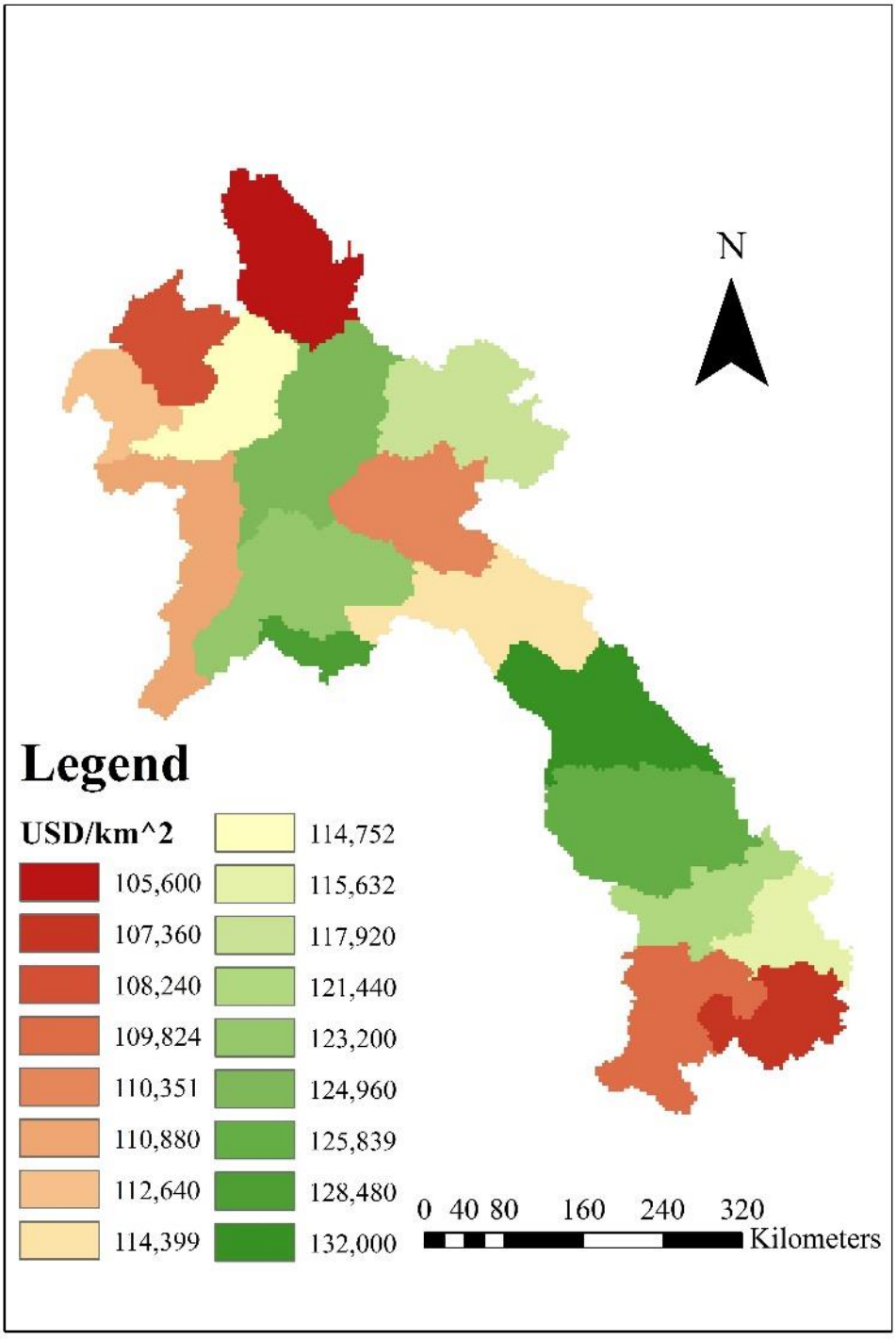

Figure 3-5: Rice price map of Lao PDR

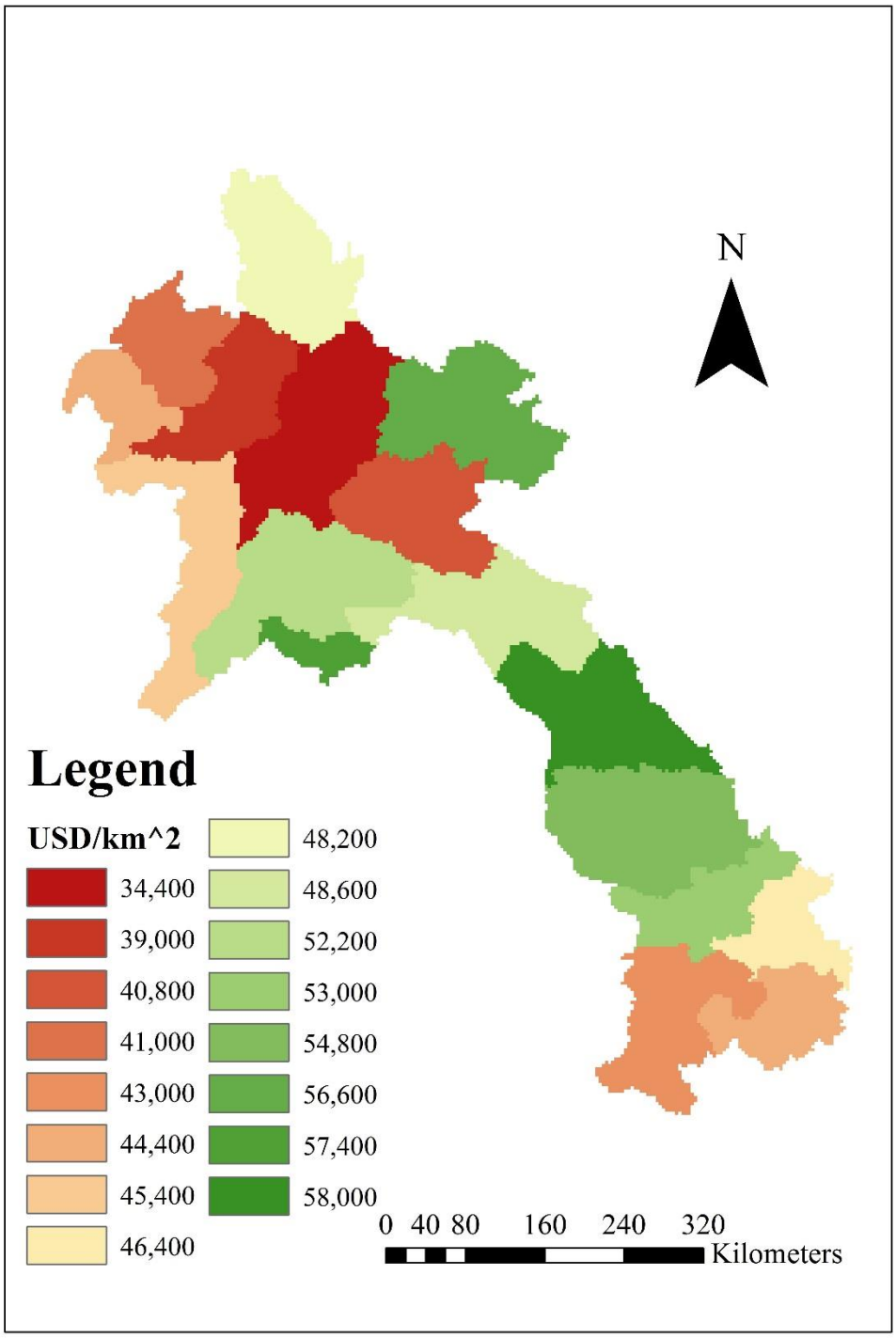

Figure 3-6: Agricultural production price map of Lao PDR

3.1.4 Soil type

Soil data were based on the Harmonized World Soil Database (Fischer et al., 2008; HWSD, 2012), the HWSD is a 30 arc-second raster database with over 16000 different soil mapping units that combine existing regional and national updates of soil information worldwide with the information contained within the 1:5,000,000 scale FAO-UNESCO Soil Map of the World. The original soil type data based on the Soil Unit (SU) Global was convert to the soil texture class. The soil type data plays an important role in the infiltration factor of hydrological distribution (Figure 3-5).

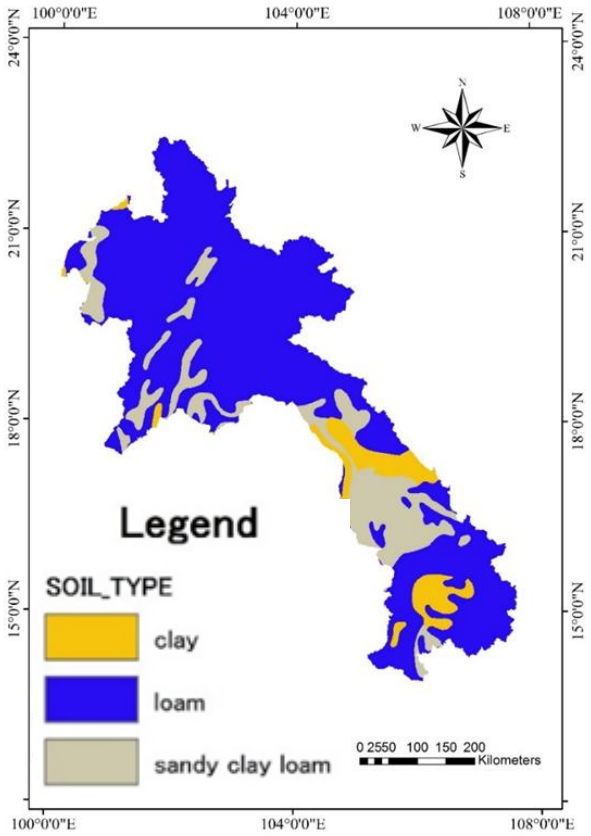

Figure 3-7 Soil type of Lao PDR

3.2 Data sources

3.2.1 Meteorological and hydrological data

For this study, we used hydrological and meteorological dataset from Mekong River Commission. Daily rainfall dataset range from 1970 to 2000 (30 years) from 40 stations were used in this study (the location of all station will be provide in chapter 5). These stations were selected to cover all of study area. The rainfall data were interpolated into 1km x 1km resolution using Inverse Distant Weight (IDW). After that, Log-Pearson type III distribution used for estimated the 100 year return period of extreme rainfall in Laos by use the annual maximum daily rainfalls for each grid area. The hydrological data were used as input data for the rainfall-runoff model and probability of landslide model and it was used for calibrate the rainfall-runoff model. In this study, 100 year return period is use because most of the hazard events (more detail will be explain in Chapter 5-6) was occur by 100 year return period extreme rainfall. In addition, In addition to the rainfall data, daily maximum data is selected to analyse the rainfall intensity return period. The data also used for bias correction between Global Climate Models (GCMs) and observation data.

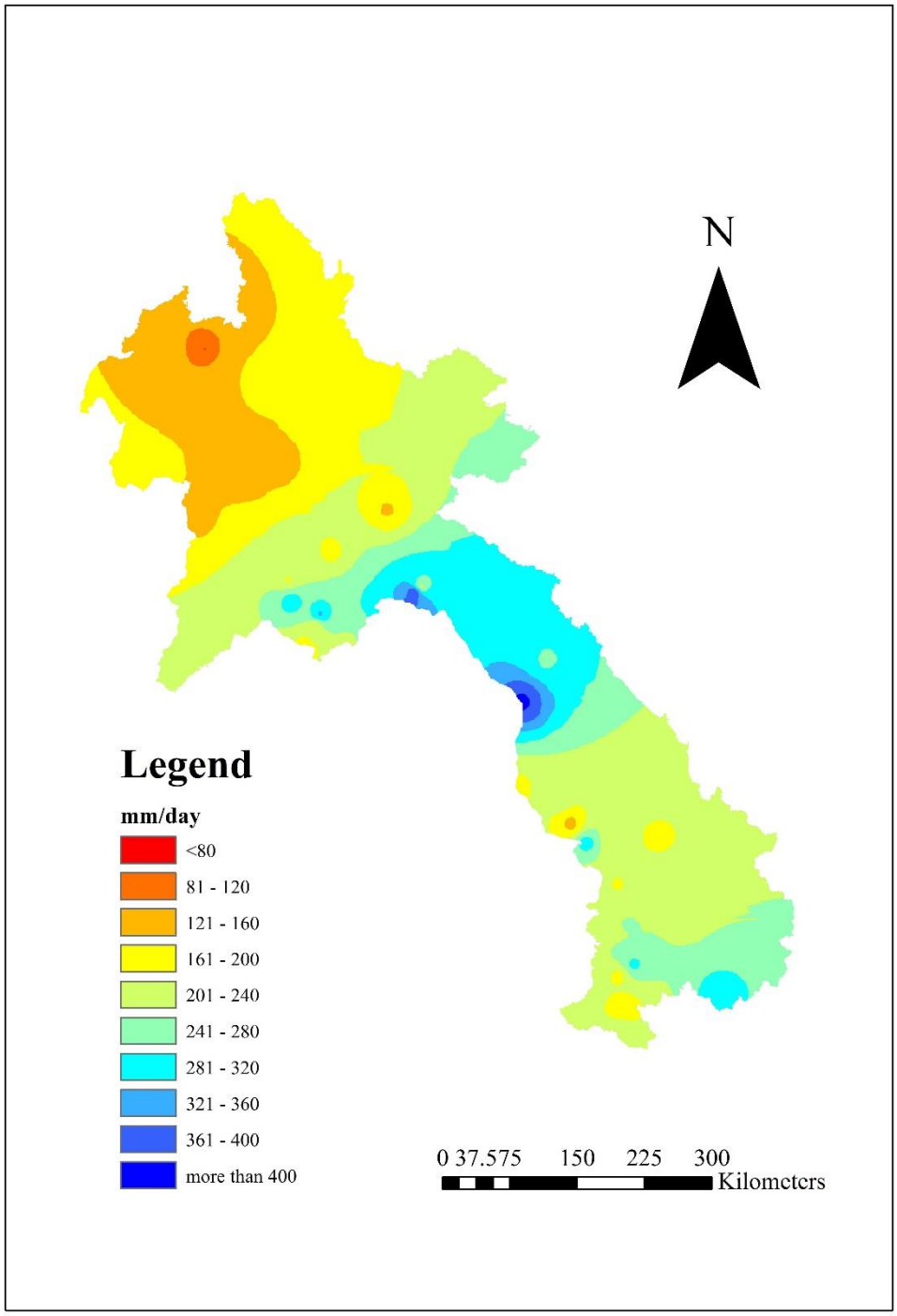

Figure 3-8 100 year return period rainfall in Laos

3.2.2 Digital elevation model and GIS data

In this study we have 3 main based maps consist of topography, soil and land use. Shuttle Radar Topographic Mission (SRTM) Digital Elevation Map (DEM) were used in this study. The original DEM data have a spatial resolution of 90 m x 90 m then we resample is to 1 km x 1km to meet distributed hydrological model spatial resolution. DEM data that used in this study were obtain from National University of Laos. DEM data is a principal source for extract topographic factors, is one of the most important data which has been used in various research works (Tehrany et al., 2013).

3.2.3 Future scenario data

Estimates of global warming are generally based on the application of General Circulation Models (GCMs), which attempt to predict the impact of increased atmospheric CO_2 concentrations on climate variables. Results from numerical experiments with state of the art, GCMs are the main basis for estimates of the greenhouse gas induced anthropogenic climate change. The climate change predictions, determined from different GCM models, indicate that the global warming has clearly been increasing during recent decades and that the trend may worsen in the future. Considering the complex mechanics in the atmosphere and the uncertainty of the model structure, different GCMs produce different prediction. However, despite differing predictions, trends in weather variables were coincident (IPCC, 2007)

Climate change is expected to increase both the magnitude and the frequency of extreme precipitation events, which may lead to more intense and frequent river flooding. Several studies have shown that the climate has been a contributing factor to flooding risk by increasing the amount of precipitation relative to the average annual rainfall (Hirabayashi et al., 2008; Li et al., 2013). Until now, IPCC have proposed 2 scenarios of future climate change Special Report on Emissions Scenarios (SRES) and Representative Concentration Pathways (RCPs). In this study, RCPs scenarios was used for future climate change projection because RCPs scenarios area based on of radiative forcing projection and it is allow for policy change to be implemented. Seven GCMs, namely, CanESM2, CNRM-CM5, GFDL-ESM2 M, MPI_ESM_LR, MRI-CGCM3, Miroc-ESM and Miroc-ESM-CHEM (details about each GCM are shown in Table 3-1), were selected to create future scenarios of spatially distributed heavy rainfall. Rainfall data from GCMs have different time resolution, therefore we convert all of 3 h rainfall data to daily data by summation of rainfall data in same day. The rainfall data period was from 2006 to 2100, and three representative concentration pathways (RCPs) were used, including 2.6 (RCP2.6) 4.5 (RCP4.5) and 8.5 (RCP8.5). In addition, the number 2.6, 4.5 and 8.5 from RCP mean a prediction range of radiative forcing value in the end of year 2100. The first, RCP2.6, is a scenario where the annual concentration level of greenhouse gases (GHG) peaks in approximately 2020 and then decreases afterwards. The second, RCP 4.6, is a scenario in which the GHG concentration peak occurred in approximately 2040 and stabilized before 2100. The third, RCP 8.5, is the scenario where the GHG concentration is at the highest level.

The resolution of GCMs data is bigger than our dataset resolution, therefore, we apply statistical downscale bias correction quartile mapping method to downscale GCMs rainfall data (more detail is explain in Chapter 4.5). Then we use average daily rainfall data of 7 GCMs as future projection daily rainfall. The future projection daily rainfall data were interpolated in to 1km x 1 km resolution using IDW method (more detail in Chapter 4.11). Subsequently, the annual maximum daily rainfalls were selected for each grid. The calculation of future projection return period rainfall was don based on grid calculation using Pearson type III (more detail in Chapter 4.12)

Table 3-1 List of Global Climate Models (GCMs) used in this study

Model	Institution	Time resolution	Resolution (Lon×Lat)
MIROC-ESM	Atmosphere and Ocean Research Institute (the University of Tokyo), National Institute for Environmental Studies and Japan Agency for Marine-Earth Science and Technology, Japan	3h	2.8°×2.8°
MIROC-ESM-CHEM	Atmosphere and Ocean Research Institute (the University of Tokyo), National Institute for Environmental Studies and Japan Agency for Marine-Earth Science and Technology, Japan	3h	2.8°×2.8°
CanESM2	Canadian Center for Climate Modeling and Analysis, Canada	24h	2.8°×2.8°
CNRM-CM5	Center National de Recherches Meteorologiques / Center Europeen de Recherche et Formation Avancees en Calcul Scientifique	3h	1.4°×1.4°
GFDL-ESM2 M	NOAA Geophysical Fluid Dynamics Laboratory	3h	2.5°×2.0°
MPI-ESM-LR	Max Planck Institute for Meteorology, Germany	24h	1.87°×1.86°
MRI-CGCM3	Meteorological Research Institute	24h	1.12°×1.12°

CHAPTER 4: METHODOLOGY

4.1 Outline of method

The integrated risk maps for this study are created based on integrated hazard maps and land use categories. The integrated hazard maps consist of five hazard maps: flood, land use change, landslide, climate change leading to flood and climate change leading to landslide hazard maps.

4.2 Flood hazard

To evaluate flood hazard a distributed hydrological model was utilized (Kazama et al., 2004; Phrakonkham et al., 2019). The hydrological models are simplified, conceptual representations of a part of the hydrologic cycle. A lot of theoretical and experimental studies have been conduct to get better understanding of hydrological processes and simulate their dynamic mathematically. Hydrological cycle is a complex multifactor process and not yet well understood, simplified representation hydrological models are widely used to delineate the hydrological cycle mechanism before a satisfactory physical delineation is found.

The model consider the meteorological dataset as input into an output hydrological dataset such as stream flow over a time period. A hydrological model is made of mathematical representations of the key process like precipitation, infiltration and transfer into stream; the hydrological processes considered in this model are precipitation, infiltration, surface runoff, base water flow and water balance in each layers. The model

technically consists in a set of hydrological parameters describing the catchment properties, and algorithms describing the physical processes, in this model the catchment is divided into land glow planes and channel segments. In the land, for each grid cell, two layers are considered in vertical direction: base water layer and surface layer. For distributed system models information on geological and topographical characteristics of a river catchment in required in order to derive or measure the necessary parameters. The river basin characteristics were described by the set of data (elevation, flow direction, catchment area and stream network), derived from the digital elevation model.

The model is includes a direct flow and base flow models and used to estimate the river flow. Direct flow is calculated using Kinematic wave concepts which pursues meteoric water runoff using a momentum equation and a continuity equation. This concept will be true on the basic of assuming that the downstream condition has no effect to the upstream. This method fundamentally intended for surface flow, but for a freshet of downpour, it can be applied to direct flow, which includes surface and intermediate flow. With an assumption of a rectangular section of grid.

Continuity equation

$$\frac{\partial A}{\partial t} + \frac{\partial Q}{\partial x} = (r_e)B \qquad (4.1)$$

$$\frac{\Delta H * B}{\Delta t} + \frac{Q_{out} - Q_{in}}{\Delta x} = (r_e)B \qquad (4.2)$$

$$\Delta H = \frac{\Delta t}{B\Delta x}(Q_{in} - Q_{out}) + (r_e)\Delta t \qquad (4.3)$$

Where, ΔH is variation of depth (m), Δt is time interval of flow direction (d), Δx mash interval of flow direction (m), r_e is precipitation (m/d), and B is width of flow

path (m). For the first and second term mean a variation of water depth by inflow and outflow respectively. Calculating the second term for each cell and then adding its result in the next downstream cell, water depth of each cell is calculated.

The flow rates was calculated form Manning equation

$$Q = \frac{1}{n} B h^{\frac{5}{3}} I^{\frac{1}{2}} \quad (4.4)$$

Where Q is flow rate (m^3/d), h is water depth (m), I is gradient slope and n is the Manning roughness coefficient ($d/ [m^{1/3}]$).

The infiltration water was determined by the following equation

$$R_{in} = k_a * h \quad (4.5)$$

Where R_{in} is the amount of infiltration (m/d), k_a is the infiltration coefficient (d^{-1}) and h is water depth (m). Base flow is calculated with the storage function method because of its simplicity

Storage function method

$$s = kq^p;\ q = \left(\frac{s}{k}\right)^{\frac{1}{p}} \quad (4.6)$$

Where s is apparent storage level (m) q outflow level of base flow (m/d), k and p are constant.

4.3 Landslide hazard

Landslides are one of the most dangerous natural hazards, and they cause major damage to affected areas. To identify the locations of landslide hazard areas throughout Laos, a probabilistic model based on multiple logistic regression analysis was used. The model considers several important physical parameters, including hydraulic and geographical parameters. Among these, the hydrological parameter (i.e., hydraulic gradient) is the most important factor for determining the probability of a landslide. (Kawagoe et al. 2010). The statistical approaches used for evaluation are indirect hazard mapping methodologies that involve a statistical determination based on a combination of variables that have identified land use occurrence (Ohlmacher and Davis, 2003; van Westen et al., 2006). In addition, probabilistic methods are used to determine the probability over a large area where numerous natural slopes exist. Hence, the hydraulic gradient is the main hydraulic parameter. Due to the lack of data in Laos, data from Thailand were used for this study on Laos (Kawagoe et al., 2010; Komori et al., 2018; Ono et al., 2011), in which Equation. (4.7) was derived:

$$L_p = \frac{1}{1 + exp[-(-17.494 + 1179.25 \times hydro \times 0.0097 \times relief)]} \quad (4.7)$$

Where L_p is the probability of a landslide, which we consider to be the hazard index of a landslide, $hydro$ is the hydraulic gradient and $relief$ is the relative relief (m).

Relative relief defined as the elevation difference between the highest location and lowest location. Relief energy is an index that could show the complexity of geographical features considering the active development of landform. Therefore, in this study relief energy is defined as the elevation difference between the highest and the lowest elevation in each grid cell and the relief energy for each 1km×1km resolution grid cell is estimated using the digital elevation model (DEM) data.

Hydraulic gradient in a significant factor for initiation of landslide. Change in hydraulic gradient in slope area can lead to landslide. In this study we use unsaturated infiltration analysis based on Richards equation to find the change in hydraulic gradient($\Delta h/L$). The equation used rainfall, soil type and slope angle as main parameter (Figure 4-1).

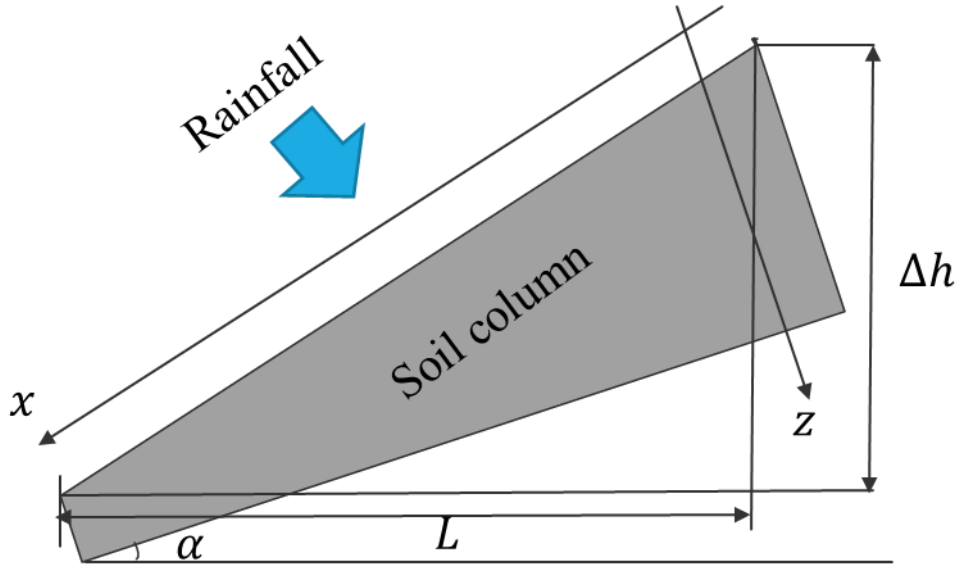

Figure 4-1 Schematic diagram for infiltration analysis to obtain the hydraulic gradient

From Richards equation water volume content (θ) is shows in Equation (4.8)

$$\frac{\partial \theta}{\partial t} = -\left(\frac{\partial V_x}{\partial x} + \frac{\partial V_z}{\partial z}\right) \quad (4.8)$$

Where, θ is water volume content, t is time interval, V_x is the velocity in the horizontal direction (m/d) and V_z is the velocity in vertical direction (m/d), which V_x and $V_z$can be obtain from :

$$V_x = -K_x \frac{\partial hh}{\partial x} \quad (4.9)$$

$$V_z = -K_z \frac{\partial hh}{\partial z} \quad (4.10)$$

Where, K_x is the unsaturated hydraulic conductivity in horizontal direction, K_z is the unsaturated hydraulic conductivity in vertical direction. hh is the total hydraulic head (m), it can obtain from summation of the hydraulic pressure head ψ (m) and elevation head. The elevation head can be estimated using horizontal and vertical length components (L_x = grid size in horizontal (m) and L_z = grid size in vertical (m)), as $-L_x \sin\alpha - L_z \cos\alpha$, α is slope angle therefore total head is

$$hh = \psi - L_x \sin\alpha - L_z \cos\alpha \quad (4.11)$$

Combining Equation (4.9), (4.10) and (4.11) two dimensional hydraulic head can be analysed (Richards, 1931)

$$C\frac{\partial\psi}{\partial t} = \frac{\partial}{\partial x}\left(K_x\frac{\partial hh}{\partial x}\right) + \frac{\partial}{\partial z}\left(K_z\frac{\partial hh}{\partial z}\right) \quad (4.12)$$

$$C\frac{\partial\psi}{\partial t} = \frac{\partial}{\partial x}\left(K_x\frac{\partial\psi}{\partial x} - K_x\sin\alpha\right) + \frac{\partial}{\partial z}\left(K_z\frac{\partial\psi}{\partial z} - K_z\cos\alpha\right) \quad (4.13)$$

Where, C is the specific moisture capacity, it is can calculate from gradient of the soil moisture characteristic curves (Gosh, 1980, Ahuja et al., 1985, Kawakami, 2003). For analyse the specific moisture capacity, two relationship have been used.

First the relation between unsaturated hydraulic conductivity (K) and water volume content (θ)

$$K_x = Ks_x\left(\frac{\theta-\theta_r}{\theta_s-\theta_r}\right)^{\beta} \quad (4\text{-}14)$$

$$K_z = Ks_z\left(\frac{\theta-\theta_r}{\theta_s-\theta_r}\right)^{\beta} \quad (4\text{-}15)$$

Where, Ks is the saturated hydraulic conductivity (m/d), β is a soil characteristic value, θ_r is the residual water volume content θ_s is the saturation water volume content.

Second is relationship between water volume content (θ) and pressure head ψ

$$\theta = (\theta_r - \theta_s)\left(\frac{\psi'}{\psi_0}+1\right)exp\left(-\frac{\psi'}{\psi_0}\right) + \theta_r \quad (4\text{-}16)$$

$$\psi' = \begin{cases}\psi\ (\psi < 0)\\ 0\ (\psi \geq 0)\end{cases} \quad (4\text{-}17)$$

where ψ_0 is used as the initial condition (initial pressure (m)) and ψ' is used as the saturated condition (saturated pressure (m)).

Table 4-1 Properties of soil types used for infiltration analysis

Soil type	Hydraulic conductivity Ks (m/d)	Saturation water volume content θ_s	Residue water volume content θ_r	Soil characteristic value β
Sandy clay loam	0.864	0.35	0.067	3
Loam	0.864	0.42	0.064	3
clay	$8.64x10^{-3}$	0.5	0.10	20

4.4 Land use change hazard

The scenario in which reduced forest and increased cropland area are included was first used to assess the impacts of various land use scenarios on the flood hazard map in this study area. To investigate the sensitive areas of the flood hazard map, this selection was chosen. Hence, the reduction of forest, all forest areas and cropland was considered and converted to the worst scenario. One of the suitable geo-environmental factors of crop fields is the slope (Ceballos-Silva and López-Blanco, 2003; Huynh, 2008). As shown by these studies, a slope of approximately 6-12% will increase the growth of vegetation. Consequently, in the scenario designed first, the forest area with a slope angle less than 12% was converted to cropland and the slope angle more than 12% was remained unchanged. Second, based on the probability of an increased population, an expansion of urban areas was created to represent the process from rural areas to urban areas.

4.5 Climate change hazard

Climate change hazard is estimated as a future projection of the climate change impact on the future flood and future landslide hazard. It is obtained by the future projection of precipitation from the GCMs data set. In this study, the average precipitation from 7 GCMs (Table 3-1) and three RCP scenarios were selected. Because most GCMs offer information at scales greater than a few hundred kilometers, statistical downscale bias correction quantile mapping was deployed (Equation (4-18)) to reduce bias for precipitation output from the GCMs (Boé et al., 2007; Fajar Januriyadi et al., 2018; Fang et al., 2015; Lafon et al., 2013; Salem et al., 2018). First, the method for bias correction quantile mapping presented by Salem (2018) is used. Then, the near and far future trends in rainfall are chosen as the average future precipitation data of the GCMs from 2010 to 2050 (2050s) and 2051 to 2099 (2100s). Additionally, log-Pearson type III method was used for calculated return period rainfall for all future rainfall patterns.

$$z_{cor} = CDF_0^{-1}\left(CDF_{gcm}(z_{gcm})\right) \quad (4\text{-}18)$$

Where, $z_{cor}$is precipitation after correcting the bias, z_{gcm} is precipitation from GCMs before bias correction, CDF_{gcm} is the Cumulative Distribution Function (CDF) of z_{gcm} and CDF_0^{-1} is the inverse CDF of observed rainfall

4.6 Hazard index

4.6.1 Flood hazard index classification

We propose a hazard index, which is adapted from the relationship between velocity and flood depth (Sally et al., 2008). By considering the water depth of every grid in the flood map, we converted the value to a hazard index. The scenario was as follows: the water velocity from the flooded areas was low, and the depth can be transformed into a hazard index. The index is scaled from zero to one, with zero representing the lowest hazard and one representing the highest hazard. The hazard index was classified into four categories, i.e., small, medium, high and very high hazard, which correspond to the inundation depths of 0.0-0.3, 0.31-0.6, 0.61-2.0 and more than 2.1 m, respectively. Subsequently, we can find relationship between flood depth and hazard index as shown in Figure 4-3 and flood depth and hazard index curve can be derived (Figure 4-4)

Velocity (m/s)	Depth of flooding (m)											
	0.05	0.1	0.2	0.3	0.4	0.5	0.6	0.8	1	1.5	2	2.5
0												
0.1												
0.25												
0.5												
1												
1.5												
2												
2.5												
3												
3.5												
4												
4.5												
5												

Figure 4.2 Flood depth-velocity relationship to hazard index.

Flood depth (m)	hazard index
Small hazard < 0.3	0-0.25
Medium hazard < 0.6	0.25-0.5
High risk< 2	0.5-0.75
Very high risk > 2	0.75-1

Figure 4.3 Flood depth-hazard index relationship.

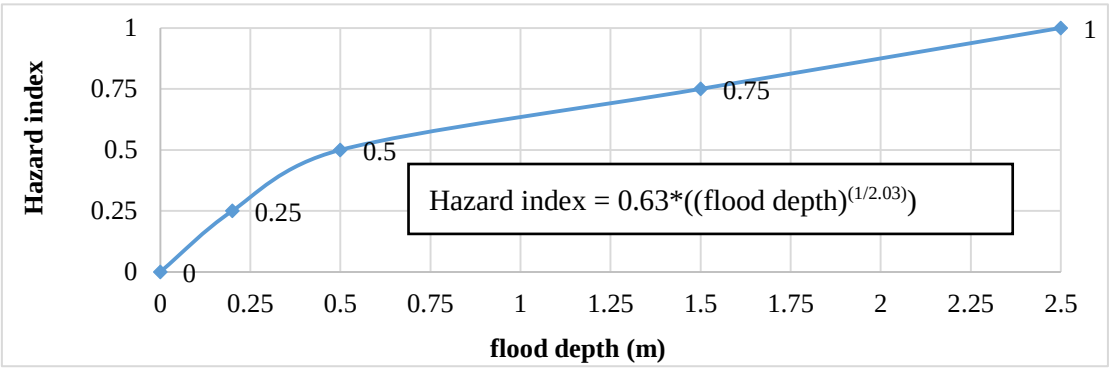

Figure 4-4 Flood depth and hazard index relationship curve.

4.6.2 Land slide hazard index classification

Probability of landslide (0-1) is used directly as land slide hazard index (0-1). Landslide hazard map was classified, using the natural breaks method that provided in ArcGIS program. The natural breaks method is a data classification method designed for determined best arrangement in term of representation data's spatial distribution (Bednarik et al., 2010; Constantin et al., 2011; Erener and Düzgün, 2010; Falaschi et al., 2009; MohanV and RajT, 2011; Pourghasemi et al., 2012). The natural breaks method is identified break point by picking the class break that best group similar values and maximize the difference between classes. By using different break point in the dataset to determine which set of break has the smallest in class variance. The natural breaks method works by optimizing the goodness of variance fit, a value from 0 to 1 where 0 = no fit and 1 = perfect fit. In this study we want to classification our data into 4 class which similar to flood hazard map and for convenience for comparison to other hazard maps.

Sum of squared Deviations from Array Mean ($SDAM$)

$$SDAM = \sum_{id=1}^{tg} (X_{id} - X_{mean})^2 \quad (4\text{-}19)$$

Sum of squared Deviations from the Class Mean ($SDCM$)

$$SDCM = \sum_{id1=1}^{cl1} (X_{id1} - X_{class1})^2 + \sum_{id2=cl1+1}^{cl2} (X_{id2} - X_{class2})^2 + \sum_{id3=cl2+1}^{cl3} (X_{id3} - X_{class3})^2 + \sum_{id4=cl3+1}^{tg} (X_{id4} - X_{class4})^2 \quad (4\text{-}20)$$

Goodness of Variance Fit (GVF)

$$GVF = (SDAM - SDCM)/SDAM \quad (4\text{-}21)$$

Where X_{id} (id = 1, 2, 3…., tg) is id^{th} probability grid data of land slide hazard map (from smallest to largest probability), tg is total number of grid from land slide hazard map, X_{mean} is mean of probability grid data, we divide X_{id} data into 4 group as group 1 = X_{id1} $(id1 = 1,2,3, \dots cl1)$ group 2 = $X_{id2} = (id2 = cl1 + 1, cl1 + 2, \dots\dots, cl2)$, group 3 = $X_{id3} = (id3 = cl2 + 1, cl2 + 2, \dots, cl3)$ and group 4 = $X_{id4} = (id4 = cl3 + 1, cl3 + 2, \dots\dots, tg)$, $cl1, cl2, cl3$ are group break point in X_{id} data $X_{class1}, X_{class2}, X_{class3}$ and X_{class4} are mean of probability grid data from group 1,2 3 and 4, respectively. The method first specifies arbitrary grouping of data. $SDAM$ is constant and does not change unless data change. The mean of each class is computed and the $SDCM$ is calculated. Data are then move from on class to another class in an effort to reduce the sum of $SDCM$ and therefore increase the GVF statistic. This process continues until the GVFvalue can no longer increase. Finally, land slide hazard map is graded into 4 class: low (0-0.23), medium (0.23-0.54), intermediate (0.54-0.85) and high (0.85-1).

4.7 Analytical Hierarchy Process (AHP)

AHP is a powerful tool for multi-criteria decision-making (Saaty, 1994). To provide the relative weights of the criteria, it is necessary to define each criterion's relative importance, and thus, a pair-wise comparison matrix for each criterion is created to enable significance comparisons. We have 5 criteria, which include Flood, land use change, landslide, climate change impact to flood and climate change impact to landslide, and thus, the matrix is 5 by 5, and the diagonal elements are equal to 1. The value of each row of pair-wise comparisons is determined based on expert judgments.

To obtain the criteria relative priority value, expert judgments are required. We de-signed

and conducted a questionnaire at the Ministry of Natural Resource and Environment of Laos because most of the officers that work in this ministry have knowledge of flood hazards, climate changes, and land use impacts in Laos (Table 4-2). All of expert and who have experience in field of our concerned hazards and risk were asked to do a questionnaire. Approximately 41 samples were collected from all expert officer Ministry of Natural Resource and Environment. By using Equation (4-22), we obtained a value for each pair-wise comparison from each row of questionnaire.

$$Rel_j = \sqrt[m]{\frac{\prod_{i=1}^{m} A_{m,j}}{\prod_{i=1}^{m} B_{m,j}}} \quad (4\text{-}22)$$

Where Rel_j is relative important of pairwise of criteria in jth row from questionnaire, for example row $j = 1^{st}$ represent pairwise comparison between flood and land use change according to Table 4-2, and m is the number of samples (in this study m = 41).

Table 4-2 Questionnaire of preference for AHP approach.

Which respect to damage, using the scale from 1 to 9 (where 9 is extremely and 1 is equally important), please indicate (x) the relative importance of opinions *A* (left column) to opinions *B* (right column), here scale value are consider as (9 (*A*) to 9 (*B*))

Options *A*	Extremely		Very Strongly		Strongly		Moderately		Equally		Moderately		Strongly		Very Strongly		Extremely	Options *B*	
Flood	9	8	7	6	5	4	3	2	1	2	3	4	5	6	7	8	9	Land use change	$j = 1$
Flood	9	8	7	6	5	4	3	2	1	2	3	4	5	6	7	8	9	Landslide	$j = 2$
Flood	9	8	7	6	5	4	3	2	1	2	3	4	5	6	7	8	9	Climate change to flood	$j = 3$
Flood	9	8	7	6	5	4	3	2	1	2	3	4	5	6	7	8	9	Climate change to landslide	
Land use change	9	8	7	6	5	4	3	2	1	2	3	4	5	6	7	8	9	Landslide	
Land use change	9	8	7	6	5	4	3	2	1	2	3	4	5	6	7	8	9	Climate change to flood	
Land use change	9	8	7	6	5	4	3	2	1	2	3	4	5	6	7	8	9	Climate change to landslide	
Landslide	9	8	7	6	5	4	3	2	1	2	3	4	5	6	7	8	9	Climate change to flood	
Landslide	9	8	7	6	5	4	3	2	1	2	3	4	5	6	7	8	9	Climate change to landslide	
Climate change to flood	9	8	7	6	5	4	3	2	1	2	3	4	5	6	7	8	9	Climate change to landslide	$j = 10$

Options *A*	Extremely		Very Strongly		Strongly		Moderately		Equally		Moderately		Strongly		Very Strongly		Extremely	Options *B*	
Flood	✖	8	7	6	5	4	3	2	1	2	3	4	5	6	7	8	9	Land use change	$j = 1$

A_j and B_j are the responses value that expert given from questionnaire in row jth, when the value was given to option A or B due to the experts' judgment the opposite value will be 1 for in stand from above example, first expert (m =1) was given his/her judgment that in row 1 ($j = 1$) the comparison between flood and land use change, in term of damage flood extremely more important than land use change results from the

questionnaires are shown in Table 4-3

Table 4-3 Result of pairwise comparison from questionnaires

Option A	Option B	Rel_j
Flood	Land use change	4.2
	Land slide	7.1
	Climate change to flood	0.714
	Climate change to land slide	4.1
Land use change	Land slide	3.6
	Climate change to flood	0.185
	Climate change to land slide	1.6
Land slide	Climate change to flood	0.17
	Climate change to land slide	0.34
Climate change to flood	Climate change to land slide	5.5

The results form Table 4-3 then transferred into comparison matrix ($\boldsymbol{D}_{i,k}$) as shows in Table 4-4 below. The comparison of same criteria will consider as equally important (scale value = 1). When we compare the inverse of the pair-wise values, the scale value is the reciprocal value. For example, the value for flooding vs. land use change is 4.20, and thus, the value for land use change compared to flooding is 1/4.20 $\approx$ 0.24, which is shown in Table 4-4

Table 4-4 AHP pairwise comparison matrix ($\boldsymbol{D}_{i,k}$)

Option B(k) / Option A (i)	Flood ($k=1$)	Land use change ($k=2$)	Landslide	Climate change to flood	Climate change to landslide ($k=5$)	
Flood	1.00	4.20	7.10	0.71	4.10	$i=1$
Land use change	0.24	1.00	3.60	0.18	1.60	$i=2$
Landslide	0.14	0.28	1.00	0.17	0.34	
Climate change to flood	1.4	5.4	5.7	1.00	5.50	
Climate change to landslide	0.24	0.63	2.9	0.18	1.00	$i=5$

Next step we have to find relative priority or weight ($\boldsymbol{w}_i$) of each criteria. According to Saaty (1994), the weight ($\boldsymbol{w}_i$) is the normalized eigenvector of the matrix ($\boldsymbol{D}_{i,k}$) associated with the largest eigenvalue λ_{max} of the matrix ($\boldsymbol{D}_{i,k}$). $\boldsymbol{w}_i$ (i= 1, 2,…, 5) is a weight of each hazard correspond to hazard from ith row of Table 4-5 for example $\boldsymbol{w}_1$ ($i = 1$) is a weight of flood hazard ($\boldsymbol{w}_1 = \boldsymbol{w}_{flood}$) according to Table 4-4 ($\boldsymbol{w}_2 = \boldsymbol{w}_{land\ use\ change}$, $\boldsymbol{w}_3 = \boldsymbol{w}_{landslide}$, $\boldsymbol{w}_4 = \boldsymbol{w}_{climate\ change\ to\ flood}$ & $\boldsymbol{w}_5 = \boldsymbol{w}_{climate\ change\ to\ landslide}$). The weights for pairwise comparison matrix is present in Table 4-5

Table 4-5 Pairwise comparison matrix, with the weight of each criteria

$k = 1$ $k = 2$ ---------- $k = 5$

Option B (k) / Option A (i)	Flood	Land use change	Landslide	Climate change to flood	Climate change to landslide	Weight ($\boldsymbol{w}_i$)	
Flood	1.00	4.20	7.10	0.71	4.10	0.33	$i = 1$
Land use change	0.24	1.00	3.60	0.18	1.60	0.11	$i = 2$
Landslide	0.14	0.28	1.00	0.17	0.34	0.045	
Climate change to flood	1.4	5.4	5.7	1.00	5.50	0.42	
Climate change to landslide	0.24	0.63	2.9	0.18	1.00	0.09	$i = 5$
Sum	3.02	11.50	20.30	2.26	12.54	1	

In practice, it is impossible to expect the decision maker to provide a pair-wise comparison matrix that is completely consistent. Therefore, after obtaining $\boldsymbol{w}_i$, the consistency needs to be evaluated.

The consistency ratio is evaluated as follows:

$$CR = \frac{CI}{Ri} \tag{4-23}$$

Where CR is the consistency ratio, CI is the consistency index and Ri is a random

index that is dependent on the sample size, which is shown in Table 4-6, where the values of Ri are tabulated. There are five criteria, and as a result, Ri = 1.12.

Table 4-6 Random index (Ri) used to compute consistency ratio.

N	1	2	3	4	5	6	7	8	9
Ri	0	0	0.58	0.9	1.12	1.24	1.32	1.41	1.45

According to AHP theory (Saaty, 1994), CR must be less than 0.1. CI can be calculated as follows:

$$CI = \frac{\lambda_{max} - N}{N - 1} \quad (4\text{-}24)$$

$$\lambda_{max} = \frac{1}{N} Trace(diag(\boldsymbol{u}_i)) \quad (4\text{-}25)$$

$$\boldsymbol{u}_i = diag(\boldsymbol{v}_i) \times diag(\boldsymbol{w}_i)^{-1} \times (1,1)^T \quad (4\text{-}26)$$

$$\boldsymbol{v}_k = \boldsymbol{D}_{i,k} \times \boldsymbol{w}_i \quad (4\text{-}27)$$

Where, λ_{max} is the maximum eigenvalue of the comparison matrix $\boldsymbol{D}_{i,k}$ and N is number of criteria. $\boldsymbol{D}_{i,k}$ is a pair-wise comparison matrix from Table 4-4, i, k = 1,2,…., N

From Equation (4-24) to (4-27), we can obtain CI = 0.04.and λ_{max} = 5.18. Finally, the consistency ratio was calculated to be CR = 0.03. Since, the CR value is lower than the threshold (0.1), this indicates that the expert judgments are reasonably consistent.

4.8 AHP-based integrated hazard

To integrate the above flooding, land use, landslide, climate change leading to flood and climate change leading to landslide hazard maps, the AHP-based hazard index is used. This index is also deployed to assimilate the weight of each criterion used to assign its role in the final map. Each grid must therefore be evaluated based on all criteria. The AHP-based hazard index can be derived as follows:

$$AHP_{\bar{x},\bar{z}}hazard\ index = \left(HI_{\bar{x},\bar{z},flood} \times \boldsymbol{w}_{flood}\right) + \left(HI_{\bar{x},\bar{z},land\ use\ change} \times \boldsymbol{w}_{\ land\ use\ change}\right) + \left(HI_{\bar{x},\bar{z},land\ slide} \times \boldsymbol{w}_{land\ slide}\right) + \left(HI_{\bar{x},\bar{z},climate\ change\ to\ flood} \times \boldsymbol{w}_{climate\ chnage\ to\ flood}\right) + \left(HI_{\bar{x},\bar{z},climate\ change\ to\ landslide} \times \boldsymbol{w}_{climate\ chnage\ to\ landslide}\right) \quad (4\text{-}28)$$

Where $HI_{\bar{x},\bar{z},flood}$ ($\bar{x}$ = 1, 2,…..,$\overline{xx}$; $\bar{z} = 1, 2, \ldots\ldots, \overline{zz}$) is a value of hazard index from flood hazard map, $HI_{\bar{x},\bar{z},land\ use\ change}$, $HI_{\bar{x},\bar{z},land\ slide}$, $HI_{\bar{x},\bar{z},climate\ change\ to\ flood}$, $HI_{\bar{x},\bar{z},climate\ change\ to\ landslide}$ is a value of hazard index from land use change, land slide, climate change to flood and climate change to landslide hazard map, respectively. $\bar{x}$ is a vertical coordination grid in map and $\bar{y}$ is a horizontal coordination grid in map. Every hazard maps (flood, landslide, and so on) have an equal number of grid in horizontal and vertical. $\overline{xx}$ is number of grid in vertical and $\overline{zz}$ is number of grid in horizontal from hazard map. For the classification of integrated hazard maps, we apply natural break method from section 4.6.2 for the classification because the method can determine the best arrangement of value into different classes. Integrated hazard map was classified to four hazard areas corresponding to low (0-0.21), medium (0.22-0.43), high (0.44-0.68)

and very high hazard (0.69-1.0) areas.

4.9 Risk assessment

In this study, the term "risk" means the cost damage from the hazards by the land use categories. The land use categories consist of urban, agricultural, paddy field, forest and river areas. As there are more consistent available data for the first three areas than for the last two, this study will mainly focus on urban, agricultural and paddy field areas. Price of agricultural and paddy field data were collected by the Ministry of Agriculture and Forestry of Laos (Ministry of agriculture and Forestry, 2018) (Figure 3-5 and 3-6). The damage costs in agricultural and paddy areas are shown by Equation (4-29). In addition, the damage costs in urban areas are defined in Equation (4-30); the equation to estimate the value of the house content (HC) was proposed by Nural (2018) and defined in Equation (4-30 and 4-31).

$$DC_x = hazard\ index * price * \frac{production}{area} \quad (4\text{-}29)$$

$$DC_{urban} = hazard\ index * HC \quad (4\text{-}30)$$

$$HC = (0.06GDP - 9.53Pop + 2663) * 1{,}000{,}000 \quad (4\text{-}31)$$

Where DC_x damage cost in x area (USD/km^2), x is either agricultural or paddy field, DC_{urban} damage cost in an urban area (USD/km^2), HC asset value of house content (USD/km^2), GDP total gross domestic product in billions USD (GDP of Lao PDR is 18. 13 billion USD), and Pop population in millions (population of Lao PDR is 7.06 million), both of GDP and population data were retrieved from World bank(2017).

4.10 Cost-benefit analysis

The costs benefits analysis is widely adopts methods as a decision making tool in order to find the adaptation measures to tackle with environmental problems in practical works.

$$TB = \sum_{i=1}^{T} \frac{Benefit}{(1+r)^i} \quad (4\text{-}32)$$

$$TC = \sum_{i=1}^{T} \frac{Costs\ of\ adaptation\ measure}{(1+r)^i} \quad (4\text{-}33)$$

where T = the period over the project is analyzed (year) and r = the discount rate, for the discount rate central bank of Lao PDR (2018) suggested the rate of discount in Lao PDR around 0.05 to 0.1 . TB means the total benefits from the project from start of project until end (USD), $benefit$ the project benefit per year (USD/year) while TC is the total costs of project (USD), $Costs\ of\ adaptation\ measure$ is cost for adaptation per year (USD/year). The ratio of costs and benefits (B/C) can be computed from by TB over TC as shown in Equation (4-34)

$$B/C = \frac{TB}{TC} \quad (4\text{-}34)$$

The results of B/C can summary as bellow

B/C < 1	B/C = 1	B/C > 1
In economic terms, the costs exceed the benefits. Solely on this criterion, the project should not proceed.	Costs equal the benefits, which means the project should be allowed to proceed, but with little viability.	The benefits exceed the costs, and the project should be allowed to proceed.

4.11 Inverse Weight Distance

Inverse Weight Distance (IDW) is deterministic spatial interpolation method based on the assumption that interpolating should be influenced most by the nearby points and less by more the distance increase.

$$Z_p = \frac{\sum_{ib=1}^{M}(\frac{Z_{ib}}{d_{ib}^{pw}})}{\sum_{ib=1}^{M}(\frac{1}{d_{ib}^{pw}})} \quad (4\text{-}35)$$

Where Z_p is estimation value for location p, points surrounding p location, Z_{ib}, ib = 1,2,…, M are value at sample point, M is the number of sample points, d_{ib}, ib = 1,2,…, M are the Euclidean distance between estimated location to sample location, and exponent pw is the power or distant exponent power. In this study, ArcGIS program was used for IDW interpolation. We use the optimize setup from ArcGIS for exponent power (pw=2) and the number of sample points M is depend on how many sample points are located in radius of 5 km around location p

4.12 Log Pearson type III

The Log Pearson type III (LP3) distribution is statistical technique and widely used for evaluate the frequency distribution it is similar to normal distribution, when the skewness is small, the LP3 distribution can approximates as normal distribution. The LP3 was recommended by the U.S Water Resource Council (WRC) in 1976 as the based method of flood frequency analysis

$$F_{Tr,Cs} = \bar{F} + K_{Tr,Cs} S_F \quad (4\text{-}36)$$

$$Cs = \frac{f \sum_{ic=1}^{f} (F_{ic} - \bar{F})^3}{(f-1)(f-2)(S_F)^3} \quad (4\text{-}37)$$

Where, $F_{Tr,Cs}$ is the logarithm of input data at return period (recurrence interval in years) Tr (year), $\bar{F}$ is an average of input data logarithms (m/d), $K_{Tr,Cs}$ is a function of the skew coefficient (Cs) and return period Tr from table 4-7, F_{ic} (ic =1, 2, 3…., f) is logarithm of input data f is the number of input data and S_F is standard deviation of input data

Table 4-7 Frequency Factors K for Gamma and log-Pearson Type III Distributions (Haan, 1977)

	Recurrence Interval In Years (Tr)							
	1.0101	2	5	10	25	50	100	200
SKEW COEFFICIENT	Percent Chance (>=) = 1-F							
Cs	99	50	20	10	4	2	1	0.5
3	-0.667	-0.396	0.42	1.18	2.278	3.152	4.051	4.97
2.9	-0.69	-0.39	0.44	1.195	2.277	3.134	4.013	4.904
2.8	-0.714	-0.384	0.46	1.21	2.275	3.114	3.973	4.847
2.7	-0.74	-0.376	0.479	1.224	2.272	3.093	3.932	4.783
2.6	-0.769	-0.368	0.499	1.238	2.267	3.071	3.889	4.718
2.5	-0.799	-0.36	0.518	1.25	2.262	3.048	3.845	4.652
2.4	-0.832	-0.351	0.537	1.262	2.256	3.023	3.8	4.584
2.3	-0.867	-0.341	0.555	1.274	2.248	2.997	3.753	4.515
2.2	-0.905	-0.33	0.574	1.284	2.24	2.97	3.705	4.444
2.1	-0.946	-0.319	0.592	1.294	2.23	2.942	3.656	4.372
2	-0.99	-0.307	0.609	1.302	2.219	2.912	3.605	4.298
1.9	-1.037	-0.294	0.627	1.31	2.207	2.881	3.553	4.223
1.8	-1.087	-0.282	0.643	1.318	2.193	2.848	3.499	4.147
1.7	-1.14	-0.268	0.66	1.324	2.179	2.815	3.444	4.069
1.6	-1.197	-0.254	0.675	1.329	2.163	2.78	3.388	3.99
1.5	-1.256	-0.24	0.69	1.333	2.146	2.743	3.33	3.91
1.4	-1.318	-0.225	0.705	1.337	2.128	2.706	3.271	3.828
1.3	-1.383	-0.21	0.719	1.339	2.108	2.666	3.211	3.745
1.2	-1.449	-0.195	0.732	1.34	2.087	2.626	3.149	3.661
1.1	-1.518	-0.18	0.745	1.341	2.066	2.585	3.087	3.575
1	-1.588	-0.164	0.758	1.34	2.043	2.542	3.022	3.489
0.9	-1.66	-0.148	0.769	1.339	2.018	2.498	2.957	3.401
0.8	-1.733	-0.132	0.78	1.336	1.993	2.453	2.891	3.312
0.7	-1.806	-0.116	0.79	1.333	1.967	2.407	2.824	3.223
0.6	-1.88	-0.099	0.8	1.328	1.939	2.359	2.755	3.132
0.5	-1.955	-0.083	0.808	1.323	1.91	2.311	2.686	3.041
0.4	-2.029	-0.066	0.816	1.317	1.88	2.261	2.615	2.949
0.3	-2.104	-0.05	0.824	1.309	1.849	2.211	2.544	2.856

Table 4-7 Frequency Factors K for Gamma and log-Pearson Type III Distributions (Haan, 1977)

	Recurrence Interval In Years							
Weighted SKEW COEFFICIENT	1.0101	2	5	10	25	50	100	200
	Percent Chance (>=) = 1-F							
Cw	99	50	20	10	4	2	1	0.5
0.2	-2.178	-0.033	0.83	1.301	1.818	2.159	2.472	2.763
0.1	-2.252	-0.017	0.836	1.292	1.785	2.107	2.4	2.67
0	-2.326	0	0.842	1.282	1.751	2.054	2.326	2.576
-0.1	-2.4	0.017	0.846	1.27	1.716	2	2.252	2.482
-0.2	-2.472	0.033	0.85	1.258	1.68	1.945	2.178	2.388
-0.3	-2.544	0.05	0.853	1.245	1.643	1.89	2.104	2.294
-0.4	-2.615	0.066	0.855	1.231	1.606	1.834	2.029	2.201
-0.5	-2.686	0.083	0.856	1.216	1.567	1.777	1.955	2.108
-0.6	-2.755	0.099	0.857	1.2	1.528	1.72	1.88	2.016
-0.7	-2.824	0.116	0.857	1.183	1.488	1.663	1.806	1.926
-0.8	-2.891	0.132	0.856	1.166	1.448	1.606	1.733	1.837
-0.9	-2.957	0.148	0.854	1.147	1.407	1.549	1.66	1.749
-1	-3.022	0.164	0.852	1.128	1.366	1.492	1.588	1.664
-1.1	-3.087	0.18	0.848	1.107	1.324	1.435	1.518	1.581
-1.2	-3.149	0.195	0.844	1.086	1.282	1.379	1.449	1.501
-1.3	-3.211	0.21	0.838	1.064	1.24	1.324	1.383	1.424
-1.4	-3.271	0.225	0.832	1.041	1.198	1.27	1.318	1.351
-1.5	-3.33	0.24	0.825	1.018	1.157	1.217	1.256	1.282
-1.6	-3.88	0.254	0.817	0.994	1.116	1.166	1.197	1.216
-1.7	-3.444	0.268	0.808	0.97	1.075	1.116	1.14	1.155
-1.8	-3.499	0.282	0.799	0.945	1.035	1.069	1.087	1.097
-1.9	-3.553	0.294	0.788	0.92	0.996	1.023	1.037	1.044
-2	-3.605	0.307	0.777	0.895	0.959	0.98	0.99	0.995
-2.1	-3.656	0.319	0.765	0.869	0.923	0.939	0.946	0.949
-2.2	-3.705	0.33	0.752	0.844	0.888	0.9	0.905	0.907
-2.3	-3.753	0.341	0.739	0.819	0.855	0.864	0.867	0.869

Table 4-7 Frequency Factors K for Gamma and log-Pearson Type III Distributions (Haan, 1977)

	Recurrence Interval In Years							
Weighted SKEW COEFFICIENT	1.0101	2	5	10	25	50	100	200
	Percent Chance (>=) = 1-F							
Cw	99	50	20	10	4	2	1	0.5
-2.4	-3.8	0.351	0.725	0.795	0.823	0.83	0.832	0.833
-2.5	-3.845	0.36	0.711	0.711	0.793	0.798	0.799	0.8
-2.6	-3.899	0.368	0.696	0.747	0.764	0.768	0.769	0.769
-2.7	-3.932	0.376	0.681	0.724	0.738	0.74	0.74	0.741
-2.8	-3.973	0.384	0.666	0.702	0.712	0.714	0.714	0.714
-2.9	-4.013	0.39	0.651	0.681	0.683	0.689	0.69	0.69
-3	-4.051	0.396	0.636	0.66	0.666	0.666	0.667	0.667
-2.4	-3.8	0.351	0.725	0.795	0.823	0.83	0.832	0.833
-2.5	-3.845	0.36	0.711	0.711	0.793	0.798	0.799	0.8
-2.6	-3.899	0.368	0.696	0.747	0.764	0.768	0.769	0.769
-2.7	-3.932	0.376	0.681	0.724	0.738	0.74	0.74	0.741
-2.8	-3.973	0.384	0.666	0.702	0.712	0.714	0.714	0.714
-2.9	-4.013	0.39	0.651	0.681	0.683	0.689	0.69	0.69
-3	-4.051	0.396	0.636	0.66	0.666	0.666	0.667	0.667

4.13 Model performance indicator

The performance of model was determined using two commonly statistical performance measure, first is coefficient of determination R^2 and second is Nash-Sutcliffe efficiency E (Nash and Sutcliffe, 1970)

Coefficient of determination R^2

$$R^2 = \left(\frac{\sum_{ia=1}^{nn}(O_{ia}-\bar{O})(y_{ia}-\bar{y})}{\sqrt{\sum_{ia=1}^{nn}(O_i-\bar{O})^2}\sqrt{\sum_{ia=1}^{nn}(y_{ia}-\bar{y})^2}} \right)^2 \quad (4.38)$$

Where, O_{ia} (ia = 1, 2,…., nn) is iath observed data for the element being evaluated $\bar{O}$ is the mean value of observed data and y_{ia} is iath simulated data for the element being evaluated, $\bar{y}$ is the mean value of simulated data, nn is number of evaluated data. R^2 can also be expressed as the square ratio between the covariance and the multiplied standard deviations of the observed and predicted values. Therefore, it estimates the combined dispersion against the single dispersion of the observed and predicted values. The ranges of R^2 lies between 0 and 1 which described how much of the observed dispersion is explained by the prediction. A value of zero means no correlation at all, where a value of 1 means that the dispersion of the prediction is equal to that of the observation

Nash-Sutcliffe efficiency E

The efficiency E is defined as one minus the sum of the absolute squared differences between the predicted and observed value normalized by the variance of the observed value.

$$E = 1 - \frac{\sum_{ia=1}^{nn}(O_{ia}-\bar{y})^2}{\sum_{ia=1}^{nn}(O_{ia}-\bar{O})^2} \quad (4.39)$$

The range of E lies between one and -∞. An efficiency of lower than zero indicated that the mean value of the observed time series would have been a better predictor than the model.

CHAPTER 5: ASSESSMENT OF INDIVIDUAL MAP AND INTEGRATED HAZARD MAPS

5.1 Introduction

Floods are among the most dangerous natural hazards. Flooding can happen anywhere, and sometimes, it is unavoidable. The economy, people's livelihood and the infrastructure of many countries around the world have been affected by flooding (Golian et al., 2010). Lao PDR suffers from flooding every year. Lao PDR is a developing country located in Southeast Asia. The country's people depend heavily on agriculture and natural resources for their livelihood. Currently, the water supply system in the country is not well distributed, particularly in rural areas. Therefore, most people living in rural areas are resettled downstream of dams and irrigation areas(Baird and Shoemaker, 2007). Changes in land use, such as decreases in forest density, can lead to increases in flood magnitude (Jongman et al., 2012; Winsemius et al., 2016). In recent years, many researchers have conducted global studies on the impact of climate change on the water cycle and its effect on people's livelihood (Adeloye et al., 2013; Parmesan and Yohe, 2003b; Westra et al., 2014). However, there have been only a few assessments and analyses for predictions on the country's environmental impacts when considering possible climate changes. According to the Intergovernmental Panel on Climate Change (IPCC) report, Southeast Asia will suffer from increasing flood frequency in the future (IPCC, 2007). General Circulation Models (GCMs) have been developed to study future climate scenarios and the associated impacts, and they help support strategies and

mitigation plans to address the effect of climate change. Lao PDR is a developing country where many ethnic groups live in mountainous areas (Laos national report, 2012). Heavy rainfall in mountainous areas can lead to floods and landslides. These can cause a significant threat to human life and the economy.

The effects of hazards on an area could be in either a single or multiple forms. In the last decade, the uses of multi-hazard assessment focusing on all scales have been considered in several studies (Cutter et al., 2000; Marzocchi et al., 2012; Sendai Framework, 2015; Sullivan-Wiley and Short Gianotti, 2017). However, exhaustive data are required in most assessments. Recently, geographic information systems (GIS) have been used as a tool for such assessment. This is an effective tool for handling large amounts of spatial data, assimilating data from several sources and undertaking analyses (Fernández and Lutz, 2010; Kazakis et al., 2015). In contrast, the tool is ineffective in performing multi-criteria analyses, and hence, it is not appropriate for executive or managerial purposes. For multi-criteria supervision, a combination of GIS and multi-criteria decision analysis (MCDA) is essential. Many studies have indicated the applicability of GIS for MCDA flood hazard maps. One of the most common MCDA methods is the analytic hierarchy process. This approach is appropriate because it offers precise results, and it is used for studying hazards in several studies (Kazakis et al., 2015; Stefanidis and Stathis, 2013). In recent development, flow accumulation, slope, elevation, land use, and rainfall intensity have been used as GIS-based map information to map flood hazards using AHP and GIS (Gigović et al., 2017).

5.2 Results

5.2.1 Flood hazard map

A distributed hydrological model was used to simulate a flood hazard map for whole country. We considered the greatest water depth in every grid cell, which was determined by contributing factors during the simulation, and these included the 100-year return periods of rainfall, land types, soil hydrologic characteristics, and elevation. The results are shown in Figure 5-1, where we can see the potential flood hazard area. The results reveal that low hazard areas cover 78.44 % of the total area, medium hazard areas cover 12.64 %, and high and very high hazard areas respectively cover 6.14 % and 2.78 %. Even though the high and very high hazard percentages are low, we still must pay attention to land use types in those areas. Total high hazard areas can be divided into 89.32 % forest, 7.18 % agricultural, 3.34 % paddy field and 0.15 % urban. Total very high hazard areas can be divided into 90.51 % forest, 7.23 % agricultural, 2 % paddy field and 0.25 % urban. In addition, most of the hazard areas are distributed around the northern and southern part, especially in agricultural area. These areas are very important to both the country and villagers because most rural areas are dependent on agricultural products as a main source of income.

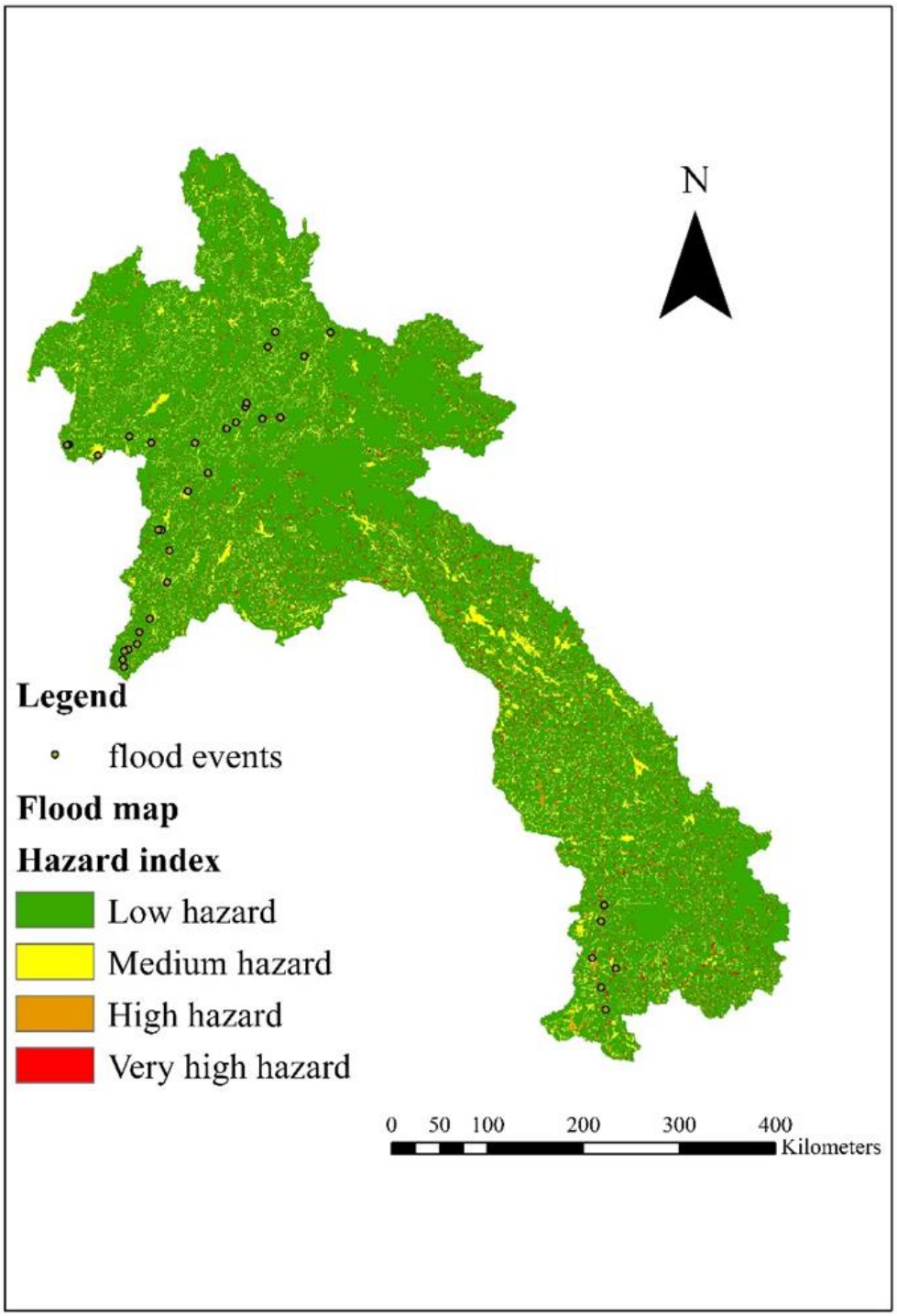

Figure 5-1 Flood hazard map and flood historical events

5.2.2 Landslide hazard map

According to the results as shown in Figure 5-2 most of the hazard area are illustrated around the central to southern part of Laos, in addition from the records of landslide events in Laos shown those landslide phenomenon events are closely related to the probability of exceeding values of rainfall. From the results reveals that low hazard area covers 92.67%, medium hazard area covers 1.83%, high hazard area covers 1.21% and very high hazard area cover 4.28% of total area. We can divide high and very high hazard area according to the land use types; for 94.01% of high hazard total area is located in forest, 4.21% located in agriculture area, 1.4% located in paddy field area and 0.17% is located in urban area. 95.76% of very high hazard area is located in forest, 3.12% located in agriculture, 0.95 % located in paddy field and only 0.16% located in urban area. Among the various type of land use cover, forest area covers a large portion of land slide affected areas. 14.86 % of total agricultural areas are located in high and very hazard area. For paddy field cover, 9.72% of total paddy field areas are located in high and very high hazard area. Both of agricultural and paddy field area are very important for ethic group who live in mountainous areas, Mostly of high and very high hazard area are near mountainous area witch explain the higher change of landslide compare to other area and most of those areas are located in around central and southern part of Laos.

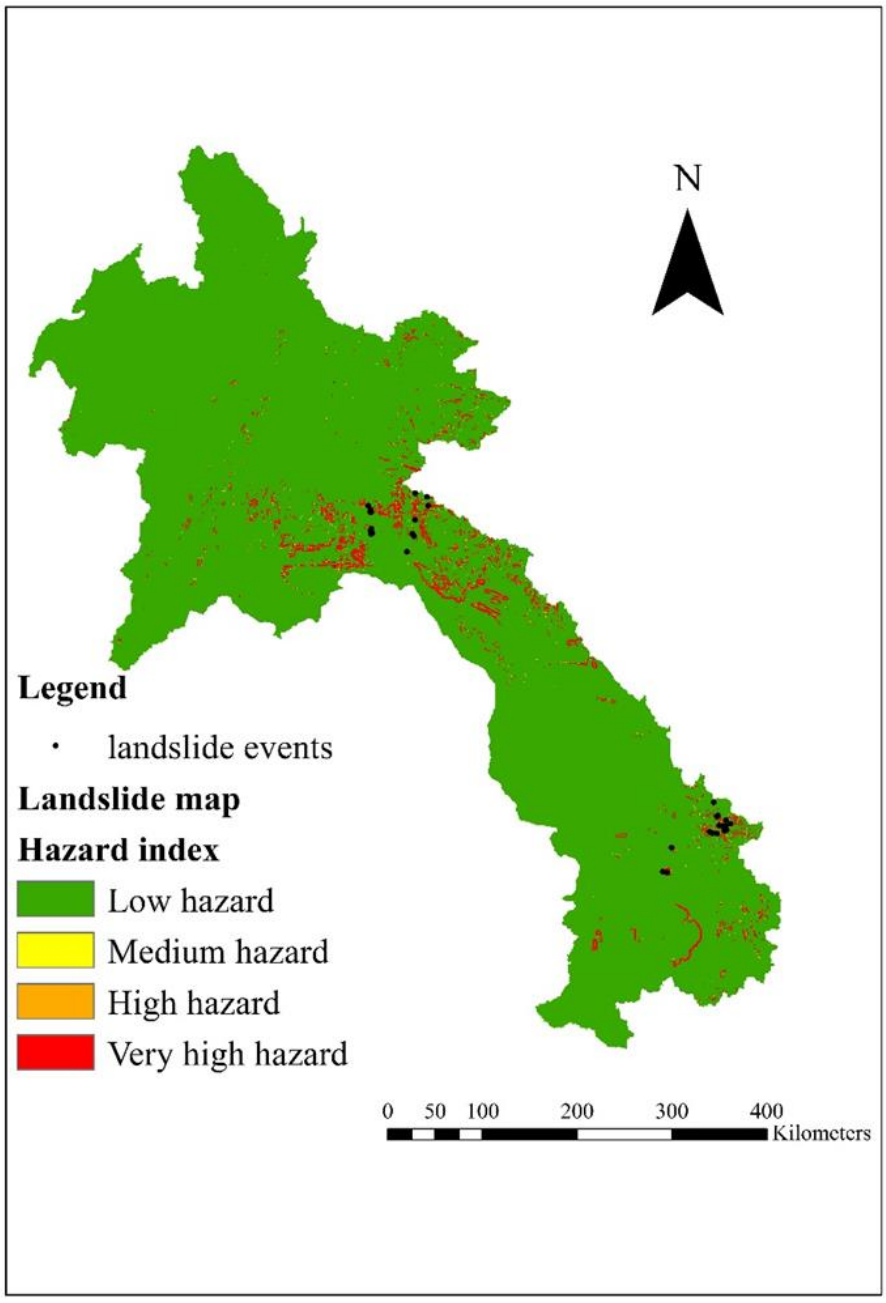

Figure 5-2 Landslide hazard map and landslide historical events

5.2.3 Land use change hazard map

The results in Figure 5-3 shows the overall impact of the hazard areas, which are growing significantly; this is mostly because of the loss of forest area that slows the rainfall runoff. Without forest area, all rainfall runoff runs directly downstream without storage or other factors to slow it down. Therefore, the hazard areas downstream are expanding. The total area of land use change impact to flood be divided into 77.08 %, 12.68 %, 6.94 % and 3.3 % of low, medium, high and very high hazard areas, respectively. High and very high hazard areas can be further divided: 89.66 % of high areas are in the forest, 8.27 % are in agricultural areas, 1.92 located in paddy field area and 0.15 % are in urban areas. We found that 90.51 % of very high hazard areas are in forests, 8.12 % are in agricultural areas, 1.12 % are in paddy field area and 0.25 % are in an urban area. Based on the results, 3 % of total urban areas located in high hazard area and 2.04 % of total urban areas located in very high hazard area. In addition, we analyzed the increase of total hazard index between flood and land use change hazard map to identify the sensitivity of the area to land use change in 3 different regional areas namely, northern area, central area, and southern area. The average of hazard index in the northern, central and southern region are 0.12, 0.16, and 0.13 respectively.

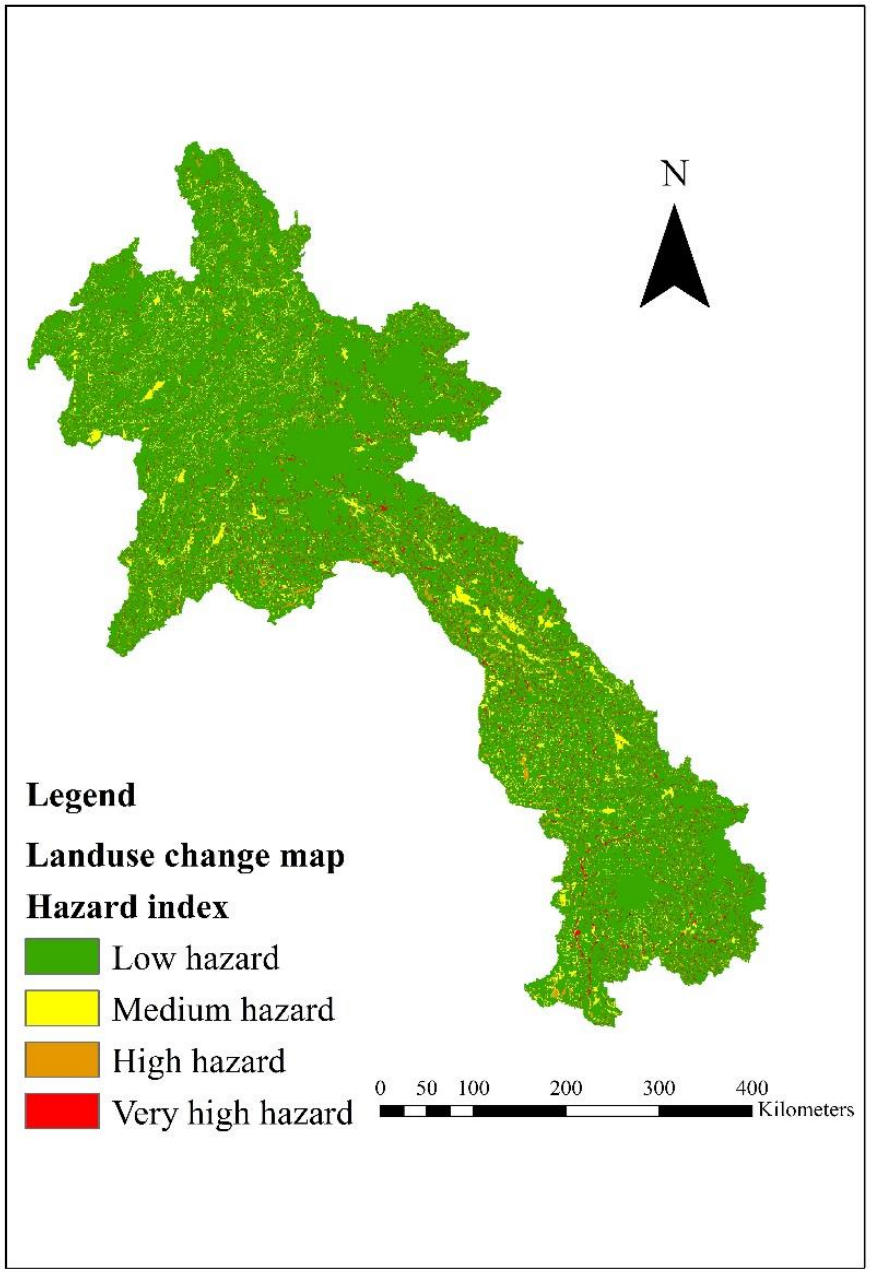

Figure 5-3 Land use change hazard map

5.2.4 Climate change hazard map

5.2.4.1 Climate change impact to flood map

Developing countries in tropical regions are highly susceptible to floods. These regions already have high levels of precipitation, and the hydrologic cycle is significantly interlinked and sensitive to the weather. Future scenarios of flood hazard map for near and far future under three scenarios is shown in Figure (5-4). Percentage of very high hazard areas for near future increased from 3.71% under RCP 2.6 to 4.05% in RCP 8.5 scenario; additionally, for far future percentage of very high hazard areas increased from 4 % under scenario of RCP 2.6 to 4.88 % of RCP 8.5 (Figure 5-5). In the climate change hazard map with respect to the change in the flood hazard map, under all scenarios, the maximum high hazard areas were 0.33% in urban, 88.77% in forest 2% in paddy field area and 9.0% in agricultural areas. It was also seen that the very high hazard areas represented 0.35, 90.09, 1.8 and 7.77% of urban, forest, paddy field and agricultural areas, respectively.

5.2.4.2 Climate change impact to landslide map

The future landslides under the three scenarios and two time periods were simulated (Figure 5-6). Percentage of very high hazard areas for near future increased from 3.71% under RCP 2.6 to 4.05% in RCP 8.5 scenario; additionally, for far future percentage of very high hazard areas increased from 4 % under scenario of RCP 2.6 to 4.88 % if RCP 8.5 (Figure 5-7). In the climate change hazard map with respect to the change in the landslide hazard map, under all scenarios, the maximum high hazard areas were 0.13%

in urban, 88.98% in forest 0.84% in paddy field area and 10.05% in agricultural areas. It was also seen that the very high hazard areas represented 0.15, 90.31, 0.77 and 8.77% of urban, forest, paddy field and agricultural areas, respectively.

Both of landslide and flood hazard areas increases with the increase of future scenarios. Among various land use cover, agricultural and paddy field affected areas are lower compare to forest area, but those areas are main source of income for people who live near mountainous area. Local authorities need to pay more attention to these areas.

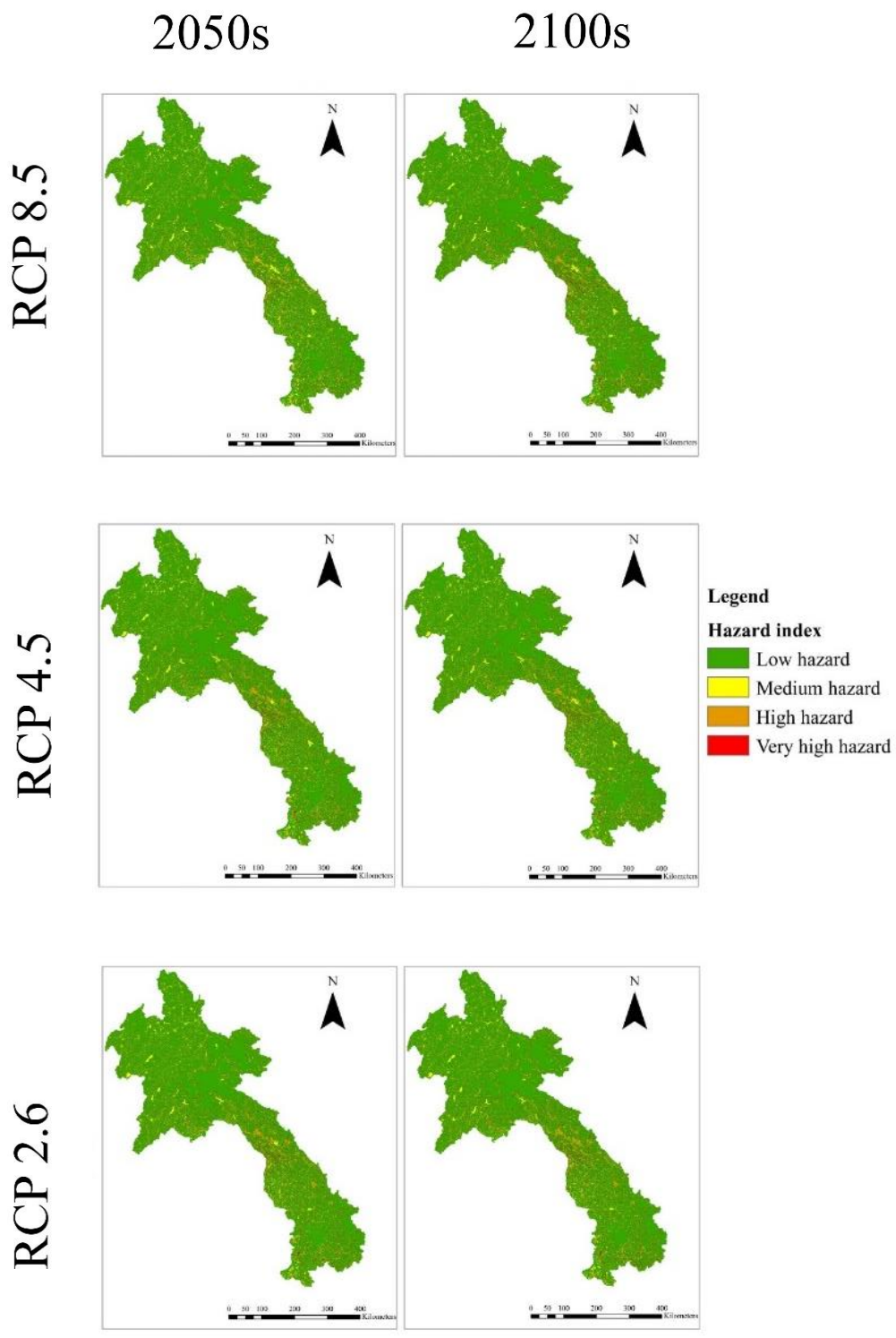

Figure 5-4 Flood hazard maps with the ensemble average of heavy rainfall from the 7 GCMs that used data under the RCP2.6, RCP4.5 and RCP8.5 scenarios

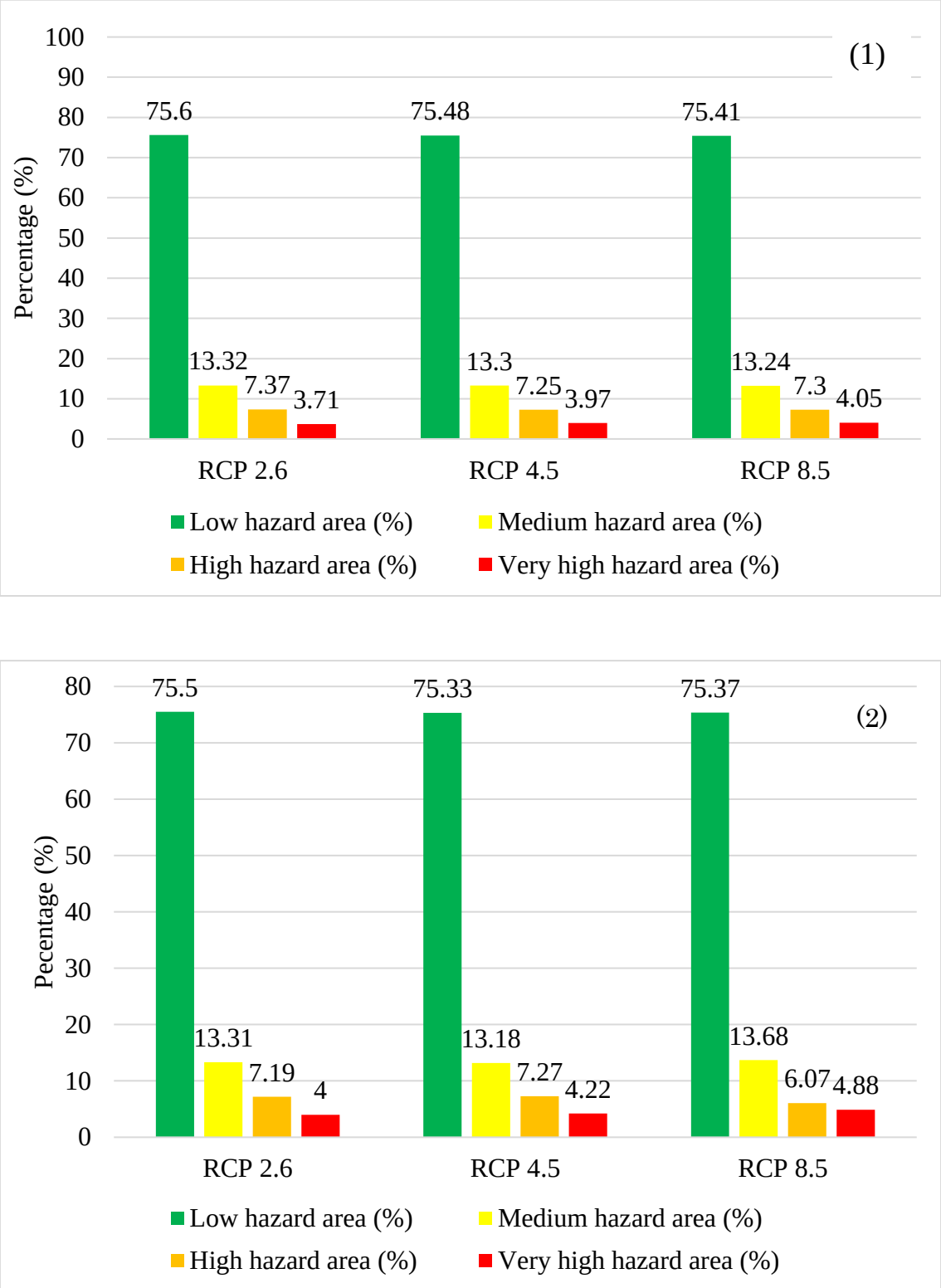

Figure 5-5 Percentage of flood hazard area in Lao PDR: (1) near future and (2) far future

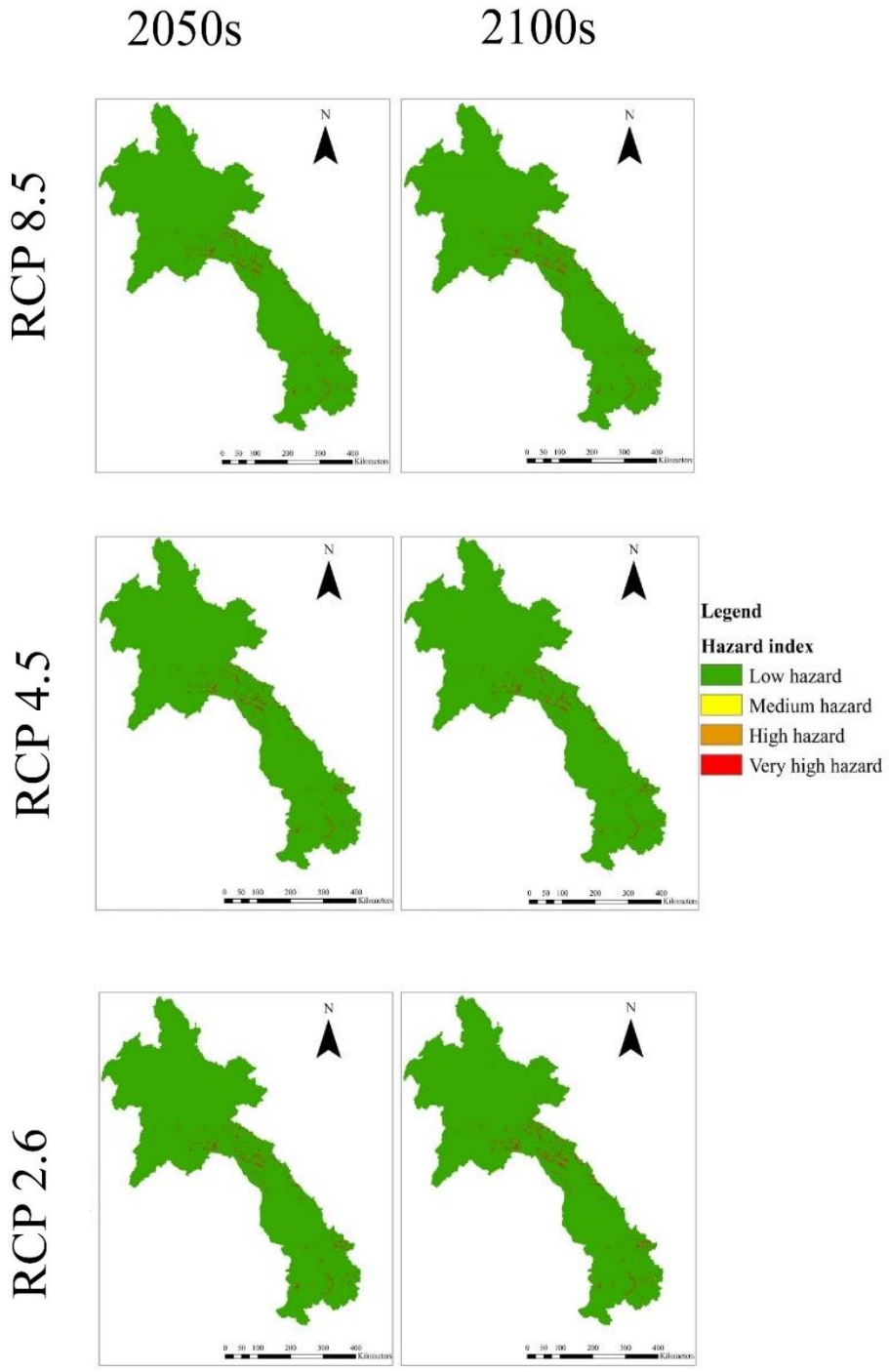

Figure 5-6 landslide hazard maps with the ensemble average of heavy rainfall from the 7 GCMs that used data under the RCP2.6, RCP4.5 and RCP8.5 scenarios

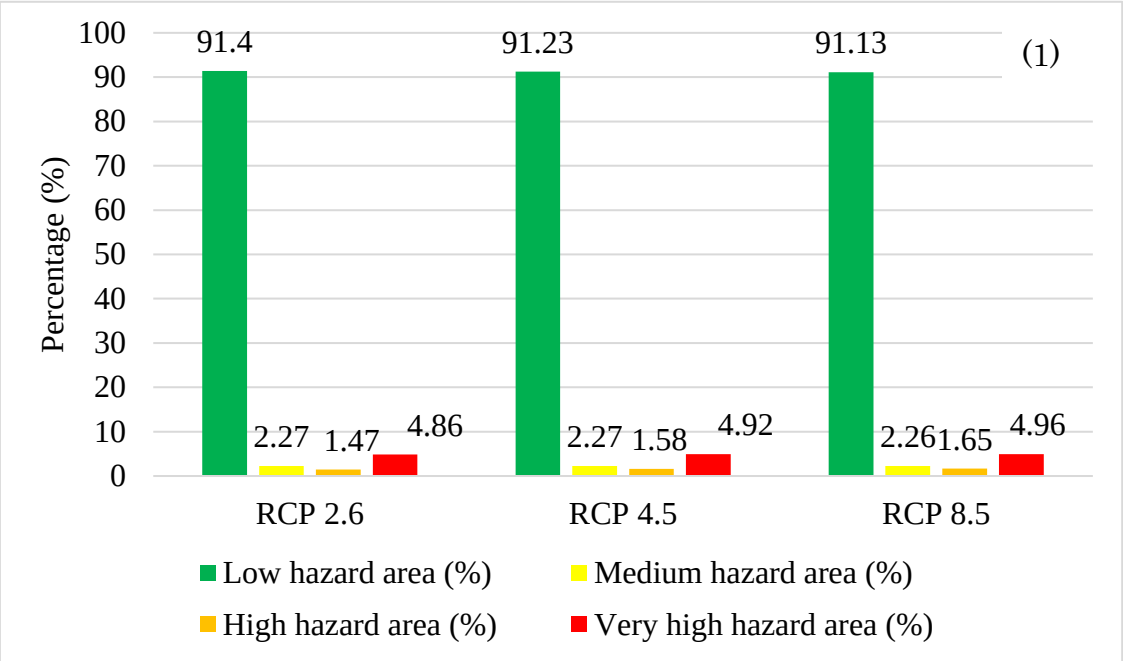

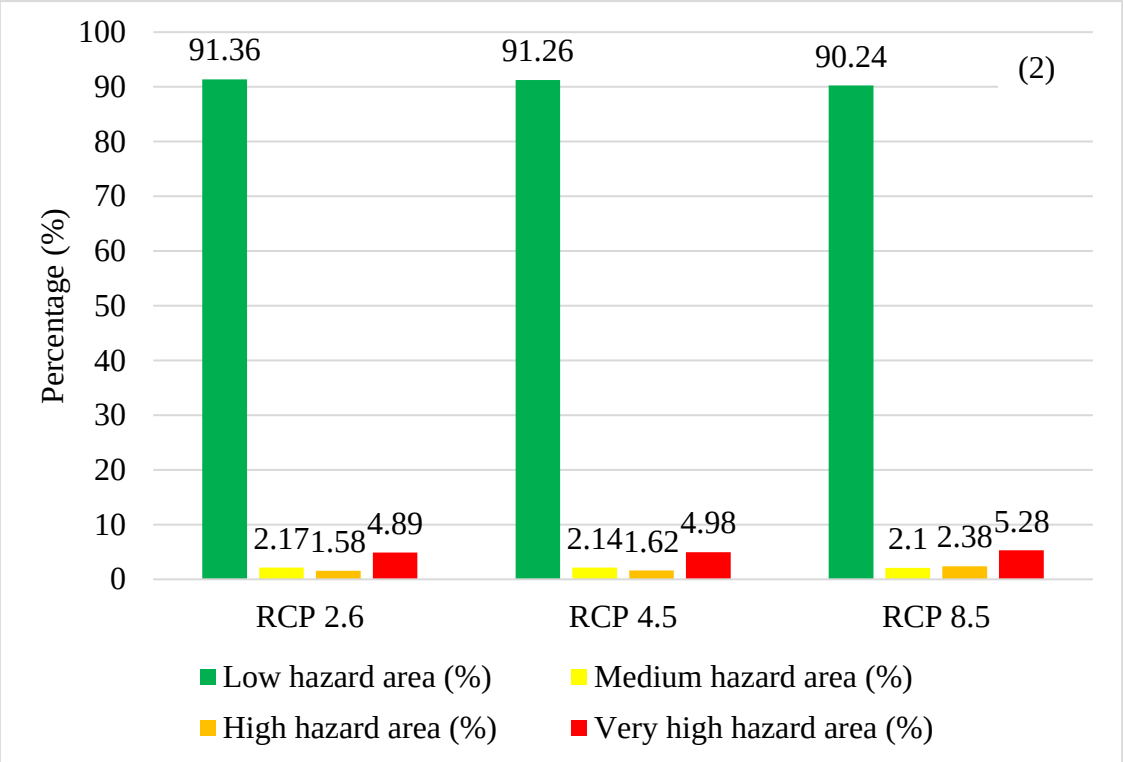

Figure 5-7 Percentage of landslide hazard area in Lao PDR: (1) near future and (2) far future

5.2.5 Integrated hazard map

The main objective of this chapter is to integrate five existing hazard maps (flood, land slide, land use change, climate change impact to flood map and climate change impact to landslide map). Phrakonkham (2019) have proposed AHP-based method for integrated multi-hazard map in Lao PDR namely flood, land use change and climate change leading to flood hazard map. Based on the results, AHP based integrated hazard map can shows potential hazard area in country scale. In this study, 6 integrated hazard maps under the 3 RCP scenarios (RCP2.6, RCP4.5 and RCP8.5) and the 2 time periods (near-future (2050s) and far-future (2100s)) were produced using the AHP method (Figure 5-8). The integrated hazard maps were categorized using the natural breaks method of classification (Tate et al., 2010). It was noticeable that the total amount of very high hazard areas increased in response to the RCP scenarios. In near future, very high hazard areas percentage increased from 3.20% under RCP 2.6 to 3.3% under RCP 8.5. Similar results are shown for far future, the high hazard area percentage increase from 3.23 under RCP 2.6 to 3.71 under RCP 8.5 as shown in Figure (5-9). The different land types under the integrated hazard maps were also analyzed. The results showed that the most affected land type is forest area (80 - 90%) followed by agricultural area (8 - 12%), and urban area (0.1 - 0.3%) was the least affected.

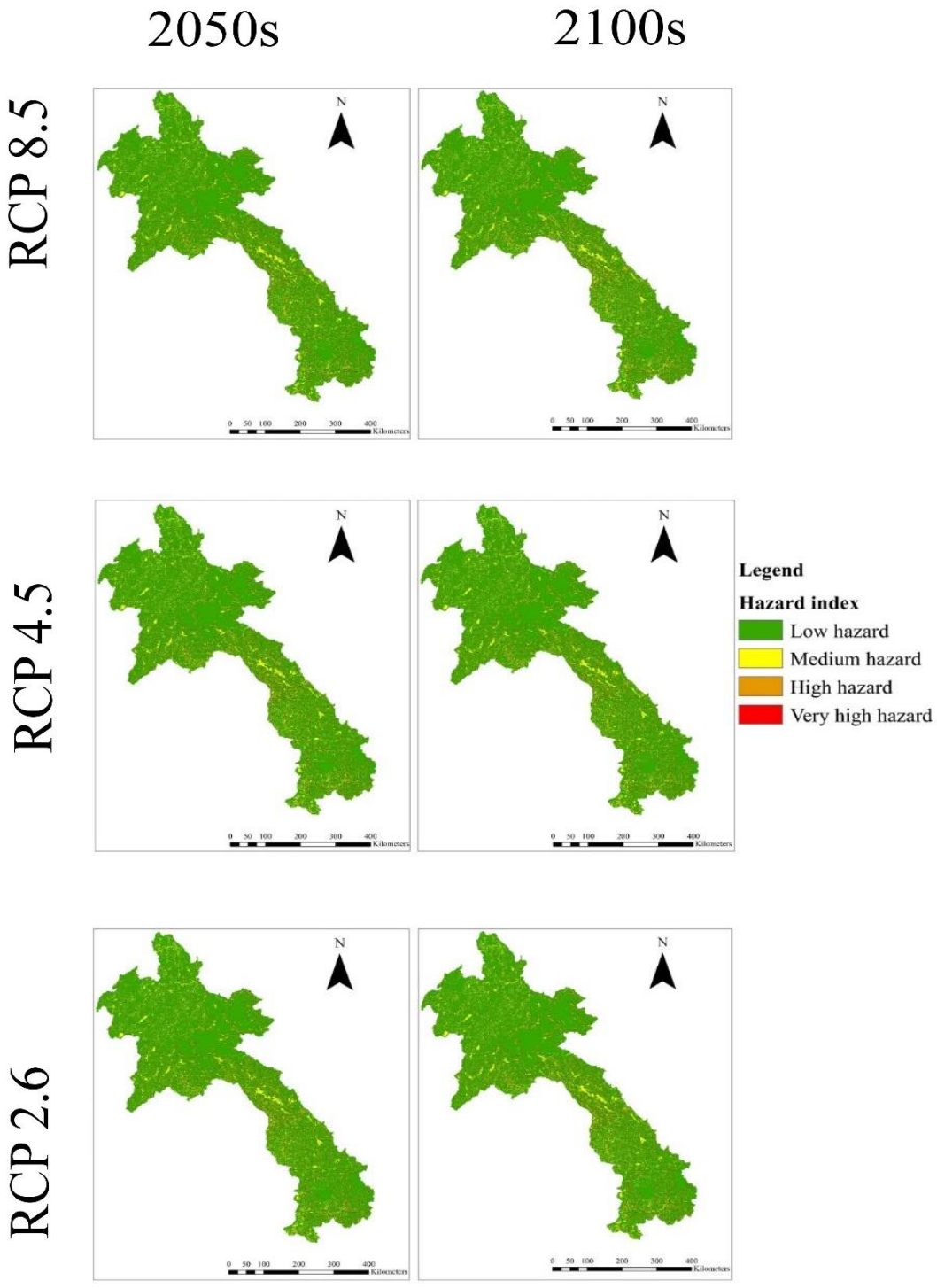

Figure 5-8 Integrated hazard maps with the ensemble average of heavy rainfall from the 7 GCMs that used data under the RCP2.6, RCP4.5 and RCP8.5 scenarios.

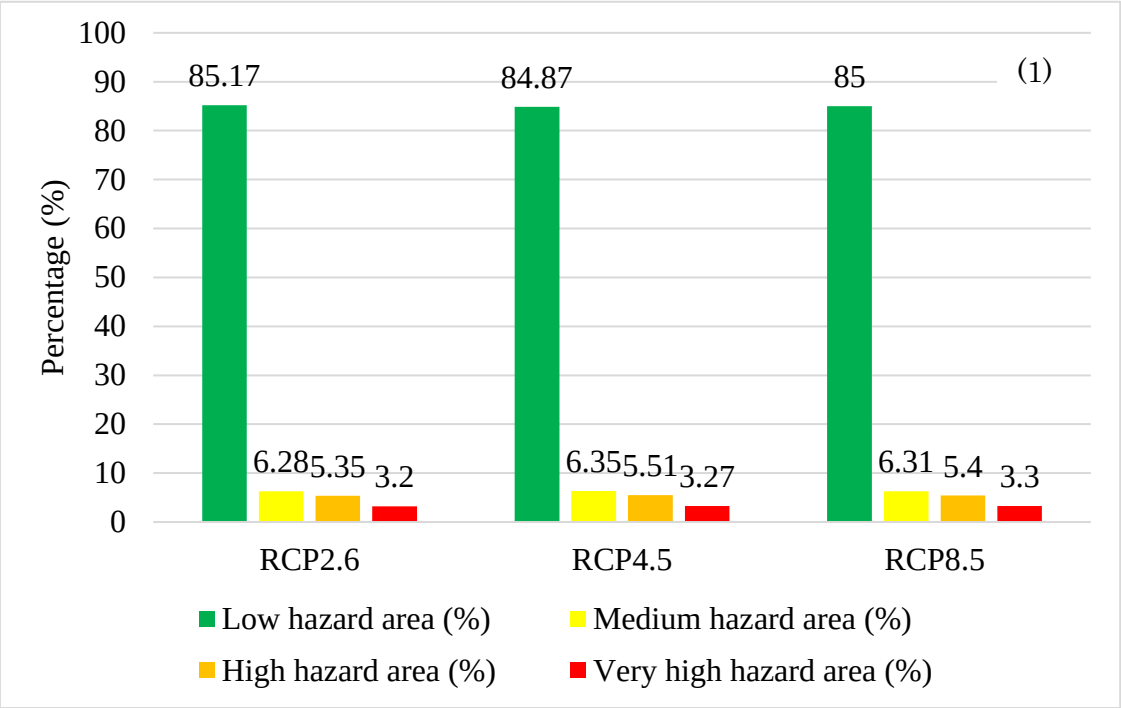

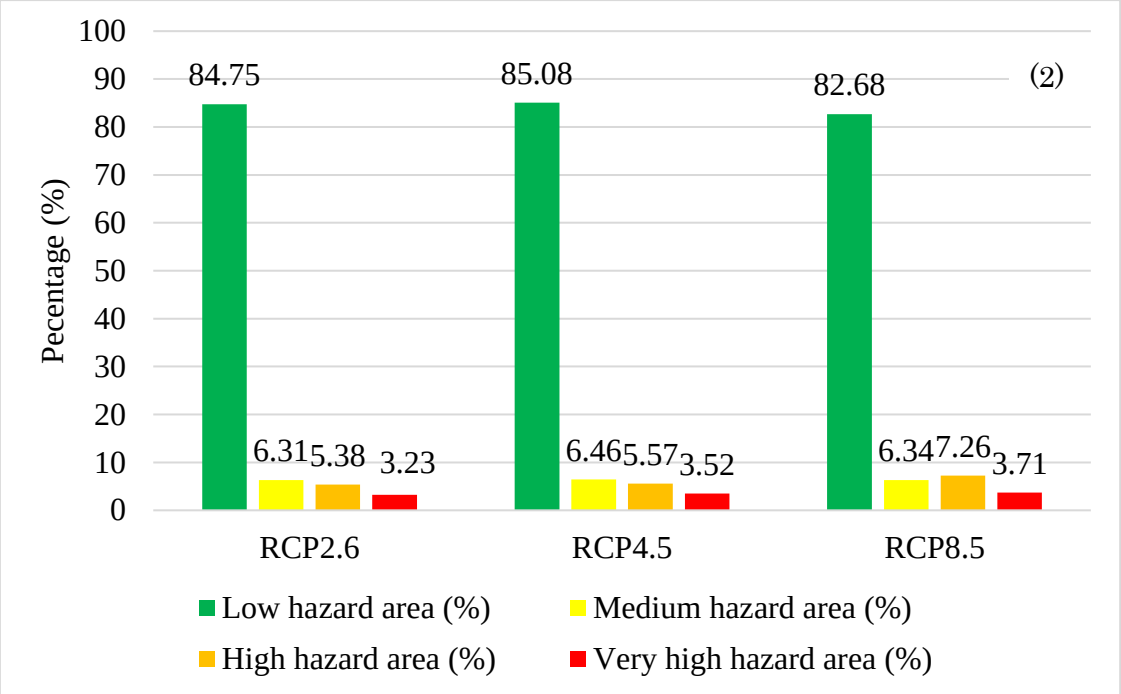

Figure 5-9 Percentage of integrated hazard area in Lao PDR: (1) near future and (2) far future

5.2.6 Validation

5.2.6.1 Flood hazard map

For validation of model, we compare discharge of simulation to observation discharge from 1 January to 31 December 2000. The performance of this model was determined using two commonly used statistical performance measures. The first is the coefficient of determination R^2, and the second is the *Nash-Sutcliffe efficiency* E, all the stations coefficients of 2000 are shown in Table 5-1. Overall, both of R^2 and E from every stations shows coefficient more than 0.6 to the observation data. Based on Moriasi D. N. et al (2007), they proposed a guideline for model evaluation. They specified that the model simulation could be classified as satisfactory and valid if the R^2 and E value are more than 0.6. Based on their guideline, the rainfall runoff model of this study can be classified as the satisfactory and the model is valid. We choose 3 station from northern region Ou river, central region Sane river and southern river Sedone river as example for comparison between the simulation and observation discharge data (Figure 5-10). 30 flood events determined by the United Nations Office for Disaster Risk Reduction (UNDRR, 2017) are used for comparison for the validation of a hazard map. Only events with a high depth of water and occurred by the extreme rainfall 100 year return period were chosen. In Figure 5-1, 4 events (13 %) are in small hazard areas (0-0.25), 9 events (30 %) are in the medium hazard areas (0.25-0.5), 7 events (23 %) are in high hazard areas (0.5-0.75), and 10 events (34 %) are in very high hazard areas (0.75-1.0). From these results, the relatively high consistency of the flood hazard map can be seen, because most of the flood events based on the historical data are in high to very high hazard areas. Hence, the reliability of the integrated hazard map is confirmed.

Table 5.1 Nash-Sutcliffe efficiency (E) and R^2 of all station in Laos from (Jan.1 to Dec31, 2000)

Station id	E	R^2	Station id	E	R^2
140501	0.81	0.82	**170207**	0.75	0.76
140504	0.83	0.87	**170404**	0.73	0.74
140505	0.66	0.72	**170501**	0.77	0.79
140506	0.74	0.77	**180203**	0.65	0.66
140507	0.7	0.72	**180205**	0.78	0.83
140705	0.85	0.89	**180206**	0.87	0.9
150504	0.9	0.95	**180207**	0.89	0.94
150506	0.84	0.88	**180213**	0.86	0.88
150508	0.76	0.81	**180303**	0.72	0.73
150602	0.73	0.74	**180306**	0.85	0.9
150607	0.79	0.8	**180307**	0.85	0.87
160405	0.81	0.83	**180308**	0.75	0.77
160504	0.74	0.77	**180501**	0.77	0.81
160505	0.8	0.81	**190101**	0.69	0.71
160507	0.76	0.78	**190103**	0.76	0.78
160508	0.74	0.77	**190205**	0.7	0.72
160601	0.87	0.9	**190301**	0.82	0.83
160602	0.82	0.86	**190302**	0.84	0.85
160603	0.88	0.9	**200101**	0.66	0.69
170203	0.78	0.8	**200204**	0.71	0.76

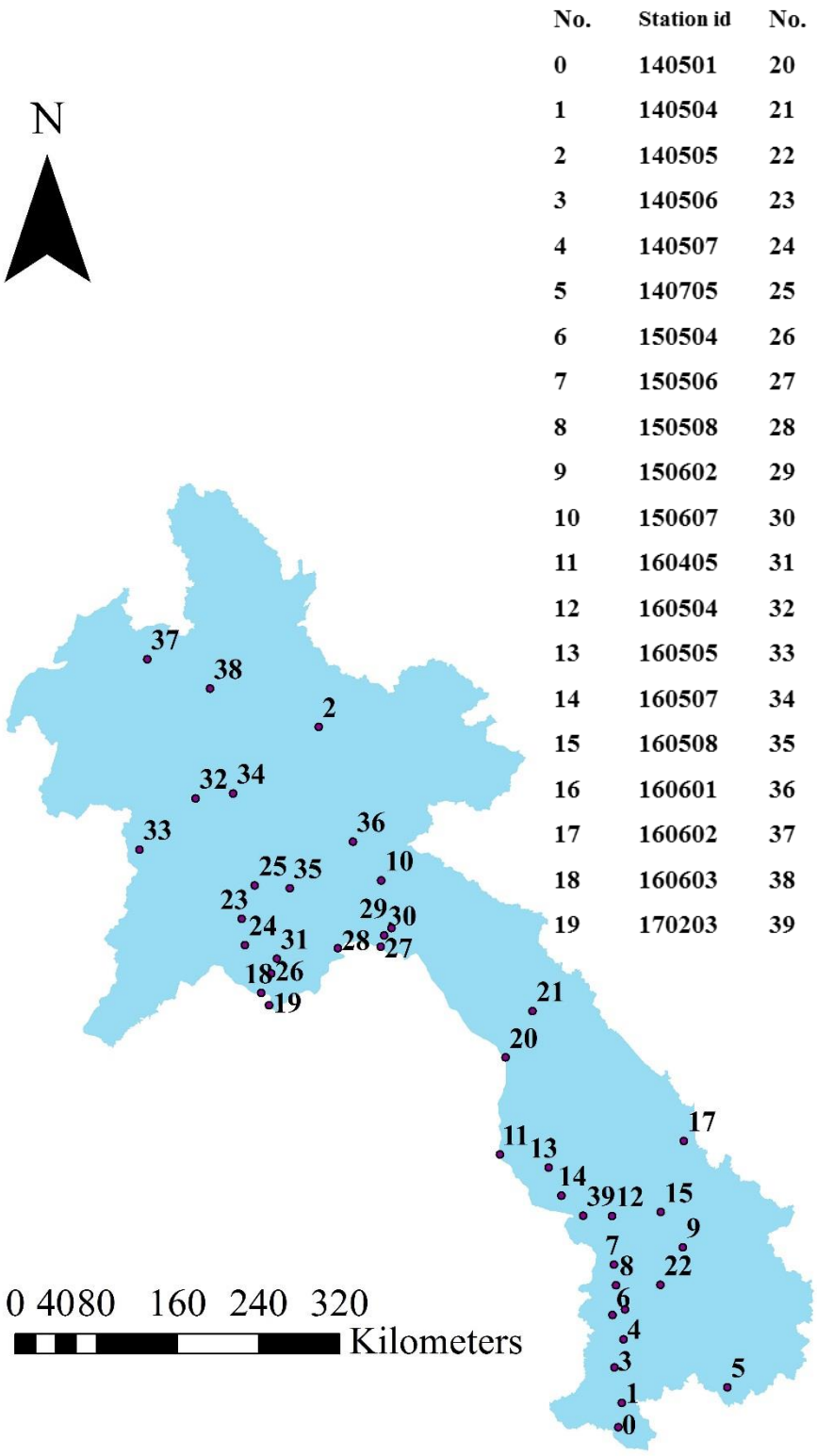

No.	Station id	No.	Station id
0	140501	20	170207
1	140504	21	170404
2	140505	22	170501
3	140506	23	180203
4	140507	24	180205
5	140705	25	180206
6	150504	26	180207
7	150506	27	180213
8	150508	28	180303
9	150602	29	180306
10	150607	30	180307
11	160405	31	180308
12	160504	32	180501
13	160505	33	190101
14	160507	34	190103
15	160508	35	190205
16	160601	36	190301
17	160602	37	190302
18	160603	38	200101
19	170203	39	200204

Figure 5-10 Rainfall station in Lao PDR

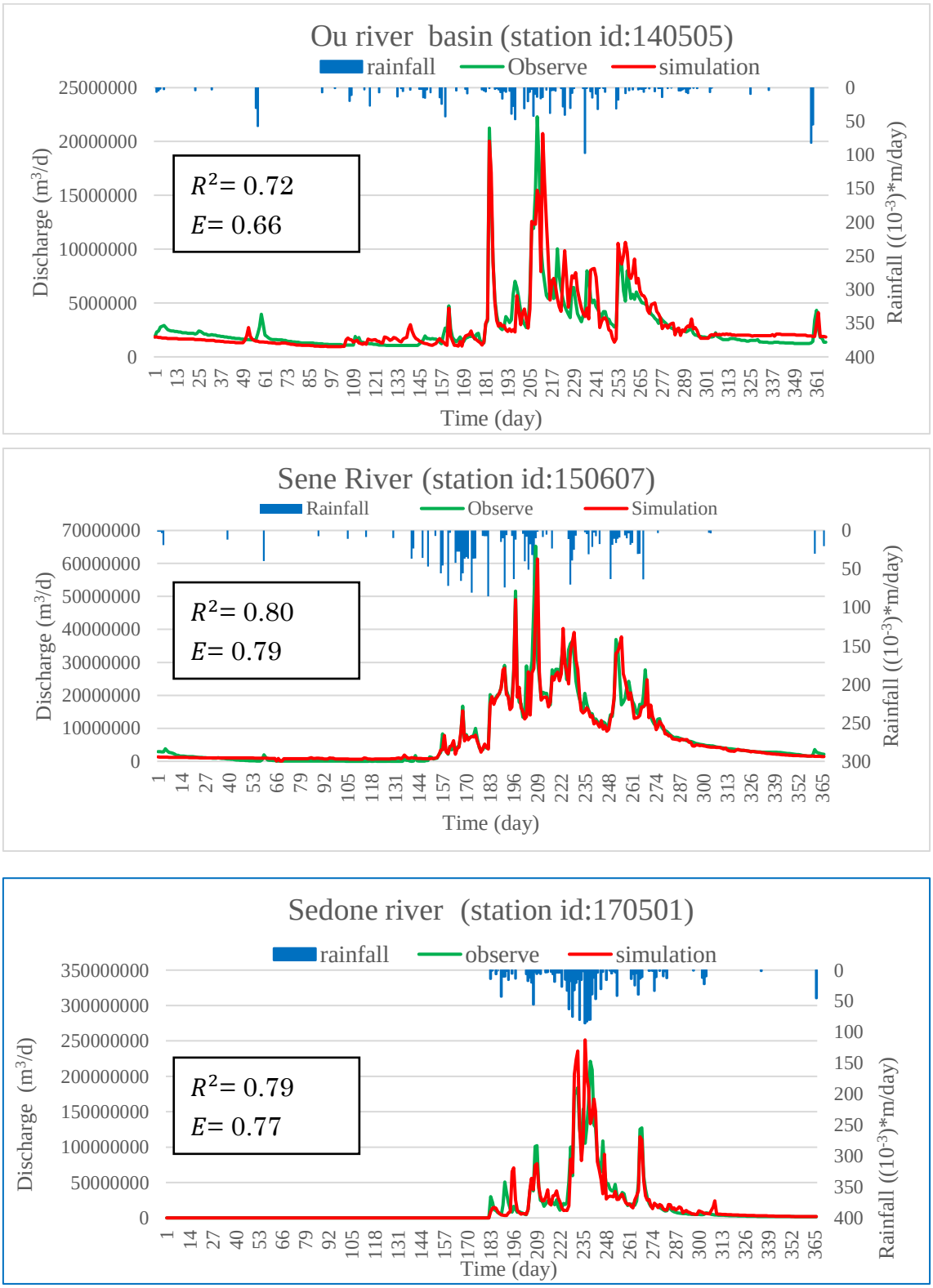

Figure 5-11 Comparison of observed and simulated discharges in 3 basins (Jan.1 to Dec.31, 2000).

Table 5-2 Comparison between flood hazard results with 100 years return period and historical flood events occurrence in Lao PDR

Hazard index	Longitude and Latitude	Dates	Kills	Injured	Missing
0.13	100.5, 19.67	20 July 1992	-	-	-
0.21	100.81, 19.58	23 Oct 1992	-	-	-
0.22	101.71, 19.26	15 Aug 1992	-	-	-
0.23	102.48, 20.63	1 Oct 1999	-	-	-
0.25	101.34, 19.71	11 Aug 1999	-	-	-
0.32	101.26, 17.93	14 Aug 2002	-	-	-
0.37	102.28, 20.1	22 Sep 1992	-	-	-
0.43	101.91, 19.44	26 Jun 2001	-	-	-
0.44	102.09, 19.86	27 Jun 2000	-	-	-
0.47	101.12, 17.6	29 Oct 1992	-	6	-
0.48	101.12, 17.75	5 Aug 2000	-	9	-
0.48	101.46, 18.89	4 Jun 2000	-	3	-
0.49	102.62, 19.97	25 July 1994	-	3	-
0.54	101.16, 17.77	10 Sep 2002	-	2	-
0.55	102.44, 19.96	5 Oct 1990	-	7	-
0.56	105.79, 15.24	12 Sep 2009	-	-	-
0.57	101.42, 18.9	23 Sep 2001	-	23	-
0.58	105.83, 14.41	22 Sep 2004	-	41	-
0.67	103.11, 20.78	5 Aug 2006	-	13	-
0.71	105.82, 15.39	3 Jun 1992	3	11	12
0.76	105.7, 14.9	16 July 1999	16	24	8
0.76	105.93, 14.8	16 Jun 2006	11	37	-
0.77	101.77, 19.72	21 Oct 1998	9	71	5
0.79	102.56, 20.78	25 Sep 1999	5	50	9
0.81	101.24, 17.82	4 Oct 2001	-	55	-
0.83	100.52, 19.68	13 July 1990	7	60	4
0.84	101.36, 18.06	23 Oct 1999	15	95	11
0.87	101.54, 18.7	3 Sep 1990	13	83	-
0.89	101.1, 17.67	17 Aug 1992	15	11	7
0.91	105.79, 14.62	6 July 1992	19	91	11

5.2.6.2 Landslide hazard map

The landslide hazard map was validated from comparison of landslide hazard map result with historical landslide events in Lao PDR, witch those events occurred with the extreme rainfall of 100 year return period. Around 33 landslide events (Figure 5-3) were used to compare with the landslide hazard map result, from the results 22 events (66.67%) were located in very high hazard area, 8 events (24.24%) located in high hazard area and 3 events (9.09%) were located in low hazard area. the land slide hazard map by our simulation corresponds to the country's historical events of landslide. These results confirm that the probability of landslide model and landslide hazard map can predict occurrence of landslide in Lao PDR.

Table 5-3 Comparison between land slide hazard results with 100 years return period and historical land slide events occurrence in Lao PDR

Hazard index	Longitude and Latitude	Dates	Kills	Injured	Missing
0.15	104.01, 19.22	5 Oct 1994	-	1	-
0.16	107.13, 16.06	1 Sep 1990	-	4	-
0.19	103.56, 19.06	1 Oct 1990	-	6	-
0.21	107.09, 16.00	27 Aug 1990	-	6	-
0.24	103.99, 18.81	3 Jun 1993	-	-	-
0.25	106.93, 15.98	17 Oct 1994	-	3	-
0.25	103.54, 19.10	11 Oct 1999	-	5	-
0.54	107.09, 16.10	7 Jun 1992	-	1	-
0.61	103.56, 18.86	26 July 1998	-	4	-
0.67	106.55, 15.84	14 Sep 1992	-	-	-
0.75	107.00, 15.97	14 Aug 1990	-	10	-
0.75	107.01, 16.14	29 Sep 1990	-	9	-
0.76	103.56, 18.82	19 Sep 1991	-	2	-
0.79	107.08, 16.04	30 Aug 1991	-	10	-

Hazard index	Longitude and Latitude	Dates	Kills	Injured	Missing
0.79	103.98, 18.83	15 July 1998	-	8	-
0.81	106.46, 15.61	25 Jun 1996	-	1-	-
0.82	103.58, 18.83	14 Aug 1996	-	4	-
0.83	107.08, 16.03	20 July 1996	-	4	-
0.84	106.99, 16.13	10 Jun 1999	7	2	5
0.88	107.07, 15.99	7 July 1995	8	11	5
0.89	106.96, 15.97	8 July 1995	6	9	4
0.89	107.06, 16.03	27 Aug 1994	6	8	2
0.93	104.00, 18.96	28 Sep 1997	9	8	3
0.94	107.02, 16.04	30 July 1993	7	-	9
0.94	103.92, 18.66	5 Jun 1999	1	11	4
0.94	104.14, 19.10	12 Aug 1995	1	9	9
0.94	103.57, 18.88	20 Aug 1990	9	5	4
0.94	103.56, 19.04	14 Oct 1990	1	3	1
0.96	107.06, 16.04	27 Jun 1997	1	4	-
0.98	106.97, 16.27	9 Sep 2000	1	1	3
0.98	103.57, 19.04	17 Sep 1992	7	6	4
0.99	106.51, 15.60	10 Jun 1994	5	13	3

5.2.6.3 Integrated hazard map

To validate the performance of integrated hazard maps, 30 flood historical events and 33 landslide historical events were compared to the integrated hazard maps (Figure 5-12). According to the results, for flood historical events 2 events (7%) located in low hazard area, 3 events (10%) located in medium hazard area, 14 (46%) events located in high hazard area and 11 (37%) events located in very high hazard areas; for land slide historical events 7 (21%) events located in low hazard area, 8 (24%) events located in medium hazard area, 11 (33%) events located in high hazard area and 7 (21%) events located in very high hazard area. The majority of landslide (54%) and flood (83%)

historical events were located in high and very high hazard areas. Hence, the reliability of the integrated hazard map was confirmed.

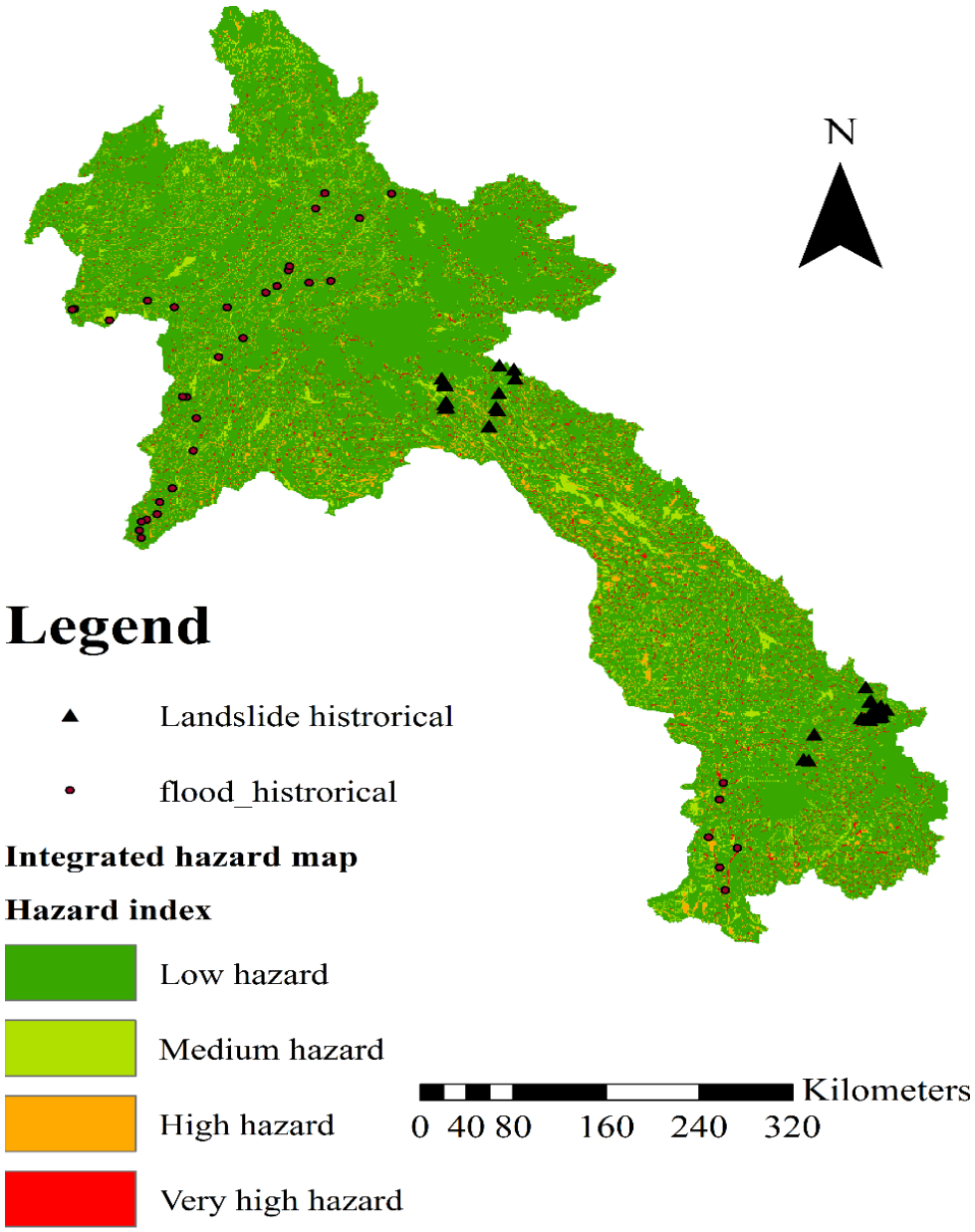

Figure 5-12 Comparison of flood and land slide historical event to integrated hazard map of scenario RCP 2.6 time period of near future

5.3 Discussion

Flood hazard map have illustrated distribution of hazard area across the study area. It is noticeable that most of distribution of hazard area were located in central and southern region of Lao PDR. Vientiane capital city is located in central region, little of area in Vientiane capital area impact by flood hazard. Based on the results, high hazard area is visible around central-southern region of Lao PDR. High and very high hazard areas in each province were divided by whole country area and their percentage of hazard areas were shows in Table 5-4. The percentage of high hazard areas in Bolikhamxai (0.73%), Khaommouan (0.87%) and Savannakhet (0.92%) province have higher percentage than other province. For very high hazard areas, Bolihamxai (0.27%), Savannakhet (0.27%) and Vientiane province (0.26%) have highest percentage of very high hazard areas. For the capital of Lao PDR, only 0.08 % of total high hazard areas and 0.04% of total very high hazard areas are located in Vientiane capital and Vientiane capital have the lowest percentage of total high and very high hazard among all the provinces. Champasak is one of the big province and developed area of Lao PDR. According to the flood historical events map from Figure 5-1, Champasak is one of the province that suffer from many flood historical events. Around 0.45% of total high hazard area and 0.18% of total very high hazard areas are located in Champasak province. Compare to Vientiane capital, Champasak have higher of both high and very high hazard areas.

Table 5-4 Percentage of high and very high hazard area from flood hazard map in each province

Province name	High hazard (percentage per whole country)	Very high hazard (percentage per whole country)
Attapeu	0.25%	0.19%
Bokeo	0.13%	0.06%
Bolikhamxai	0.73%	0.27%
Champasak	0.45%	0.18%
Houaphan	0.21%	0.20%
Khammouan	0.87%	0.24%
Louang Namtha	0.14%	0.07%
Louang Prabang	0.51%	0.17%
Oudomxai	0.22%	0.11%
Phongsaly	0.25%	0.14%
Salavan	0.16%	0.16%
Savannakhet	0.92%	0.27%
Vientiane	0.59%	0.26%
Vientiane Capital City	0.08%	0.04%
Xaignabouly	0.37%	0.16%
Xekong	0.12%	0.12%
Xiangkouang	0.14%	0.15%
Total percentage of high/very high hazard area across the country	6.14 %	2.78%

Land slide hazard map shown the distribution of potential hazard area from land slide around mountainous of central and southern region. According to the results, most of the land slide hazard area are located in forest area, second is agricultural and third is paddy field. Most of agricultural and paddy field areas are belong to ethic group who have livelihood near mountainous area. Lao PDR, many Ethic group who live in mountainous area and their source of income are mainly from production of agricultural. Compare to other provinces of Lao PDR, Vientiane, Xiangkoung, Blolikhamxai and Vientiane have high mountainous area. According to Table 5-5, Bolikhamxai have highest percentage of high hazard area (0.48%). For very high hazard area Bolikhamxai province have the highest percentage of the very hazard area (2.31%). Based on landslide historical events from Figure 5-2, Xiangkoung, Bolikhamxai and Vientiane are three provinces that several landslide occurred. Percentage of high hazard area in Xiangkoung (0.35%), Bolikhamxai (0.48%) and Vientiane (0.21%) are noticeable higher than other province. Similarly to the percentage of very high hazard area, Xiengkoung have around 0.6% of very high hazard area, Bolikhamxai have around 2.31% and Vientiane have 0.92% of very high hazard area. These provinces should be given priority for developing mitigation and countermeasure. Most of these province's mountainous area is a livelihood of ethic group people. Therefore, most of landslide hazard occurred in these area will have direct impact to agricultural and properties of ethic group people.

Table 5-5 Percentage of high and very high hazard area from landslide hazard map in each province

Province name	High hazard (percentage per whole country)	Very high hazard (percentage per whole country)
Attapeu	0.05%	0.10%
Bokeo	0.00%	0.00%
Bolikhamxai	0.48%	2.31%
Champasak	0.02%	0.07%
Houaphan	0.02%	0.01%
Khammouan	0.05%	0.18%
Louang Namtha	0.00%	0.00%
Louang Prabang	0.00%	0.00%
Oudomxai	0.00%	0.00%
Phongsaly	0.00%	0.00%
Salavan	0.01%	0.02%
Savannakhet	0.00%	0.00%
Vientiane	0.21%	0.92%
Vientiane Capital City	0.00%	0.00%
Xaignabouly	0.00%	0.00%
Xekong	0.02%	0.06%
Xiangkouang	0.35%	0.60%
Total percentage of high/very high hazard area across the country	1.21%	4.28%

Land use change hazard map illustrated similar of distribution to flood hazard map but with higher magnitude. Overall, the high hazard area and very high hazard area are increase when compare land use change hazard map to the flood hazard map (Table 5-6 and Table 5-7). The high hazard areas of land use change hazard map are increase around 13% and very high hazard area increase around 19% when compare to high and very high hazard area of current flood hazard map. Similarly to flood hazard map, Savannakhet province have the highest percentage of high (0.96%) and very high hazard area (0.3%). However compare to the flood hazard map, high and very high hazard area of Savannakhet province slightly increased. Champasak province have slightly increase in high hazard and very high hazard area when compare to current flood hazard area. The high hazard areas increase around 10% and very high hazard area increase around 17% due to impact from land use change. Vientiane capital's area got more impact compare to Champasak province. The very high hazard area in Vientiane capital increase around 82% and high hazard area increase to 60%. It is indicate that Vientiane capital is high influent by land use change more than Champasak province. It is indicate that land use change have a significant influence magnitude of flooding area. the results correspond to Huntington (2006) who found that land use change from human alterations such as conversion of forest area to agricultural or expand of urban area will lead to increase of flood hazard area.

Table 5-6 Percentage of high area from land use change impact to flood hazard map in each province and percentage of increase from current flood hazard map

Province name	High hazard (percentage area per whole country)	Percentage increase from current flood hazard map
Attapeu	0.30%	19%
Bokeo	0.18%	35%
Bolikhamxai	0.78%	6%
Champasak	0.50%	10%
Houaphan	0.25%	23%
Khammouan	0.92%	5%
Louang Namtha	0.19%	33%
Louang Prabang	0.56%	9%
Oudomxai	0.27%	22%
Phongsaly	0.30%	19%
Salavan	0.21%	30%
Savannakhet	0.96%	5%
Vientiane	0.64%	8%
Vientiane Capital City	0.12%	60%
Xaignabouly	0.42%	13%
Xekong	0.17%	39%
Xiangkouang	0.19%	33%
Total percentage of high hazard area across the country	6.94%	

Table 5-7 Percentage of very high area from land use change impact to flood hazard map in each province and percentage of increase from current flood hazard map

Province name	Very high hazard (percentage area per whole country)	Increase from current flood hazard map
Attapeu	0.22%	16%
Bokeo	0.09%	50%
Bolikhamxai	0.30%	11%
Champasak	0.21%	17%
Houaphan	0.23%	16%
Khammouan	0.27%	13%
Louang Namtha	0.10%	45%
Louang Prabang	0.20%	18%
Oudomxai	0.14%	27%
Phongsaly	0.17%	22%
Salavan	0.19%	19%
Savannakhet	0.30%	12%
Vientiane	0.29%	12%
Vientiane Capital City	0.07%	82%
Xaignabouly	0.19%	19%
Xekong	0.15%	25%
Xiangkouang	0.18%	21%
Total percentage of very high hazard area across the country	3.30%	

Climate change impacts to flood hazard maps are represented by the flood hazard map under future climate condition with 3 scenario (RCP2.6, 4.5 and 8.5) and 2 time periods (near future and far future). The flood hazard area under influences of the future rainfall condition shows the increase of hazard area across the country. By considering the near future period, the total percentage of very high hazard areas increases from 3.71% under the scenario of RCP 2.6 to 3.97% under the scenario of RCP 4.5. Luang Namtha province has the highest increase (23%) of very high hazard areas when comparing the flood hazard map under scenario RCP 2.6 to that under RCP 4.5 (Table 5-8). Under the scenario of RCP 8.5 the total percentage of very high hazard areas increases to 4.02%. Figure 5-13 (e) shows the area of the hazard index increase when comparing the scenario of RCP 8.5 and RCP 4.5. Among others, Bolikhamxai province has the highest increase (5%) of very high hazard areas when comparing the flood hazard map under scenario RCP4.5 and RCP8.5 (Table 5-9). Many provinces from climate change impacts to flood hazard map with near future have continuously increase of very high hazard area from RCP 2.6 to RCP 8.5. The very high hazard area in Bolikhamxai province increase around 6% comparing the very high hazard area under the scenario RCP 2.6 to that under RCP 4.5 and the very high hazard area in Bolikhamxai increase around 5% comparing the very high hazard area under the scenario RCP 4.5 to that under RCP 8.5. For the far future period, the total percentage of very high hazard area increases from 4% under the scenario of RCP 2.6 to 4.22% under the scenario of RCP 4.5. Figure 5-14 (d) shows the area of the hazard index increase when comparing the scenario of RCP 4.5 and RCP 2.6. Savannakhet province has the highest increase (9%) of very high hazard areas when comparing the flood hazard map under the scenario of RCP 2.6 and RCP 4.5 (Table 5-10). Under the scenario of RCP 8.5 the total very high hazard area from climate change impact

to flood hazard map is 4.88%. Figure 5-14 (e) shows the area of the hazard index increase when comparing the scenario of RCP 8.5 and RCP 4.5. Savannakhet province has the highest increase (26%) of very high hazard area when comparing the flood hazard map under the scenario of RCP 4.5 and RCP 8.5 (Table 5-11). The very high hazard area in most of the provinces from climate change impacts to flood hazard map with far future increase continually from RCP 2.6 to RCP 8.5 such as Khammouan province. The very high hazard area in Khammouan province increase around 7% comparing the very high hazard area under the scenario RCP 2.6 to that under RCP 4.5 and the very high hazard area in Bolikhamxai province increase around 19% comparing the very high hazard area under the scenario RCP 4.5 to that under RCP 8.5. Based on the results, the significantly increase in flood hazard area for all RCP scenarios is observed. In addition, the comparison between the future rainfall projection under scenario of RCP 2.6, 4.5 and 8.5 are presented in Figure 5-14 and 5-16 for near and far future respectively. Figure 5-14 (d) shows the increase of rainfall when comparing the results from future rainfall projections to those obtained by RCP 2.6 and 4.5. The results show that the rainfall increases across the country, particularly in the Southern region e.g. Savannakhet province. The areas affected by the increase of rainfall intensity and increase of very high hazard area from RCP 2.6 to RCP 4.5 are more or less on the size. Figure 5-14 (e) shows the increase of rainfall between RCP 4.5 and 8.5. It is noticed that the high increase of rainfall occurs around Khammouane province. That is, it matches with the increase of very high hazard area from flood hazard area under RCP 4.5 and 8.5. For far future, Figure 5-16 (d) and Figure 5-14 (e) show the increase of rainfall when comparing the results from future rainfall projections to those of RCP 4.5 to RCP 2.6 and RCP 8.5 to 4.5. In all, the amount of rainfall increases, particularly in Khammouan, Bolikhamxai and Attapeu province is

in line with the results in Table 5.10 and Table 5.11.

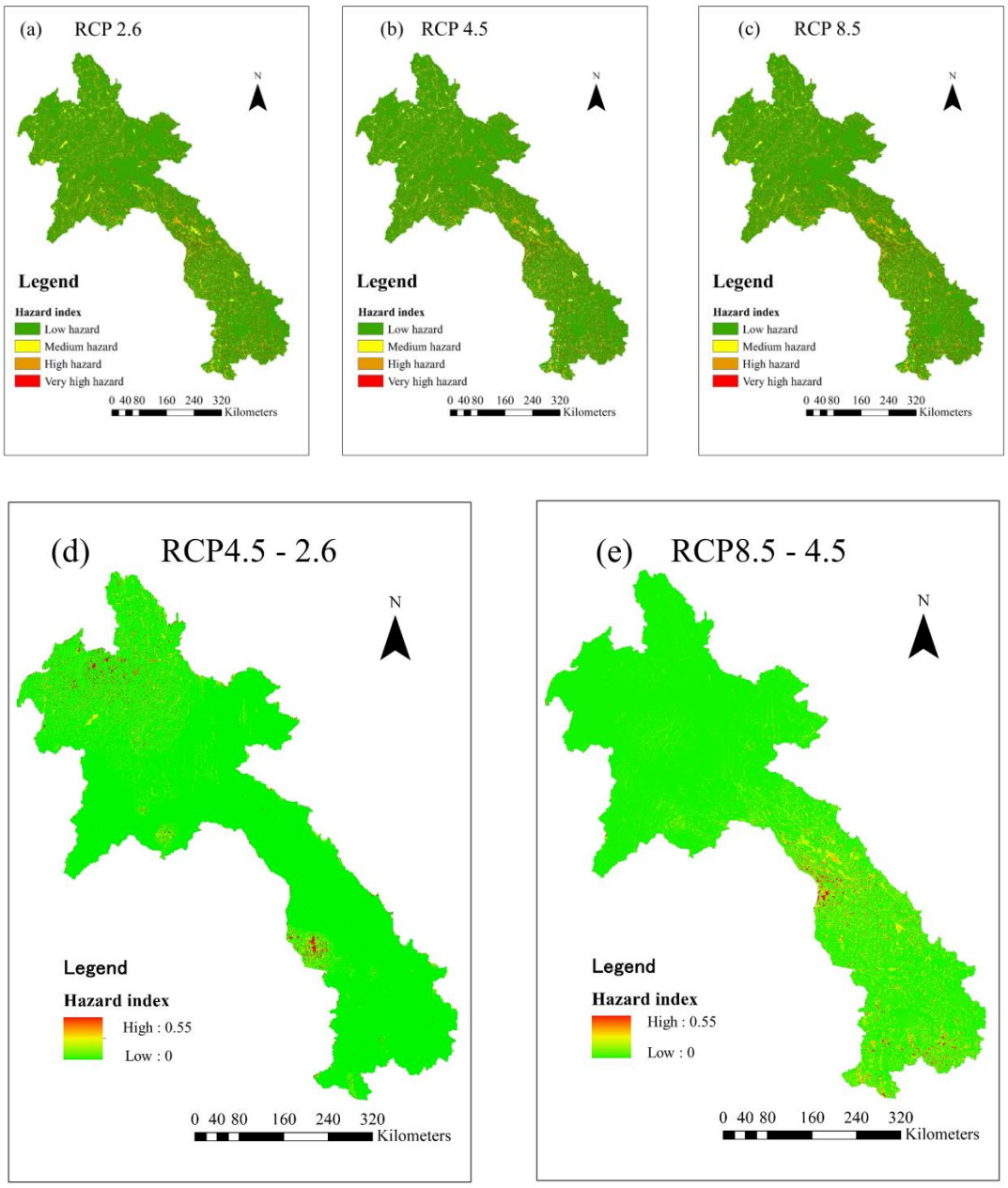

Figure 5-13 Future flood hazard maps for 100 years return period under scenario of (a) RCP 2.6, (b) RCP 4.5, (c) RCP 8.5, the difference of hazard index between (d) RCP 4.5 and RCP 2.6 scenario, and (e) RCP 8.5 and RCP 4.5 scenario during near future

Table 5-8 Percentage of very high hazard area from climate change impact to flood hazard map in each province and percentage of increase between RCP 4.5 and RCP 2.6 scenario during near future

Province name	Percentage of very high hazard area under RCP2.6	Percentage of very high hazard area under RCP 4.5	Percentage increase of very high hazard area between RCP4.5 and 2.6
Attapeu	0.25%	0.25%	2%
Bokeo	0.10%	0.10%	1%
Bolikhamxai	0.34%	0.36%	6%
Champasak	0.24%	0.25%	2%
Houaphan	0.26%	0.26%	2%
Khammouan	0.31%	0.32%	3%
Louang Namtha	0.12%	0.15%	23%
Louang Prabang	0.20%	0.23%	12%
Oudomxai	0.17%	0.19%	12%
Phongsaly	0.19%	0.19%	2%
Salavan	0.21%	0.22%	2%
Savannakhet	0.36%	0.43%	21%
Vientiane	0.31%	0.34%	9%
Vientiane Capital City	0.07%	0.08%	14%
Xaignabouly	0.21%	0.21%	2%
Xekong	0.17%	0.17%	1%
Xiangkouang	0.19%	0.20%	2%
Total percentage of very high hazard area across the country	3.71%	3.97%	

Table 5-9 Percentage of very high hazard area from climate change impact to flood hazard map in each province and percentage of increase between RCP 8.5 and RCP 4.5 scenario during near future

Province name	Percentage of very high hazard area under RCP4.5	Percentage of very high hazard area under RCP 8.5	Percentage increase of very high hazard area between RCP8.5 and 4.5
Attapeu	0.25%	0.25%	0%
Bokeo	0.10%	0.10%	0%
Bolikhamxai	0.36%	0.38%	5%
Champasak	0.25%	0.25%	2%
Houaphan	0.26%	0.26%	0%
Khammouan	0.32%	0.34%	5%
Louang Namtha	0.15%	0.15%	1%
Louang Prabang	0.23%	0.23%	0%
Oudomxai	0.19%	0.19%	0%
Phongsaly	0.19%	0.19%	0%
Salavan	0.22%	0.22%	2%
Savannakhet	0.44%	0.46%	3%
Vientiane	0.34%	0.35%	3%
Vientiane Capital City	0.08%	0.08%	1%
Xaignabouly	0.21%	0.21%	0%
Xekong	0.17%	0.17%	1%
Xiangkouang	0.20%	0.20%	2%
Total percentage of very high hazard area across the country	3.97%	4.05%	

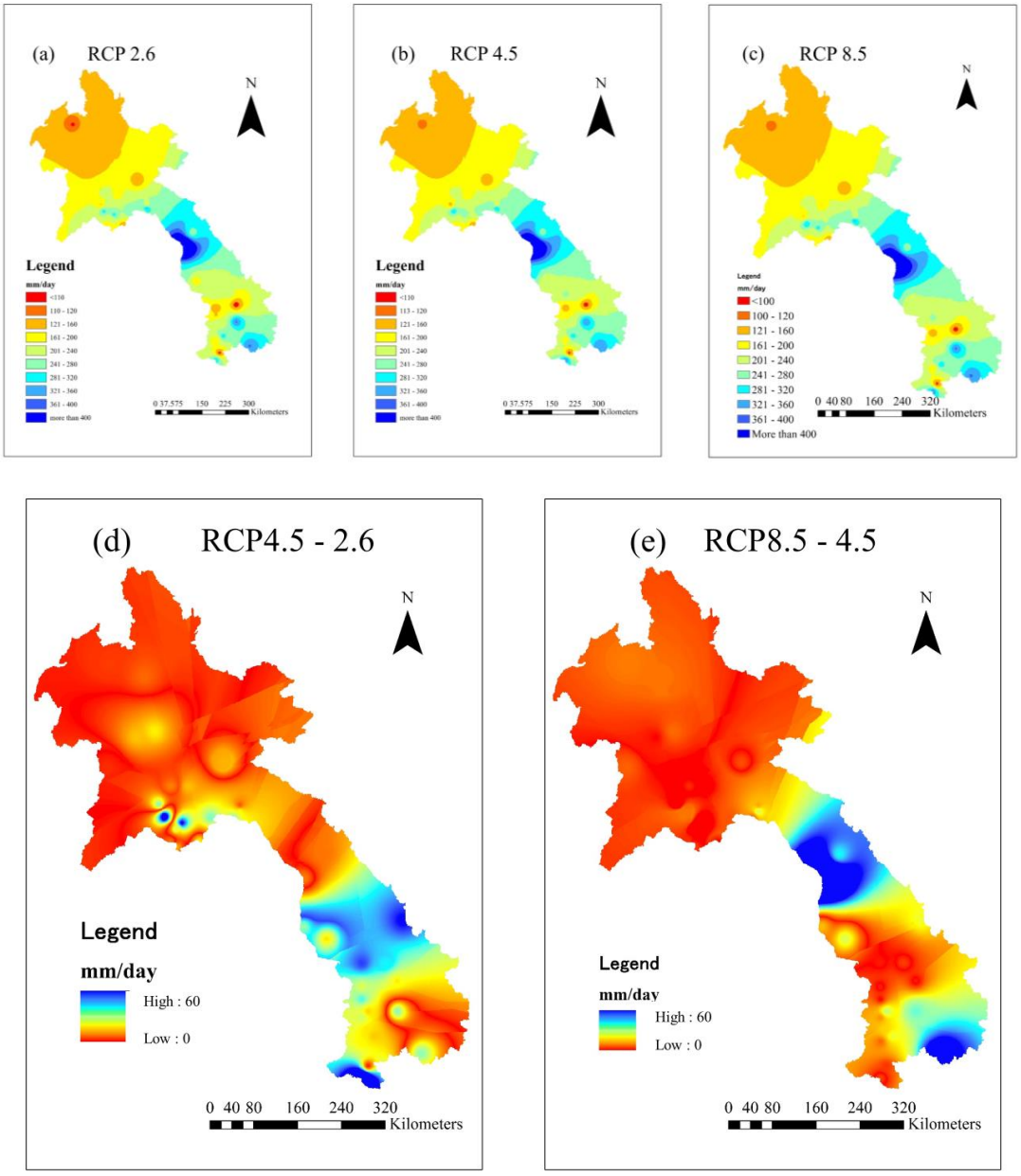

Figure 5-14 Comparison of rainfall between 3 scenarios: (a) RCP 2.6, (b) RCP 4.5, (c) RCP 8.5, the difference of rainfall between (d) RCP 4.5 and RCP 2.6 scenarios and (e) RCP 8.5 and RCP 4.5 scenarios during near future

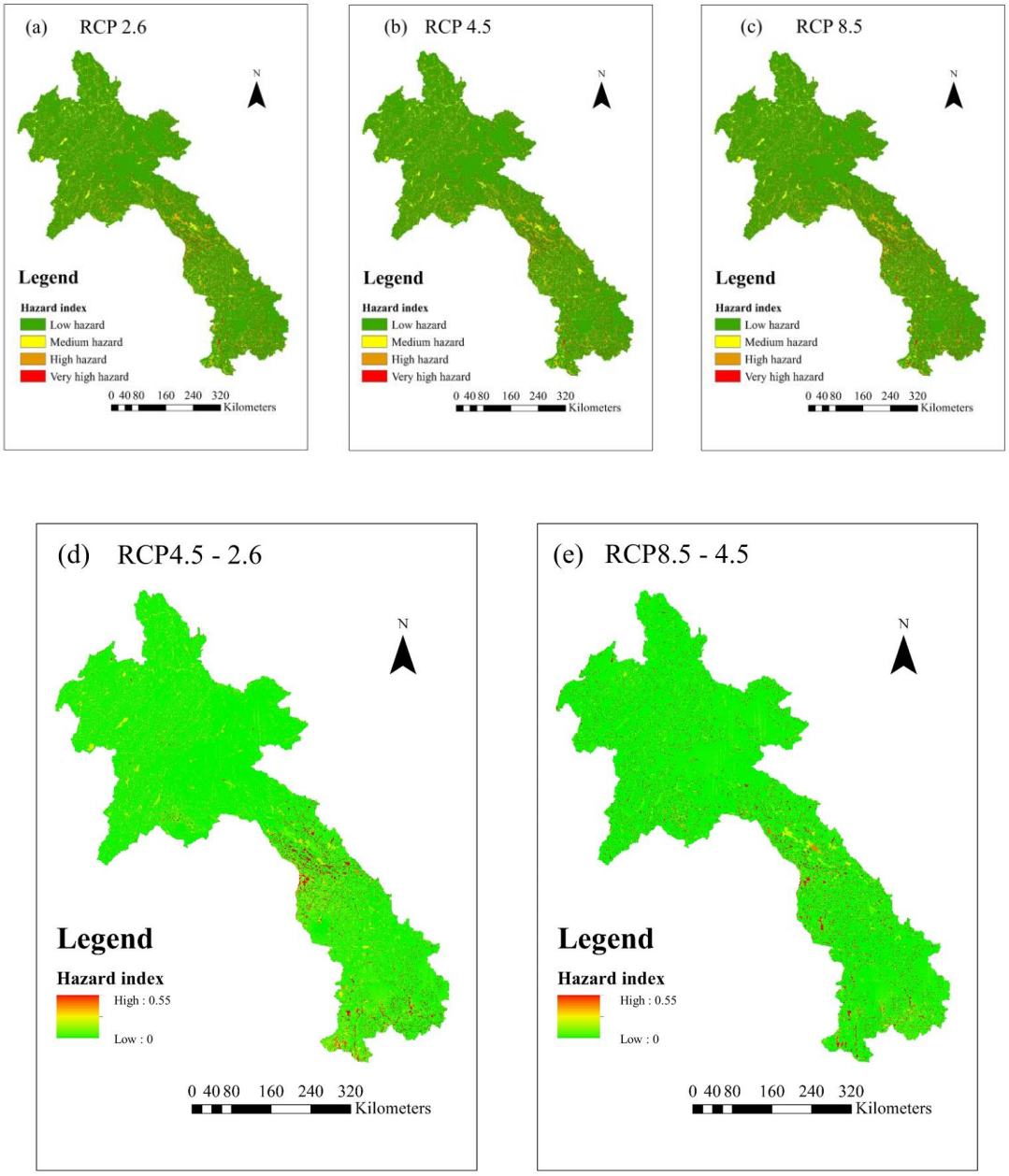

Figure 5-15 Future flood hazard maps for 100 years return period under scenario of (a) RCP 2.6, (b) RCP 4.5, (c) RCP 8.5scenario, the difference of hazard index between (d) RCP 4.5 and RCP 2.6 scenario, and (e) RCP 8.5 and RCP 4.5 scenario during far future

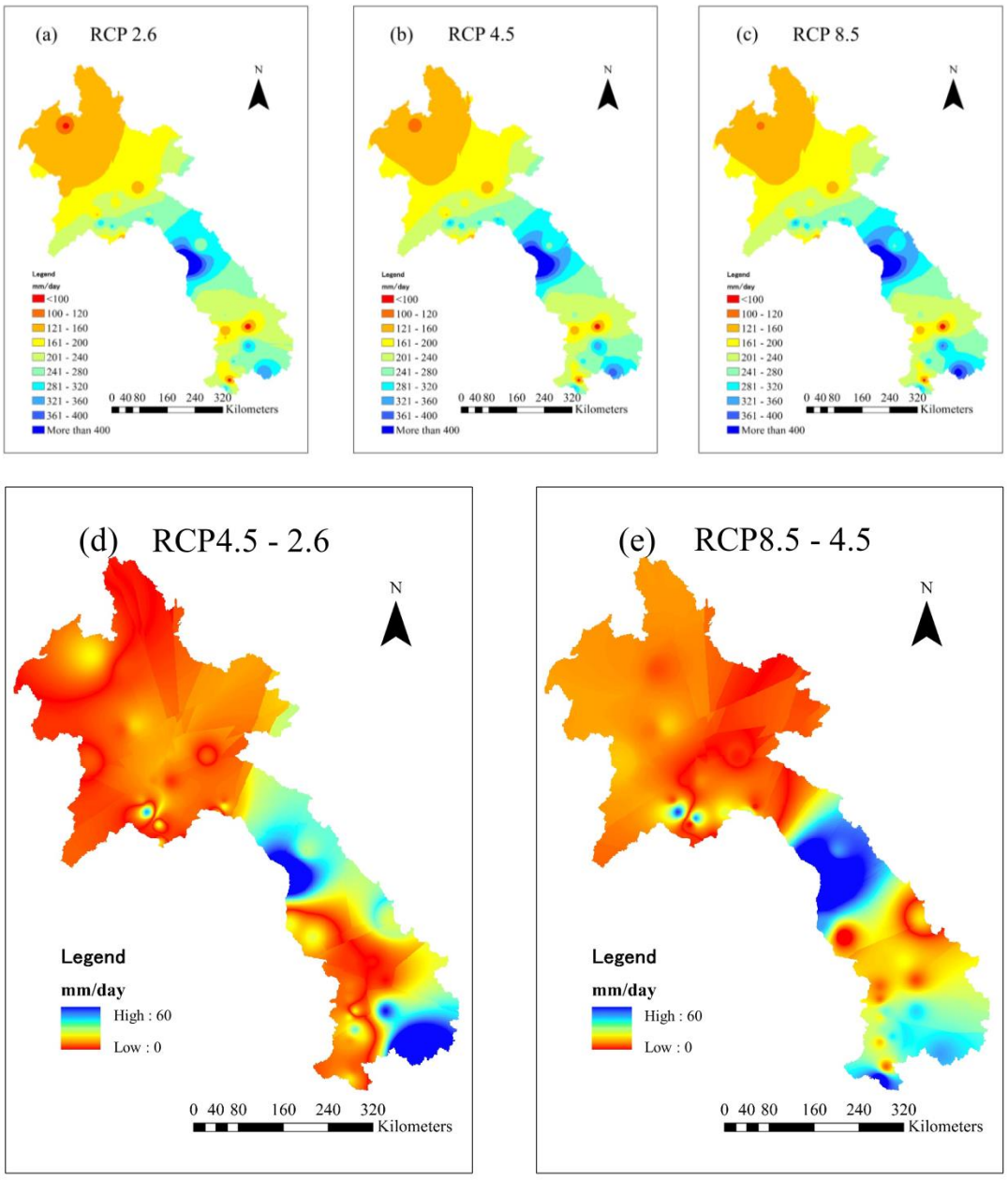

Figure 5-16 Comparison of rainfall between 3 scenarios: (a) RCP 2.6, (b) RCP 4.5, (c) RCP 8.5, the difference of rainfall between (d) RCP 4.5 and RCP 2.6 scenarios and (e) RCP 8.5 and RCP 4.5 scenarios during far future

Table 5-10 Percentage of very high hazard area from climate change impact to flood hazard map in each province and percentage of increase between RCP 4.5 and RCP 2.6 scenario during far future

Province name	Percentage of very high hazard area under RCP2.6	Percentage of very high hazard area under RCP 4.5	Percentage increase of very high hazard area between RCP4.5 and 2.6
Attapeu	0.26%	0.27%	5%
Bokeo	0.10%	0.10%	2%
Bolikhamxai	0.37%	0.40%	7%
Champasak	0.25%	0.26%	5%
Houaphan	0.26%	0.28%	5%
Khammouan	0.32%	0.35%	7%
Louang Namtha	0.15%	0.16%	3%
Louang Prabang	0.23%	0.24%	5%
Oudomxai	0.19%	0.20%	4%
Phongsaly	0.19%	0.20%	4%
Salavan	0.22%	0.23%	4%
Savannakhet	0.45%	0.49%	9%
Vientiane	0.35%	0.37%	7%
Vientiane Capital City	0.08%	0.08%	2%
Xaignabouly	0.21%	0.22%	4%
Xekong	0.17%	0.17%	3%
Xiangkouang	0.20%	0.21%	4%
Total percentage of very high hazard area across the country	4.0%	4.22%	

Table 5-11 Percentage of very high hazard area from climate change impact to flood hazard map in each province and percentage of increase between RCP 8.5 and RCP 4.5 scenario during far future

Province name	Percentage of very high hazard area under RCP4.5	Percentage of very high hazard area under RCP 8.5	Percentage increase of very high hazard area between RCP8.5 and 4.5
Attapeu	0.27%	0.31%	14%
Bokeo	0.10%	0.10%	5%
Bolikhamxai	0.40%	0.48%	21%
Champasak	0.26%	0.30%	14%
Houaphan	0.28%	0.32%	15%
Khammouan	0.35%	0.41%	19%
Louang Namtha	0.16%	0.17%	8%
Louang Prabang	0.24%	0.27%	13%
Oudomxai	0.20%	0.22%	11%
Phongsaly	0.20%	0.22%	11%
Salavan	0.23%	0.26%	12%
Savannakhet	0.49%	0.62%	26%
Vientiane	0.37%	0.45%	20%
Vientiane Capital City	0.08%	0.08%	4%
Xaignabouly	0.22%	0.25%	12%
Xekong	0.17%	0.19%	9%
Xiangkouang	0.21%	0.23%	11%
Total percentage of very high hazard area across the country	4.22%	4.88%	

Climate change impacts to landslide hazard map are represented by the land slide hazard map under future climate condition with 3 scenarios and 2 time periods. By considering the near future period, the total percentage of very high hazard area of 4.85% under the scenario of RCP 2.6 increases to 4.92% under the scenario of RCP 4.5. Figure 5-17 (d) shows the area of the hazard index increase when comparing the scenario of RCP 2.6 and RCP 4.5. The Xiengkoung province's very high hazard area increases from 0.64% under the scenario of RCP 2.6 to 0.68% under the scenario of RCP 4.5 (Table 5-12). Under the scenario of RCP 8.5 the total percentage of very high hazard area increases to 4.96%. Figure 5-17 (e) shows the aera of the hazard index increase when comparing the scenario of RCP 8.5 and RCP 4.5. Among others, Xiengkoung, Vientaine and Bolikhamxai province have the highest increase of very high hazard area when comparing landslide hazard map under scenario of RCP 4.5 and RCP 8.5 (Table 5-13). Many provinces from climate change impacts to landslide hazard map with near future have continuously increase of very high hazard area from RCP 2.6 to RCP 8.5. The very high hazard area in Vientiane province increase from 0.92% under the scenario of RCP 2.6 to 0.93% under the scenario of RCP 4.5 and increases to 0.94% under scenario of RCP 8.5. For the far future, under scenario of RCP 2.6 the total percentage of very high hazard area increases to 4.98%. Figure 5-18 (d) shows the area of the hazard index increase when comparing the scenario of RCP 4.5 and RCP 2.6. Comparing the increase of the very high hazard area between future landslide under RCP 2.6 and RCP 4.5 scenario, Bolikhamxai province has the highest increase. That is, the very high hazard area increases from 2.93% under RCP 2.6 scenario to 3.2% under RCP 4.5 scenario (Table 5-14). Under the scenario of RCP 8.5, the total very high hazard area from climate change impact to landslide hazard map increases to 5.28%. Figure 5-18 (e) shows the area of the hazard index increase when

comparing the scenario of RCP 8.5 and RCP 4.5. Bolikhamxai province has the highest increase (5%) of the very high hazard area when comparing between landslide hazard map under scenario of RCP 4.5 and RCP 8.5 (Table 5-15). The very high hazard area in most of the provinces from climate change impacts to landslide hazard map with far future increase continually from RCP 2.6 to RCP 8.5 for example Bolikhamxai province. The very high hazard area in Bolikhamxai province increase around 8.98% comparing the very high hazard area under the scenario RCP 2.6 to that under RCP 4.5 and the very high hazard area in Bolikhamxai province increase around 5% comparing the very high hazard area under the scenario RCP 4.5 to that under RCP 8.5. Based on the results, the increase of rainfall intensity (Figure 5-14 and Figure 5-16) due to climate change influences the increase of flood and landslide hazard area. Many studies in Mekong delta (Dinh et al., 2012; Lauri et al., 2012) revealed that the climate change has impacts on rainfall intensity which leads to increase in flood and landslide frequencies. Therefore, these results are in line with those of other research studies.

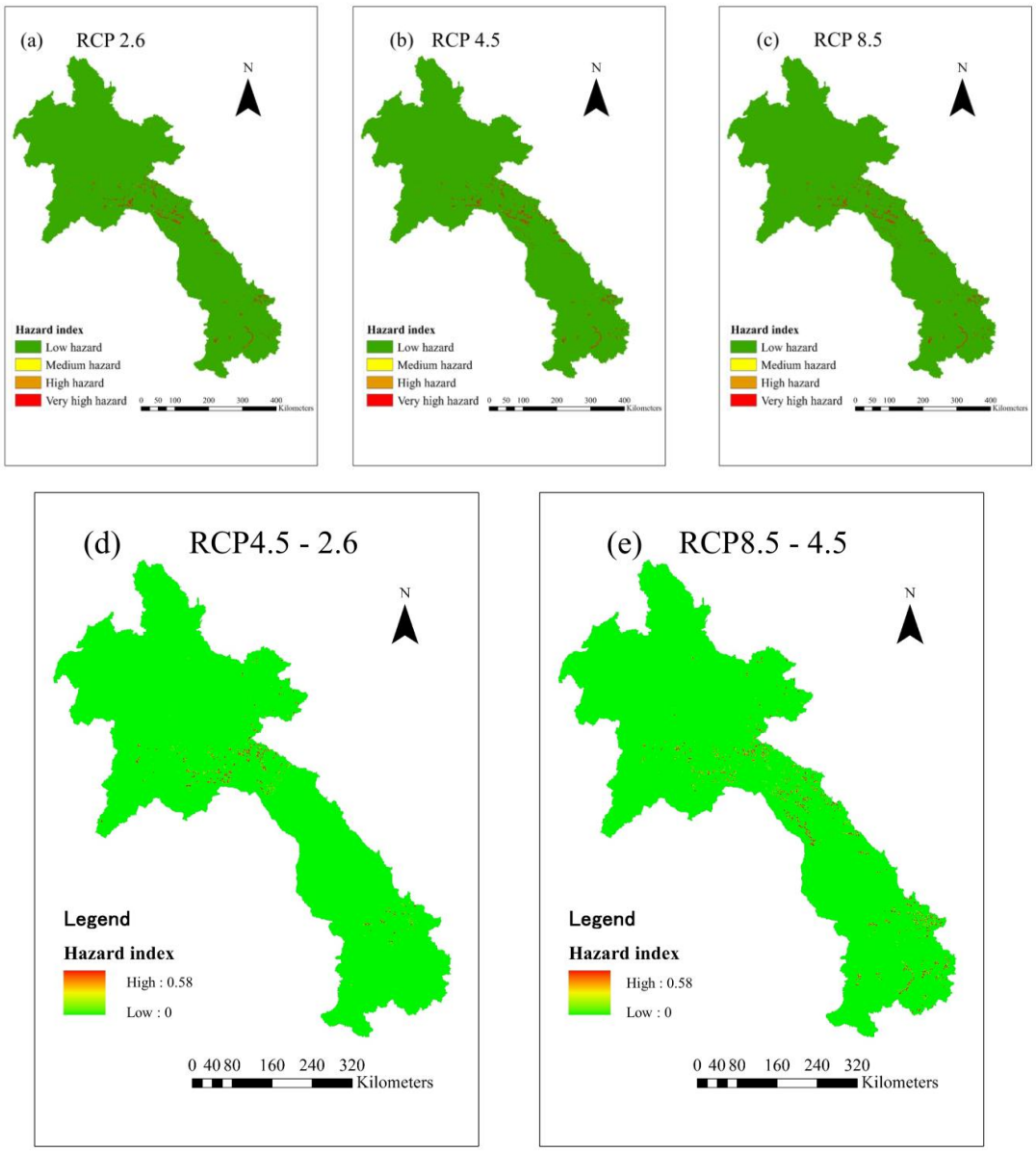

Figure 5-17 Future landslide hazard maps for 100 years return period under scenario of (a) RCP 2.6, (b) RCP 4.5, (c) RCP 8.5, the difference of hazard index between (d) RCP 4.5 and RCP 2.6 scenario, and (e) RCP 8.5 and RCP 4.5 scenario during near future

Table 5-12 Percentage of very high hazard area from climate change impact to landslide hazard map in each province and percentage of increase between RCP 4.5 and RCP 2.6 scenario during near future

Province name	Percentage of very high hazard area under RCP2.6	Percentage of very high hazard area under RCP 4.5	Percentage increase of very high hazard area between RCP4.5 and 2.6
Attapeu	0.10%	0.10%	0.06%
Bokeo	0.00%	0.00%	0.00%
Bolikhamxai	2.85%	2.86%	0.20%
Champasak	0.07%	0.07%	0.04%
Houaphan	0.01%	0.01%	0.01%
Khammouan	0.18%	0.18%	0.12%
Louang Namtha	0.00%	0.00%	0.00%
Louang Prabang	0.00%	0.00%	0.00%
Oudomxai	0.00%	0.00%	0.00%
Phongsaly	0.00%	0.00%	0.00%
Salavan	0.02%	0.02%	8.32%
Savannakhet	0.00%	0.00%	0.00%
Vientiane	0.92%	0.93%	1.64%
Vientiane Capital City	0.00%	0.00%	0.00%
Xaignabouly	0.00%	0.00%	0.00%
Xekong	0.06%	0.07%	7.46%
Xiangkouang	0.64%	0.68%	5.84%
Total percentage of very high hazard area across the country	4.86%	4.92%	

Table 5-13 Percentage of very high hazard area from climate change impact to landslide hazard map in each province and percentage of increase between RCP 8.5 and RCP 4.5 scenario during near future

Province name	Percentage of very high hazard area under RCP4.5	Percentage of very high hazard area under RCP 8.5	Percentage increase of very high hazard area between RCP8.5 and 4.5
Attapeu	0.10%	0.10%	4.69%
Bokeo	0.00%	0.00%	0.00%
Bolikhamxai	2.86%	2.87%	0.55%
Champasak	0.07%	0.07%	0.03%
Houaphan	0.01%	0.01%	0.01%
Khammouan	0.18%	0.18%	0.07%
Louang Namtha	0.00%	0.00%	0.00%
Louang Prabang	0.00%	0.00%	0.00%
Oudomxai	0.00%	0.00%	0.00%
Phongsaly	0.00%	0.00%	0.00%
Salavan	0.02%	0.02%	0.01%
Savannakhet	0.00%	0.00%	0.00%
Vientiane	0.93%	0.94%	0.35%
Vientiane Capital City	0.00%	0.00%	0.00%
Xaignabouly	0.00%	0.00%	0.00%
Xekong	0.07%	0.07%	6.93%
Xiangkouang	0.68%	0.69%	1.62%
Total percentage of very high hazard area across the country	4.92%	4.96%	

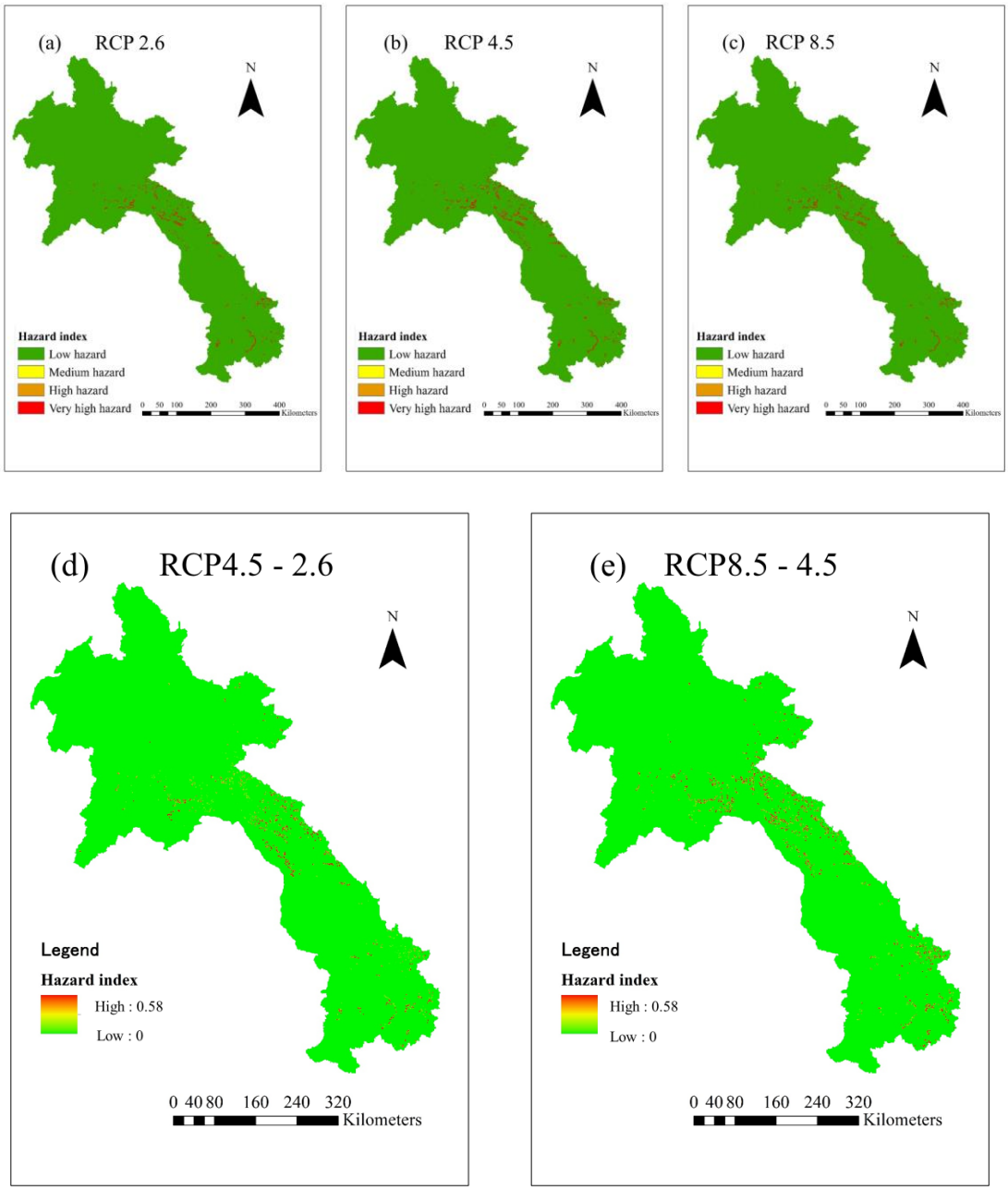

Figure 5-18 Future landslide hazard maps for 100 years return period under scenario of (a) RCP 2.6, (b) RCP 4.5, (c) RCP 8.5, the difference of hazard index between (d) RCP 4.5 and RCP 2.6 scenario, and (e) RCP 8.5 and RCP 4.5 scenario during far future

Table 5-14 Percentage of very high hazard area from climate change impact to landslide hazard map in each province and percentage of increase between RCP 4.5 and RCP 2.6 scenario during far future

Province name	Percentage of very high hazard area under RCP2.6	Percentage of very high hazard area under RCP 4.5	Percentage increase of very high hazard area between RCP4.5 and 2.6
Attapeu	0.11%	0.11%	0.33%
Bokeo	0.00%	0.00%	0.00%
Bolikhamxai	2.93%	3.20%	8.98%
Champasak	0.07%	0.07%	0.21%
Houaphan	0.01%	0.01%	0.04%
Khammouan	0.18%	0.18%	0.56%
Louang Namtha	0.00%	0.00%	0.00%
Louang Prabang	0.00%	0.00%	0.00%
Oudomxai	0.00%	0.00%	0.00%
Phongsaly	0.00%	0.00%	0.00%
Salavan	0.02%	0.02%	0.05%
Savannakhet	0.00%	0.00%	0.00%
Vientiane	0.93%	0.95%	2.84%
Vientiane Capital City	0.00%	0.00%	0.00%
Xaignabouly	0.00%	0.00%	0.01%
Xekong	0.06%	0.06%	0.19%
Xiangkouang	0.66%	0.67%	2.01%
Total percentage of very high hazard area across the country	4.89%	4.98%	

Table 5-15 Percentage of very high hazard area from climate change impact to landslide hazard map in each province and percentage of increase between RCP 8.5 and RCP 4.5 scenario during far future

Province name	Percentage of very high hazard area under RCP4.5	Percentage of very high hazard area under RCP 8.5	Percentage increase of very high hazard area between RCP8.5 and 4.5
Attapeu	0.25%	0.25%	0%
Bokeo	0.10%	0.10%	0%
Bolikhamxai	0.36%	0.38%	5%
Champasak	0.25%	0.25%	2%
Houaphan	0.26%	0.26%	0%
Khammouan	0.32%	0.34%	5%
Louang Namtha	0.15%	0.15%	1%
Louang Prabang	0.23%	0.23%	0%
Oudomxai	0.19%	0.19%	0%
Phongsaly	0.19%	0.19%	0%
Salavan	0.22%	0.22%	2%
Savannakhet	0.44%	0.46%	3%
Vientiane	0.34%	0.35%	3%
Vientiane Capital City	0.08%	0.08%	1%
Xaignabouly	0.21%	0.21%	0%
Xekong	0.17%	0.17%	1%
Xiangkouang	0.20%	0.20%	2%
Total percentage of very high hazard area across the country	4.98%	5.28%	

The integrated maps consist of flooding, land use change, landslide and climate change hazards. The maps are developed using the AHP to perform the integration. The integrated hazard map consists of 6 maps, under 3 scenario of RCP and 2 time periods. Under the scenario of RCP 2.6, for near future the total high and very high hazard area from the total integrated hazard areas are 3.2% and 5.35% respectively. For far future, the total high and very high hazard area slightly increases respectively to 3.28% and 5.38%. Under the scenario of RCP 4.5, the total high hazard area is 5.51% of the total integrated hazard area for near future and increases to 5.57% for far future. The very high hazard area increases from 3.27% for near future to 3.52% for far future. Under the scenario of RCP8.5, the total high and very high hazard area is respectively 5.4% and 3.3% of the total integrated hazard map for near future. For far future, the total high and very high hazard area increases to 7.26% and 3.71% respectively. Figure 5-19 (d) shows the area of the hazard index increase when comparing the integrated hazard map for near future under RCP2.6 and RCP 4.5 scenario. Savannakhet province is highly influenced by the climate change. The percentage of the very high hazard area from integrated hazard map increases around 4.69% when comparing the scenario of RCP 2.6 and RCP 4.5 (Table 5-16). Figure 5-19 (e) shows the area of the hazard index increase when comparing the scenario of RCP 8.5 and RCP 4.5. Among others, Khammouan, Vientiane, Savannakhet and Bolikhamxai province have higher increase of very high hazard area when comparing integrated hazard map under scenario RCP4.5 and RCP8.5 (Table 5-17). Overall, the very high hazard area in most of the provinces from integrated hazard map with near future increase continually from RCP 2.6 to RCP 8.5 for instance Savannakhet province. The very high hazard area in Savannakhet increase around 4.69% comparing the very high hazard area under the scenario RCP 2.6 to that under RCP 4.5 and the very high hazard area in Savannakhet

province increase around 1.62% comparing the very high hazard area under the scenario RCP 4.5 to that under RCP 8.5. For far future period, Figure 5-20 (d) shows the area of the hazard index increase when comparing the scenario of RCP 4.5 and RCP 2.6. Comparing the increase of very high hazard area between integrated hazard map under RCP 2.6 and RCP 4.5 scenario, Khammouan province has the highest increase (16.45%) (Table 5-18). Figure 5-20 (e) shows the area of the hazard index increase when comparing the scenario of RCP 8.5 and RCP 4.5. Khammouan province has the highest increase of very high hazard area (12.47%) when comparing between flood hazard map under scenario of RCP 2.6 and RCP 4.5 (Table 5-19). The very high hazard area in most of the provinces from integrated hazard map with far future increase continually from RCP 2.6 to RCP 8.5for example Savannakhet province. The very high hazard area in Savannakhet province increase around 11.35% comparing the very high hazard area under the scenario RCP 2.6 to that under RCP 4.5 and the very high hazard area in Savannakhet province increase around 10.72% comparing the very high hazard area under the scenario RCP 4.5 to that under RCP 8.5. The increase of very high hazard area for integrated hazard map is similar to that for the rainfall pattern from RCP 2.6 to RCP 4.5 and RCP 4.5 to RCP 8.5 scenario with near and far future period (Figure 5-14 and Figure 5-16). The southern region has the highest increase of very high hazard area, particularly Bolikhamxai, Khamouan and Savannakhet province. Special attentions must be paid to these provinces particularly on the countermeasures and adaptation planning to reduce the potential risk. The integrated hazard map can be used in combination with other maps such as the future development plan from the government or private sectors. In this way, the areas of risk in the development of agricultural areas or expansion of urban areas could be verified. These maps are applicable to the presentation of the spatial distribution of hazard areas. Thus,

the impacts on these hazard areas may be studied during the planning phase. Adequate planning can minimize the impacts from multi-hazards on the expansion of agricultural and urban areas. Moreover, local authorities can use integrated hazard maps in line with policies and multi-hazard mitigation strategies in their respective areas. This study provides an important and reliable methodology for the development of integrated hazard maps using multi-criteria decision analysis such as the AHP. The produced integrated hazard map identified suitable areas for development in the northern part of Laos, which had the greatest amount of low hazard areas (42%).

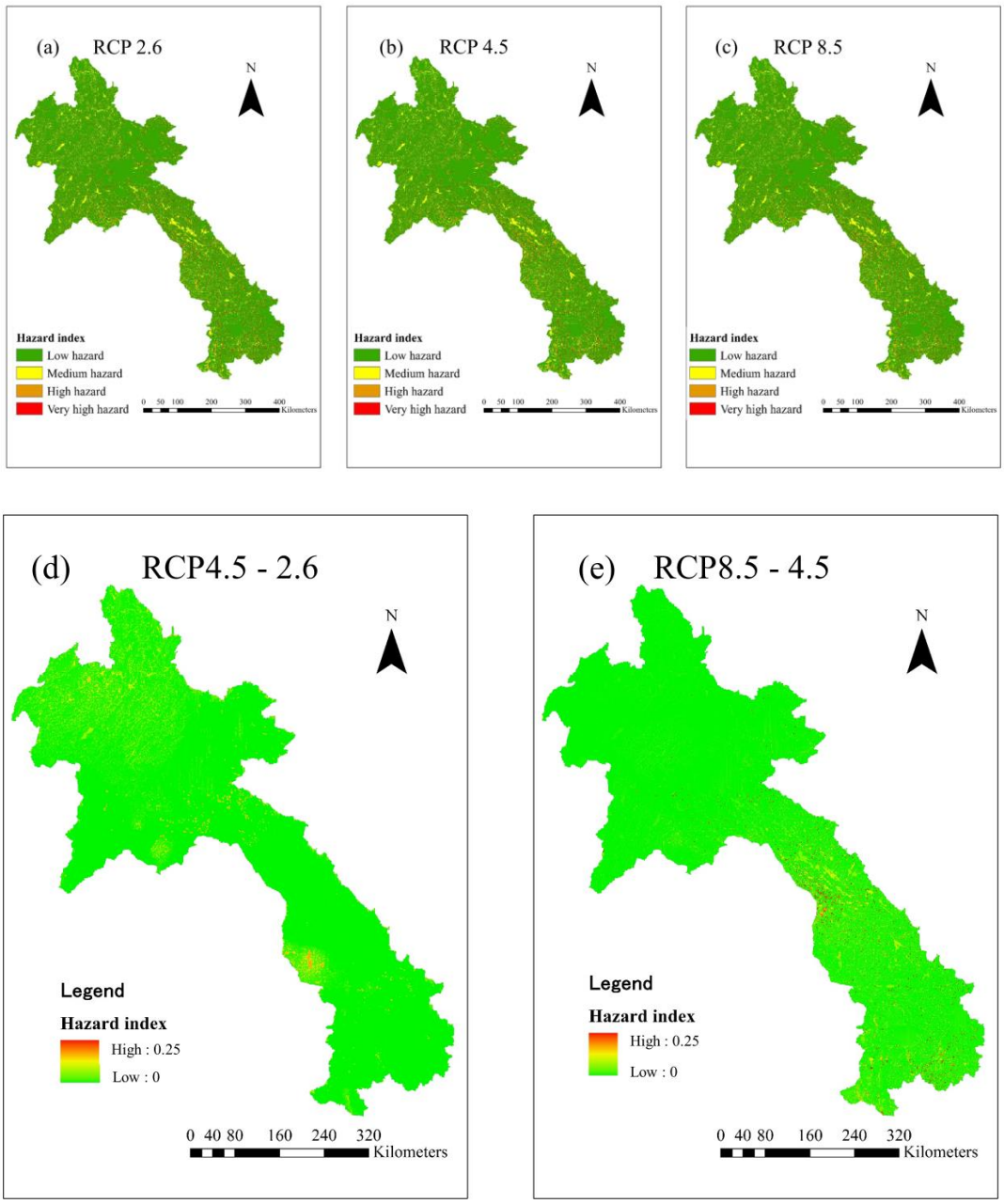

Figure 5-19 Integrated hazard maps for 100 years return period under scenario of (a) RCP 2.6, (b) RCP 4.5, (c) RCP 8.5, the difference of hazard index between (d) RCP 4.5 and RCP 2.6scenario, and (e) RCP 8.5 and RCP 4.5 scenario during near future

Table 5-16 Percentage of very high hazard area from integrated hazard map in each province and percentage of increase between RCP 4.5 and RCP 2.6 scenario during near future

Province name	Percentage of very high hazard area under RCP2.6	Percentage of very high hazard area under RCP 4.5	Percentage increase of very high hazard area between RCP4.5 and 2.6
Attapeu	0.23%	0.23%	0.31%
Bokeo	0.07%	0.07%	0.64%
Bolikhamxai	0.32%	0.33%	3.05%
Champasak	0.21%	0.22%	0.28%
Houaphan	0.22%	0.22%	0.20%
Khammouan	0.32%	0.32%	0.94%
Louang Namtha	0.08%	0.08%	4.36%
Louang Prabang	0.19%	0.20%	4.21%
Oudomxai	0.12%	0.12%	3.47%
Phongsaly	0.11%	0.11%	1.03%
Salavan	0.13%	0.13%	1.18%
Savannakhet	0.36%	0.38%	4.69%
Vientiane	0.30%	0.31%	2.86%
Vientiane Capital City	0.04%	0.04%	0.34%
Xaignabouly	0.19%	0.20%	1.80%
Xekong	0.14%	0.14%	1.30%
Xiangkouang	0.17%	0.17%	1.56%
Total percentage of very high hazard area across the country	3.2%	3.27%	

Table 5-17 Percentage of very high hazard area from integrated hazard map in each province and percentage of increase between RCP 8.5 and RCP 4.5 scenario during near future

Province name	Percentage of very high hazard area under RCP4.5	Percentage of very high hazard area under RCP 8.5	Percentage increase of very high hazard area between RCP8.5 and 4.5
Attapeu	0.23%	0.23%	0.98%
Bokeo	0.07%	0.07%	0.29%
Bolikhamxai	0.33%	0.34%	1.43%
Champasak	0.22%	0.22%	0.92%
Houaphan	0.22%	0.22%	0.95%
Khammouan	0.32%	0.32%	1.37%
Louang Namtha	0.08%	0.08%	0.34%
Louang Prabang	0.20%	0.20%	0.87%
Oudomxai	0.12%	0.12%	0.52%
Phongsaly	0.11%	0.11%	0.48%
Salavan	0.13%	0.13%	0.54%
Savannakhet	0.38%	0.39%	1.62%
Vientiane	0.31%	0.32%	1.34%
Vientiane Capital City	0.04%	0.04%	0.16%
Xaignabouly	0.20%	0.20%	0.84%
Xekong	0.14%	0.14%	0.60%
Xiangkouang	0.17%	0.17%	0.72%
Total percentage of very high hazard area across the country	3.27%	3.3%	

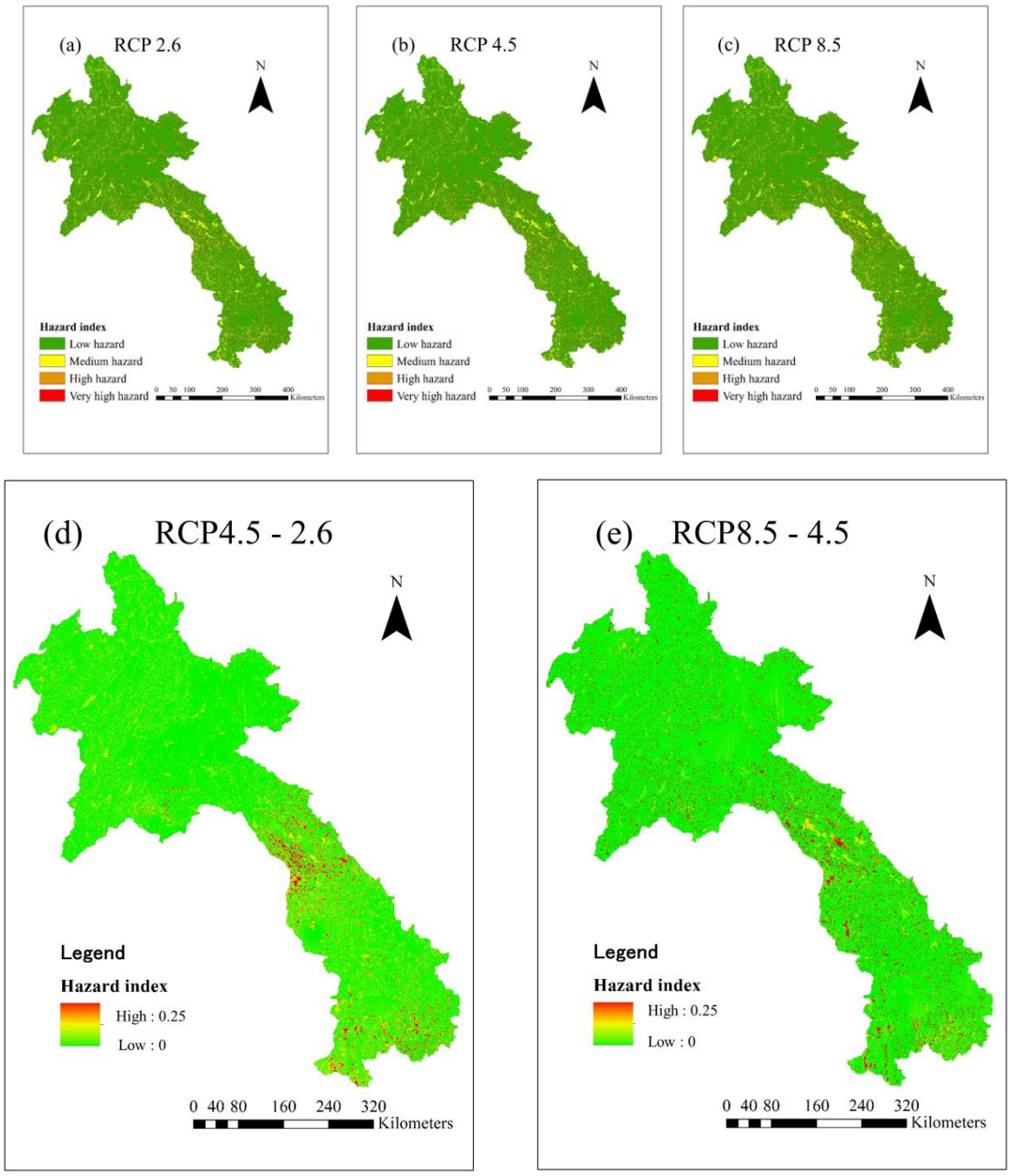

Figure 5-20 Integrated hazard maps for 100 years return period under scenario of (a) RCP 2.6, (b) RCP 4.5, (c) RCP 8.5, the difference of hazard index between (d) RCP 4.5 and RCP 2.6, and (e) RCP 8.5 and RCP 4.5 scenario during far future

Table 5-18 Percentage of very high hazard area from integrated hazard map in each province and percentage of increase between RCP 4.5 and RCP 2.6 scenario during far future

Province name	Percentage of very high hazard area under RCP2.6	Percentage of very high hazard area under RCP 4.5	Percentage increase of very high hazard area between RCP4.5 and 2.6
Attapeu	0.23%	0.25%	8.67%
Bokeo	0.07%	0.07%	2.58%
Bolikhamxai	0.33%	0.37%	12.39%
Champasak	0.22%	0.23%	8.16%
Houaphan	0.22%	0.24%	8.44%
Khammouan	0.32%	0.37%	16.45%
Louang Namtha	0.08%	0.08%	2.90%
Louang Prabang	0.20%	0.21%	7.41%
Oudomxai	0.12%	0.12%	4.48%
Phongsaly	0.11%	0.12%	4.17%
Salavan	0.13%	0.13%	4.77%
Savannakhet	0.37%	0.41%	11.35%
Vientiane	0.31%	0.34%	11.62%
Vientiane Capital City	0.04%	0.04%	1.37%
Xaignabouly	0.19%	0.21%	7.28%
Xekong	0.14%	0.15%	5.26%
Xiangkouang	0.17%	0.18%	6.31%
Total percentage of very high hazard area across the country	3.23%	3.52%	

Table 5-19 Percentage of very high hazard area from integrated hazard map in each province and percentage of increase between RCP 8.5 and RCP 4.5 scenario during far future

Province name	Percentage of very high hazard area under RCP4.5	Percentage of very high hazard area under RCP 8.5	Percentage increase of very high hazard area between RCP8.5 and 4.5
Attapeu	0.25%	0.25%	1.36%
Bokeo	0.07%	0.07%	1.42%
Bolikhamxai	0.37%	0.41%	11.90%
Champasak	0.23%	0.24%	2.77%
Houaphan	0.24%	0.25%	3.78%
Khammouan	0.36%	0.41%	12.47%
Louang Namtha	0.08%	0.08%	1.60%
Louang Prabang	0.21%	0.21%	0.99%
Oudomxai	0.12%	0.13%	0.66%
Phongsaly	0.12%	0.12%	1.13%
Salavan	0.13%	0.13%	0.59%
Savannakhet	0.42%	0.46%	10.72%
Vientiane	0.34%	0.37%	8.33%
Vientiane Capital City	0.04%	0.04%	0.75%
Xaignabouly	0.21%	0.21%	0.62%
Xekong	0.15%	0.15%	0.77%
Xiangkouang	0.18%	0.18%	1.00%
Total percentage of very high hazard area across the country	3.52%	3.71%	

CHAPTER 6: ESTIMATION OF SPATIAL RISK FOR MULTI HAZARD AND ADATATION MEASURE FOR REDUCE DAMAGE COST IN LAO PDR

6.1 Introduction

According to the Sendai Framework (2015), it is important to pay more attention to risk analysis. Single risk analysis addressing single hazards provides information about only an individual risk in a specific location; however, in a specific location, more than a single hazard can occur. For example, in mountainous areas, landslides and floods can occur together. Therefore, the integration of the risk assessment of these hazards is necessary. Phrakonkham (2019) estimated the hazards in Lao PDR due to landslides, floods, land use change to floods, climate change leading to floods and landslides, and integrated hazard maps; the results were used in the analysis of the negative consequences of these hazards. The main objective of this study was to propose integrated risk maps to detect subtle areas on the regional scale, for which there are limited data available. This modeling method combined several maps of hazards, i.e., land use change, climate change and flooding. As a priority weighting function for the maps, AHP was deployed. Integrated risk map can be used as a guide map; it provided all of the important information that can be used to develop countermeasures, not only for floods but also for other natural hazards. Both individual and integrated risk maps were used to provide the

damage costs based on land use area (urban, paddy, and agriculture). In this chapter we analyze potential damage cost from flood, land use change and land slide risk map. Furthermore, we also consider impact of climate change impact to flood and landslide risk under three scenarios (RCP 2.6, 4.5 and 8.5) for two time period (2010-2050 (2050s) and 2051-2099 (2100s)). Finally, we estimate the total damage cost of integrated risk maps.

6.2 Results

6.2.1 Damage cost form flood risk map

In recent year, flood disasters frequent are occurred in Lao PDR more often. It is lead to huge damage and impact to the development of Lao PDR (Laos national report, 2012). Therefore estimation of damage cost and potential impact area analysis is necessary. By observing the flood risk map, Total damage cost according to flood risk map is around 19.18 billion USD/year (Figure. 6-1). We analyses total damage cost based on land use type as total damage cost in urban area, total damage cost in agriculture area and total damage cost in paddy field area. The urban areas have the highest total damage costs (18.8 billion USD/year). Total damage cost in agricultural area is 314 million USD/year and total damage cost in paddy field is 68.75 million USD/year. Based on these results, floods cause greater damage to urban areas than to other land use types. It is noticeably that, the risk areas from flood were distributed around country, mostly from the central region and southern region. The central region has the highest total damage costs (13.9

billion USD/year) caused by hazards. Similarly, the southern region undergoes high total damage costs (4.4 billion USD/year), while the total damage costs of the northern region are approximately 0.88 billion USD/year. The major reason why the central region has the highest total damage costs is that it is the most developed area in Lao PDR. That is, the capital city of Lao PDR is located in the central region. In addition, the flood risk map could be used as a tool for appropriate countermeasure planning to mitigate the damage in downstream areas.

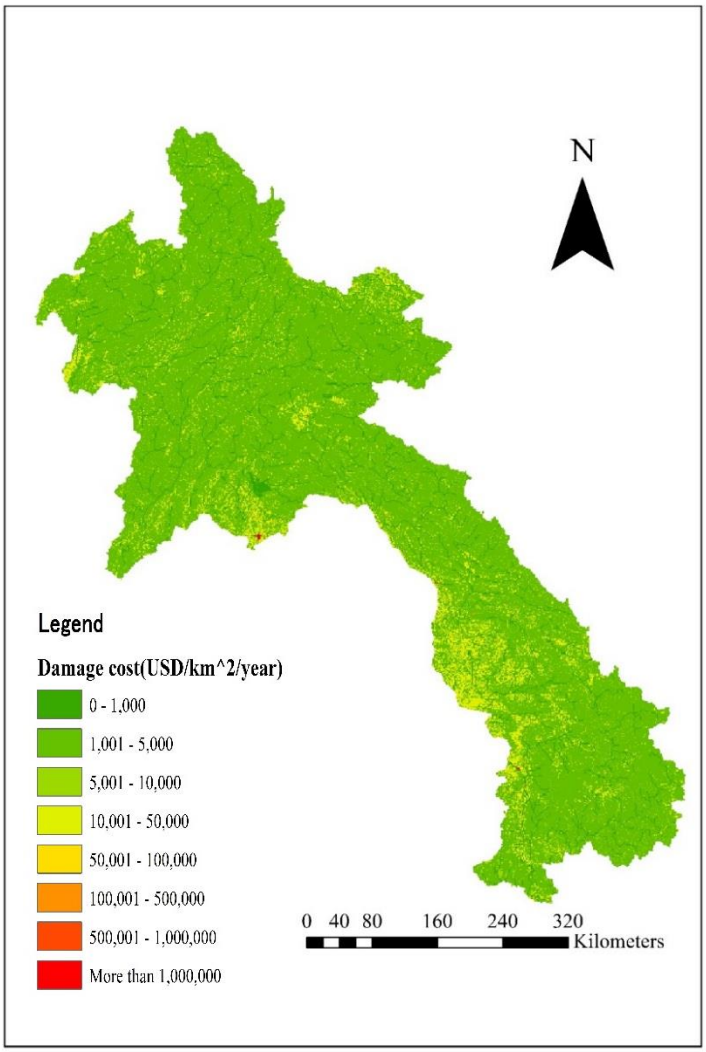

Figure 6-1 Damage cost/year of flood hazard risk map in Lao PDR

6.2.2 Damage cost from landslide risk map

Most landslide events occur near mountainous terrain. Damage from landslide can cause significant loss to agriculture production and paddy field in around mountainous area. However, when compared to the other risk maps, the landslide risk map shows the lowest total damage costs (13 million USD/year) (Figure. 6-2). The highest total damage costs from landslide risk are in agricultural areas (8.4 million USD/year). Paddy field areas has total damage cost 4.8 million USD/year, it is around 57 % of total damage cost from agricultural area. Urban area has less affected from landslide disaster, total damage cost from land slide to urban area was around 0.2 million USD/year, it is around 2 % of total damage cost from landslide disaster to agricultural area. At the region scale, the central region has the highest total damage costs (11.3 million USD/year) second is southern region (1.1 million USD/year) and total damage costs of northern region is around 0.6 million USD/year. In addition to economic uses, this map could be applied for resettlement planning for people living in the mountainous area in close cooperation with concerned agencies.

6.2.3 Damage cost form land use change risk map

The total damage costs from land use change leading to flood risk map (22 billion USD/year) are higher than total damage cost of flood risk map, with the damage costs of the urban areas caused by the land use change being the highest (21.4 billion USD/year).

In addition, total damage cost in agricultural area is 516 million USD/year and total damage cost in paddy field is around 84 million USD/year. In particular, in the central region, the total damage costs in the urban areas are the highest (16.4 billion USD/year). The total damage costs from land use change risk map for urban areas increase approximately around 12 % compare to flood risk map. For the central region, it is increase approximately around 18 % compare to flood risk map. That is, land use change has a significant impact on the total damage costs in urban areas and the central region. Furthermore, the risk map of land use change leading to floods could be deployed as a tool for a urban development planning, particularly for the urban area in the central region (Figure. 6-3).

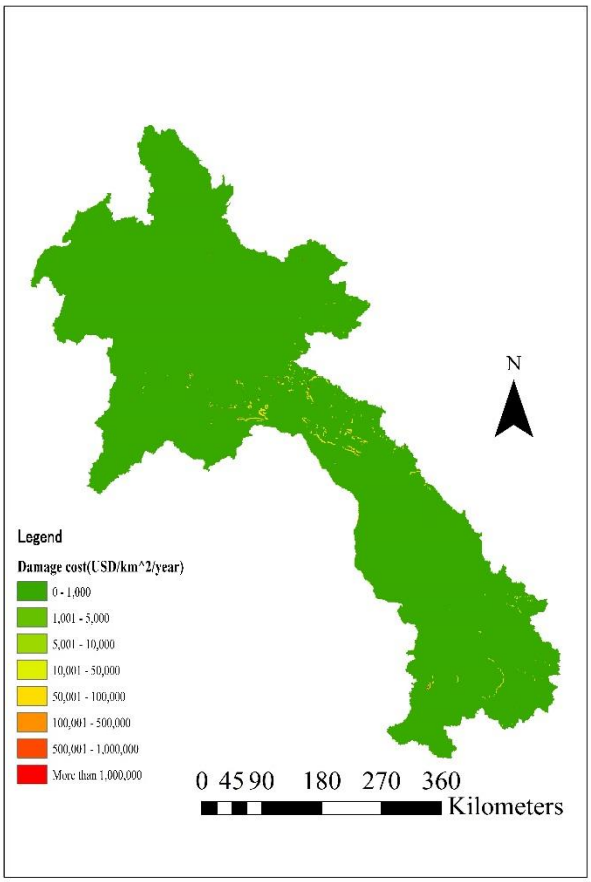

Figure 6-2 Damage cost/year of landslide hazard risk map in Lao PDR

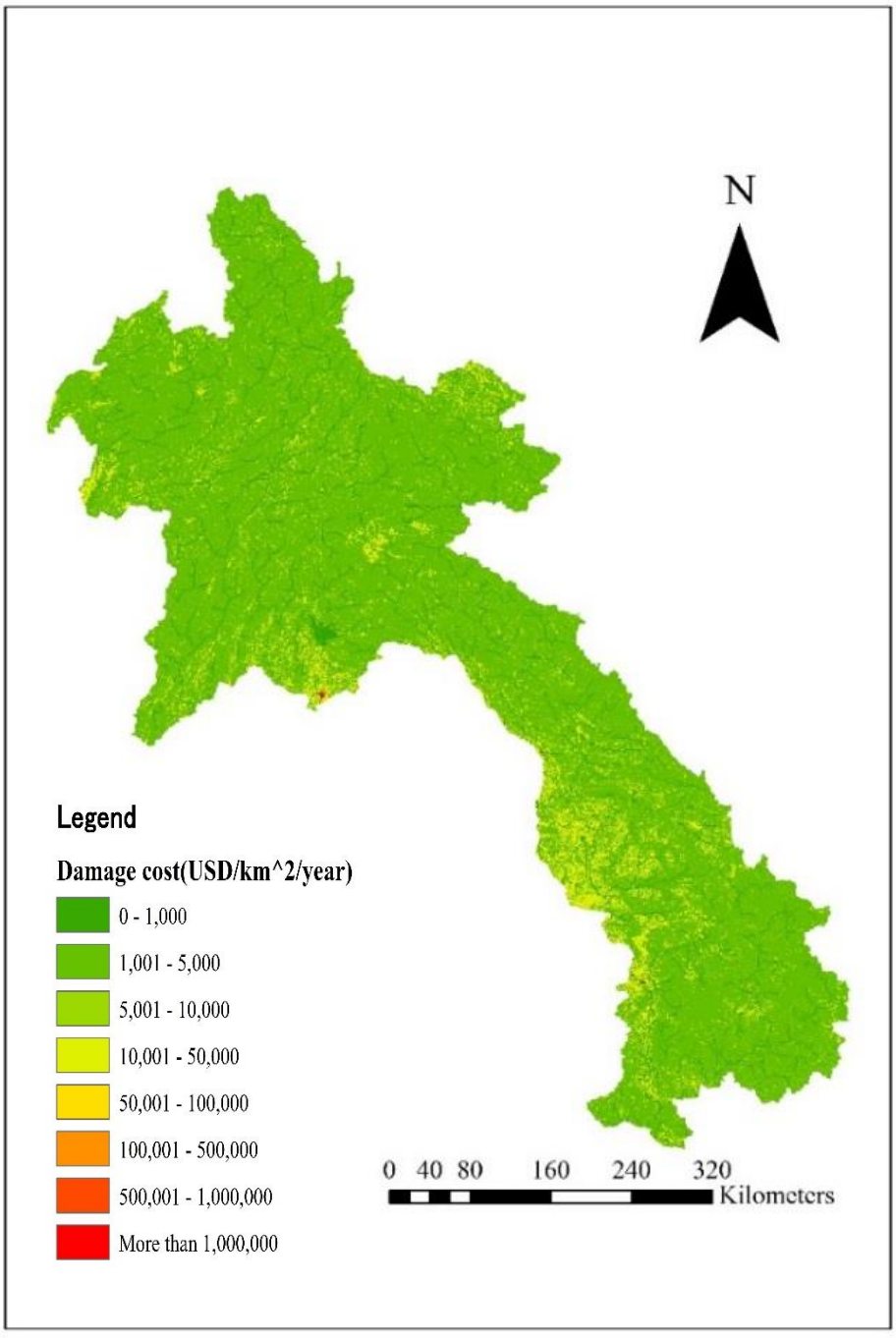

Figure 6-3 Damage cost of land use change risk map in Lao PDR

6.2.4 Damage cost form climate change hazard risk map

In the climate change risk map considering the change in the flood risk (Figure. 6-4), the total damage costs in urban area are 26.3 billion USD/year for near future and RCP 2.6 scenario, which the total damage cost is increase up to 27.63 billion USD/year for far future and RCP 8.5 scenario. The total damage costs in urban area for far future and RCP 8.5 scenario are higher than those of the flood risk (46.7%) and the land use change risk (29.11%). For the climate change risk map considering landslides (Figure. 6-5) shows that the highest total damage costs are 11.6 million USD/year in agricultural areas for far future and RCP 8.5 scenario. These costs are approximately 38.1% higher than those associated with the landslide risk. Hence, climate change has a great effect on the increasing total damage costs of the risk map. Climate change risk maps could be applied for the future design of development plans for the entire country. A comparison of the total damage costs for the flood, land use change and climate change to flood risk maps are shown in Figure. 6-6. Based on the analysis, the climate change impact to flood risk map for far future and RCP 8.5 scenario has the highest total damage costs. This result indicates that climate change is likely to expand the damage costs of the flood risk. Additionally, the change in land use also can amplify the total damage costs. Afterward, We compare the total damage costs from the landslide risk and the landslide risk impacted by climate changes. According to the results (Figure. 6-7) the total damage costs from landslide risk map increase by approximately 300% when compared to total damage cost from climate change impact to landslide map for far future and RCP 8.5 scenario. Even thought, the total damage costs of the landslide risk maps are lower than those of other

risk maps it is because most of the areas affected by landslides are only agricultural areas and paddy fields. Although the mountainous areas suffer least economic impact compare to other area, these areas are worth integrating into the risk maps because the people living in these areas suffer socially and economically from the damage.

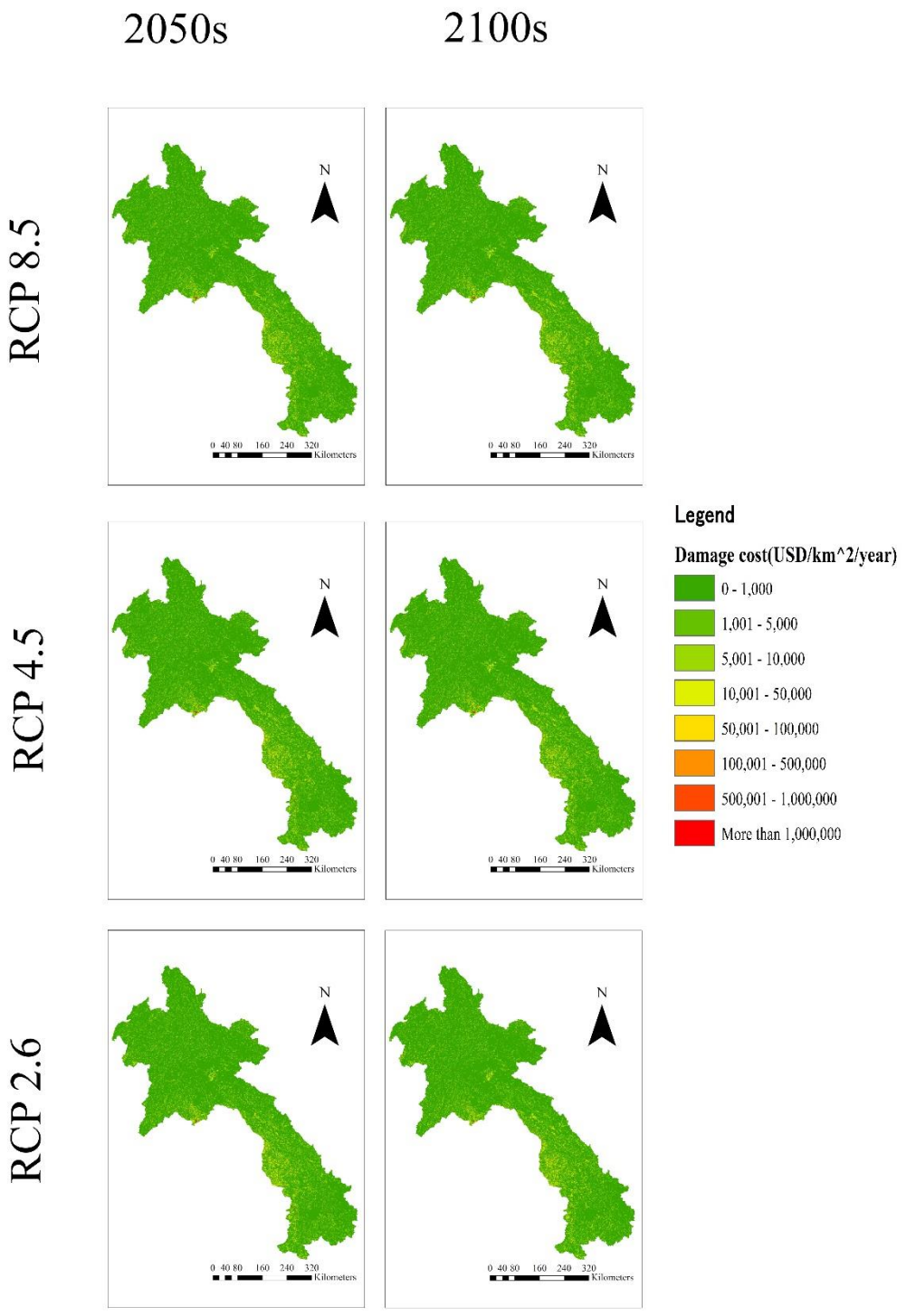

Figure 6-4 Damage cost of climate change impact to flood risk map for RCP 2.6, 4.5 and 8.5 for near future (2050s) and far future (2100s) in Lao PDR

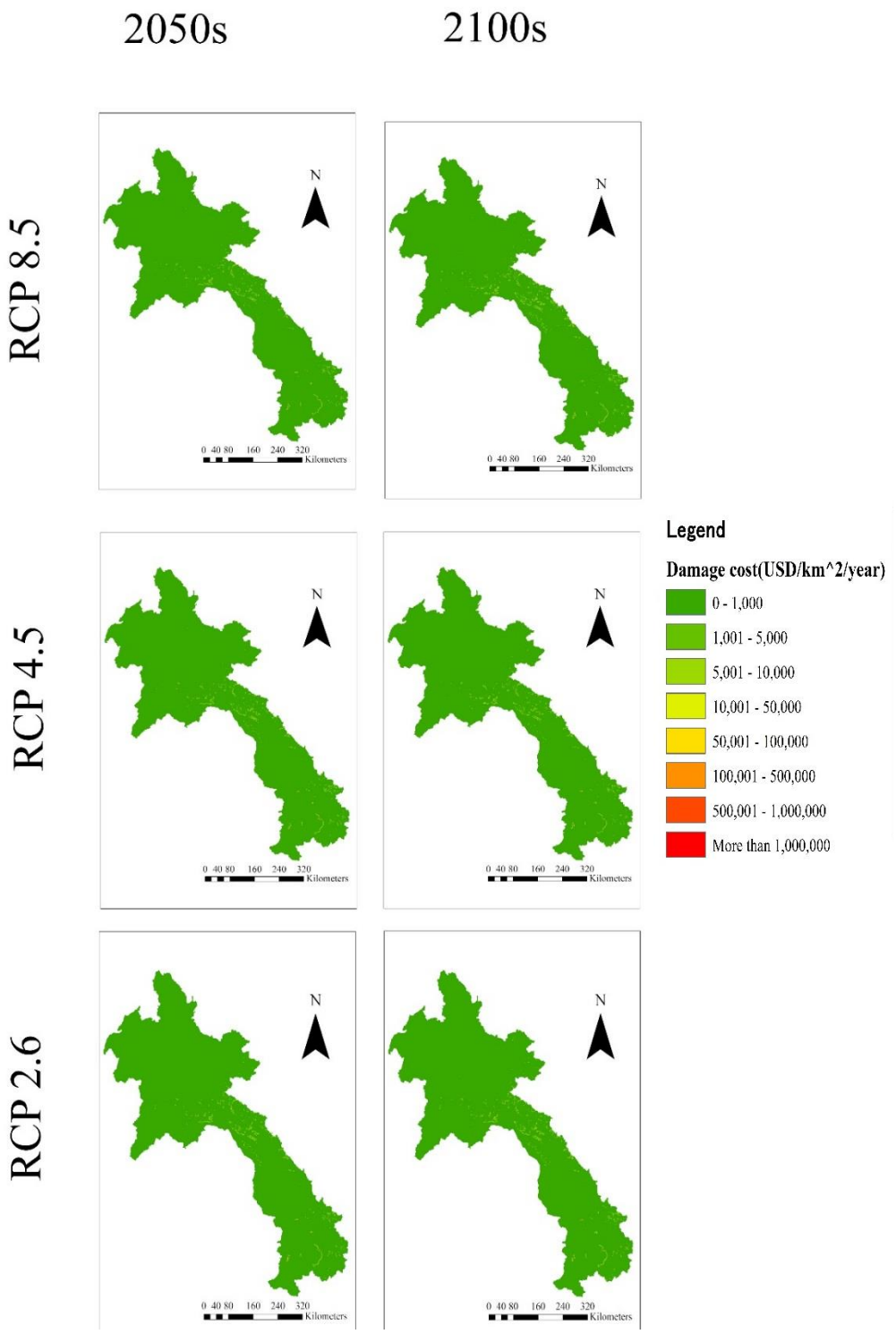

Figure 6-5 Damage cost of climate change impact to land slide risk map for RCP 2.6, 4.5 and 8.5 for near future (2050s) and far future (2100s) in Lao PDR

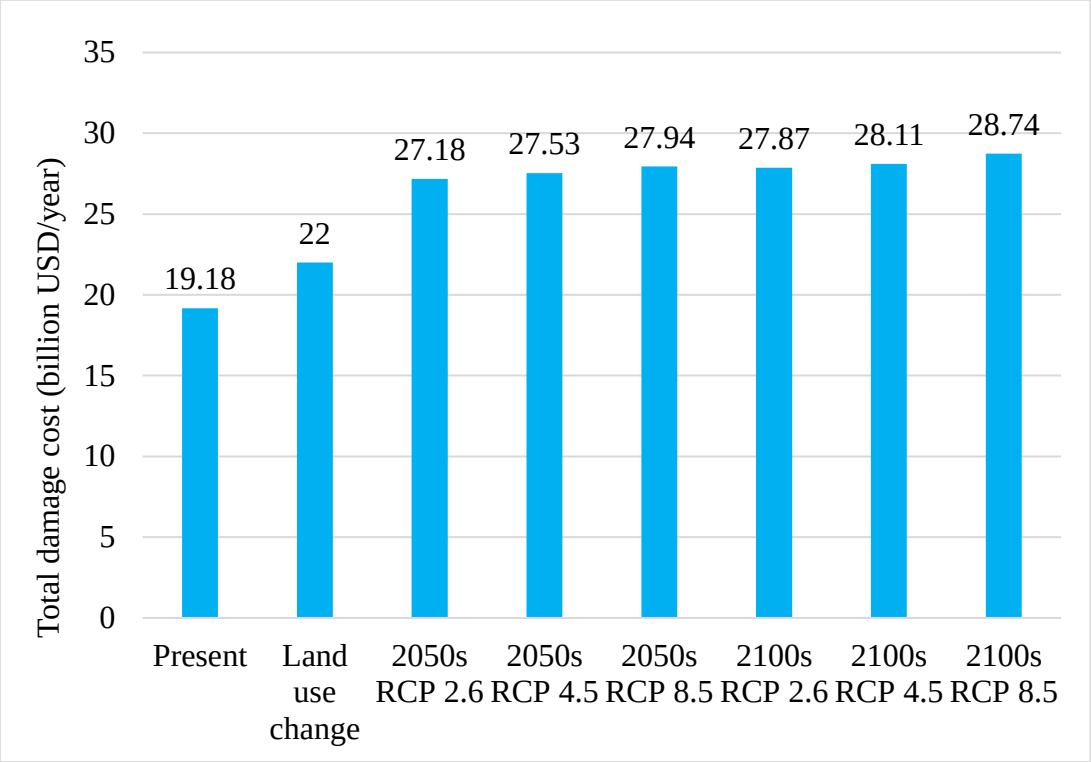

Figure 6-6 Comparison of total damage cost of flood, land use change and climate change impact to flood risks in Lao PDR

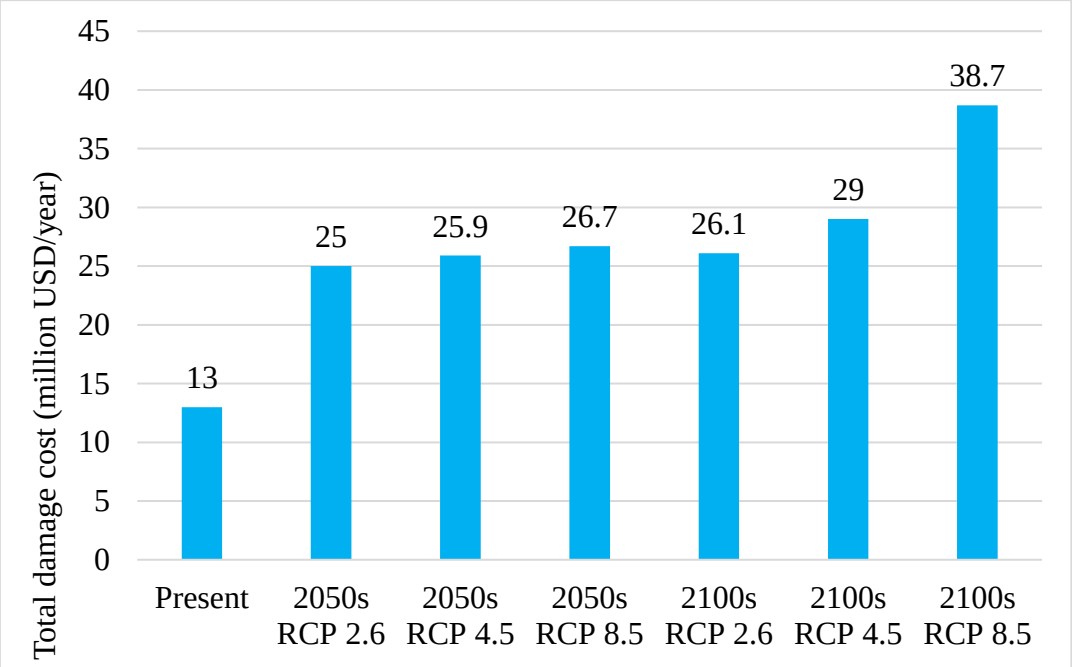

Figure 6-7 Comparison of total damage cost of landslide and climate change impact to landslide risks in Lao PDR

6.2.5 Integrated risk map

The spatial distribution of the damage costs is shown in Figure 6-8. All the integrated risk maps show a similar distribution of risk areas. Based on the Figure 6-8, huge risk areas are located in the southern region because many agricultural areas and paddy fields are located in those area. It is noticeable that very high damage cost areas (more than 1 million USD/year) are located in the central region because this location of urban area. Nevertheless, comparing the total damage costs among integrated risk maps (Figure. 6-9), the total damage costs of the integrated risk for the 2050s and scenario of RCP 2.6, 4.5 and 8.5 are 20.16, 20.31 and 20.48 billion USD/year, respectively, while those for the 2100s scenario of RCP 2.6, 4.5 and 8.5 are 20.45, 20.55 and 20.82 billion USD/year, respectively. Furthermore, the integrated risk maps are analyzed based on the different land use types. The total damage costs for agricultural areas increase in response to the RCP scenarios. Under RCP 2.6, the total damage costs in agricultural areas increase from 293 in the 2050s to 368 million USD/year in the 2100s. Under RCP 4.5, the costs increase from 329 in the 2050s to 404 million USD/year in the 2100s, and under RCP 8.5, they increase from 376 in 2050s to 421 million USD/year in the 2100s. A similar trend is observed in the total damage costs for paddy field areas. That is, the total damage costs under RCP 2.6 increase from 67 in the 2050s to 72 million USD/year in the 2100s. Under RCP 4.5, the costs increase from 71 in the 2050s to 76 million USD/year in the 2100s, and under RCP 8.5, they increase from 74 to 79 million USD/year in the 2100s. Urban areas experience the highest damage costs, among others. The total damage costs under RCP 2.6 increase from 19.8 in the 2050s to 20.01 billion USD/year in the 2100s. Under RCP 4.5, the costs increase from 19.91 in the 2050s to 20.07 billion USD/year in the

2100s, and under RCP 8.5, they increase from 20.03 to 20.32 billion USD/year in the 2100s. The results indicated that climate changes have an influence on the increase in damage costs in Lao PDR. The distribution of the integrated risk maps shows that most of the damage costs are distributed in the central and southern regions of Lao PDR. In the central region, the total damage costs of the integrated risk map under RCP 2.6 increase from 17.3 in the 2050s to 17.4 billion USD/year in the 2100s. Under RCP 4.5, they increase from 17.37 in the 2050s to 17.47 million USD/year in the 2100s, while under RCP 8.5, the costs increase from 17.5 in the 2050s to 17.6 billion USD/year in the 2100s. In the southern areas, under RCP 2.6, the total damage costs increase from 2.79 in the 2050s to 2.97 billion USD/year in the 2100s. Under RCP 4.5, they increase from 2.87 in the 2050s to 3 million USD/year in the 2100s, while under RCP 8.5, the costs increase from 2.9 in the 2050s to 3.14 billion USD/year in the 2100s.

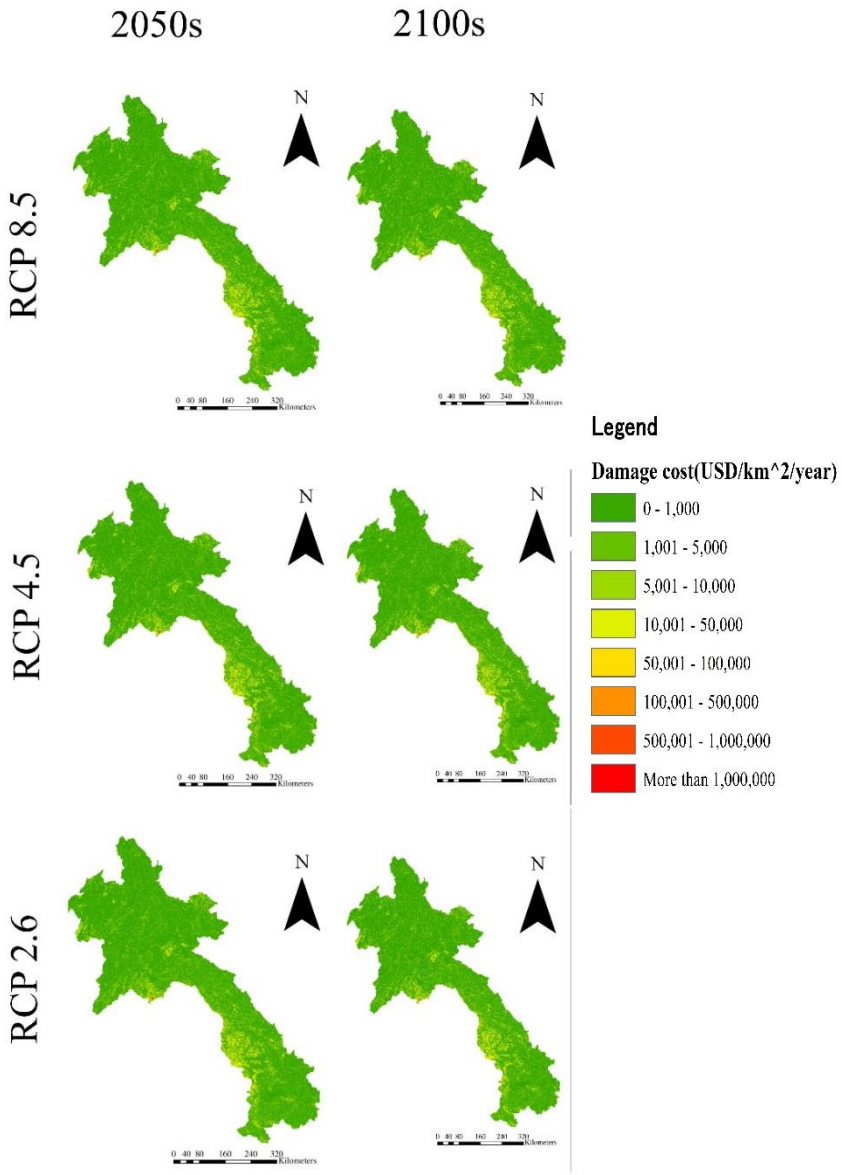

Figure 6-8 Damage cost of integrated risk map for RCP 2.6, 4.5 and 8.5 for near future (2050s) and far future (2100s)

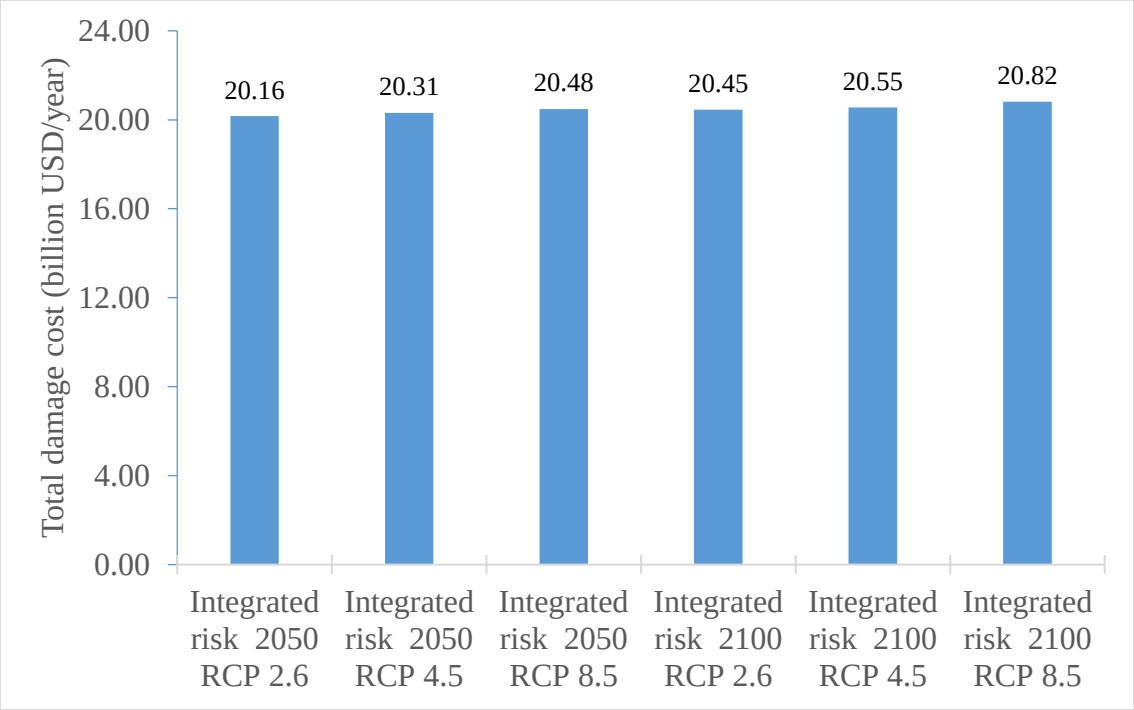

Figure 6-9 Comparison of total damage cost from integrated risks in Lao PDR

6.2.6 Adaptation measure to reduce damage costs

Climate change can results in increase of rainfall intensity lead to flood and landslide and cause serious problem to the population who live near river, downstream and mountainous area. Consequently, those hazard cause damage to crops, properties and make people in rural area stuck in cycle of poverty. One way to minimize the damage from those hazard is to move away from the hazard area (Black et al., 2011). However, before we applying an adaptation measure, effectiveness of that adaptation measure need to be evaluate in term of cost and benefit. In this study, we analyzed relocation adaptation measure of agricultural and paddy field area to reduce damage costs from integrated risk maps of three RCP scenarios. In this study, we consider various hazards. Therefore, the countermeasure have to be applicable and suitable for various hazard. Relocation is one

of basic countermeasure to reduce the damage cost from risk hazard and it can apply to all of hazards that we consider in this study. In addition, our study area Lao PDR have plenty of un-development area witch suitable for agriculture and paddy field, only manpower are lacking to develop those area. by apply relocation adaptation is can provide many advantage such as reduce potential damage cost from risk hazard, development of new agriculture and paddy field area and so on. In addition, we will use integrated risk map of near future (2010-2050) as the baseline for this study. Cost-benefit analyze was used to identify relocatable area in integrated risk maps. Relocation costs of agricultural and paddy field in Lao PDR were obtain from Ministry of Agricultural and Forestry due to the lack of quantitative data for relocation cost of urban area, in this study we consider only agricultural and paddy field area.

According to Figure 6-10 and 6-11 the relocation cost in Vientiane Capital is highest for both of agricultural and paddy field. By using cost-benefit analysis for agricultural and paddy field, the duration of project is need. In this study, we used integrated risk map of near future as a baseline map, therefore the duration of project is from 210 to 2050 (40 years). Figures 6-12 to Figure 6-14 describe the spatial distribution of the cost-benefit analysis in different RCP scenario, which each scenario have two discount rate (r = 0.05 and r =0.1). According to the results, for the discount rate = 0.05, in RCP8.5 around 81 % of agricultural and paddy field areas from integrated risk map are not suitable for relocation (B/C <1), in case of RCP 4.5 around 79 % and for RCP 2.6 78 % of agricultural and paddy field total area are not suitable for relocation. In case of discount rate = 0.1 for all RCP over 89-91% of agricultural and paddy field area not suitable for relocation. If we assume that all of those area will relocate from risk area, the total damage cost from integrated risk map will decrease from 5-7 % (discount rate = 0.05) and 1-3 % (discount

rate = 0.1)

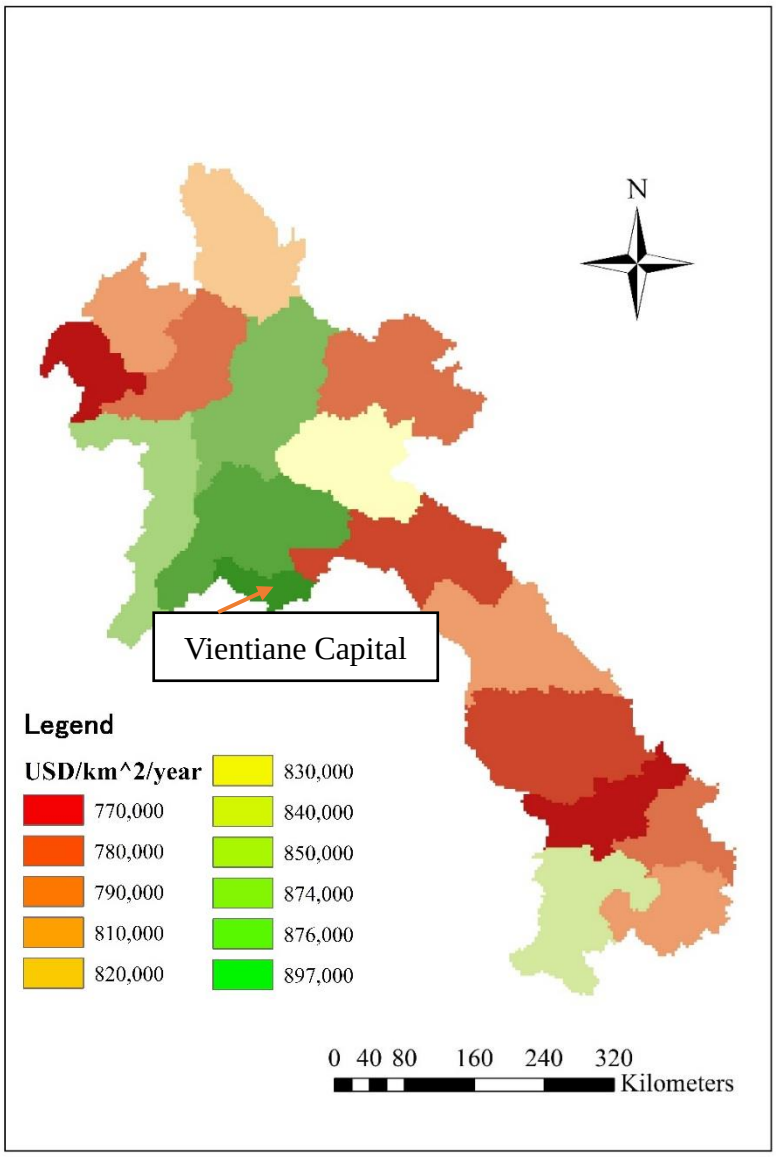

Figure 6-10 Relocation cost of agricultural area

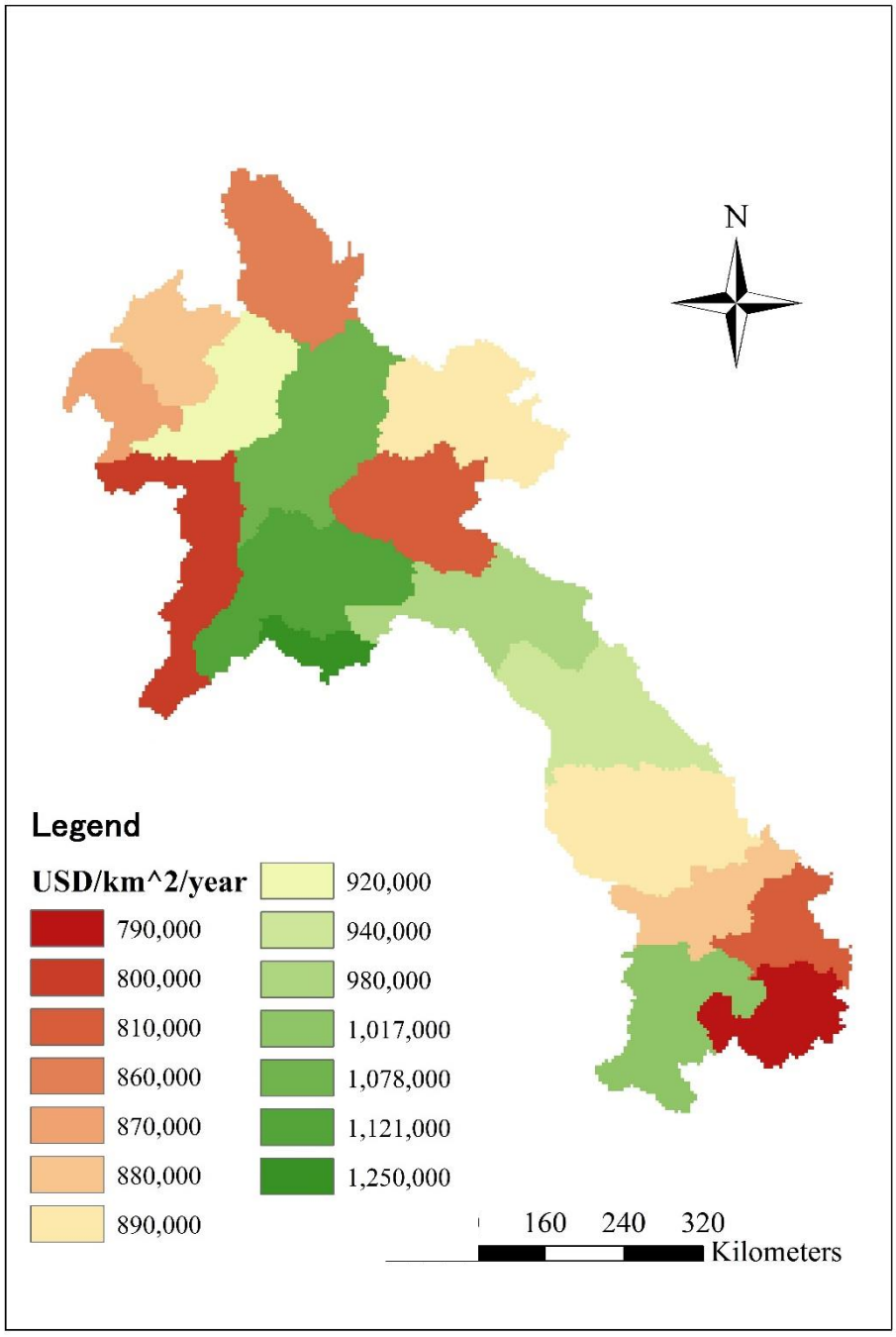

Figure 6-11 Relocation cost of paddy field

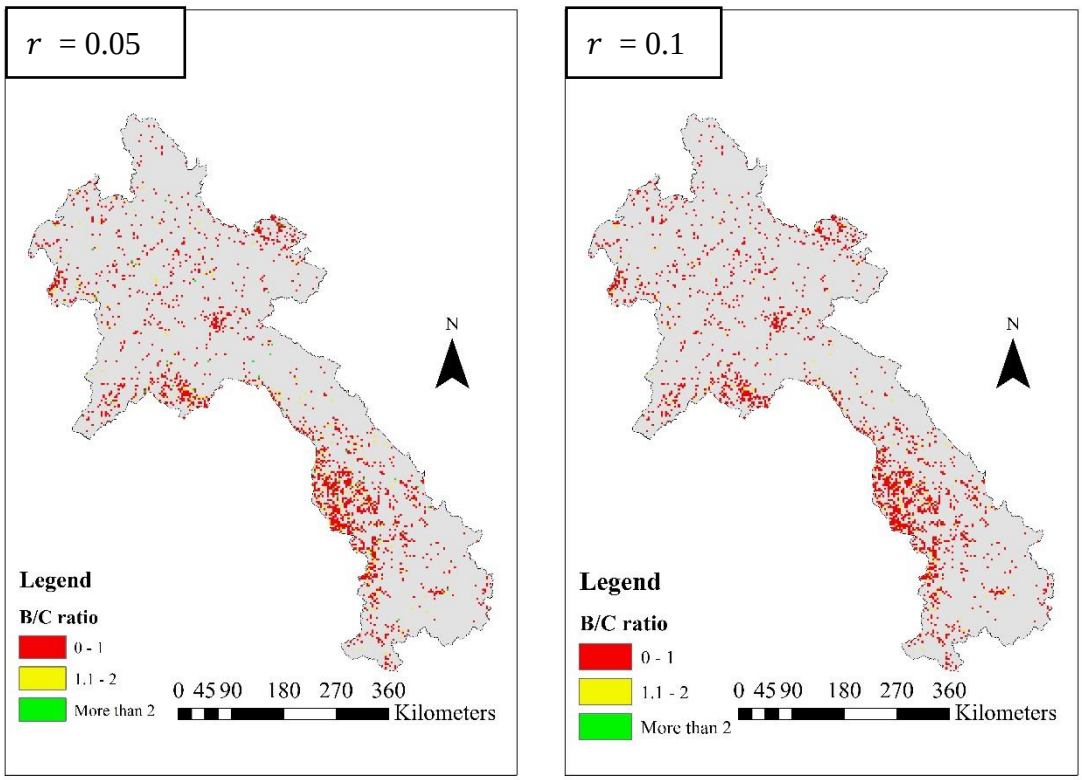

Figure 6-12 B/C ratio with discount rates (r = 0.05 and 0.1) in the case of relocation from agricultural and paddy field with RCP 2.6 scenario for the intergrated risk map

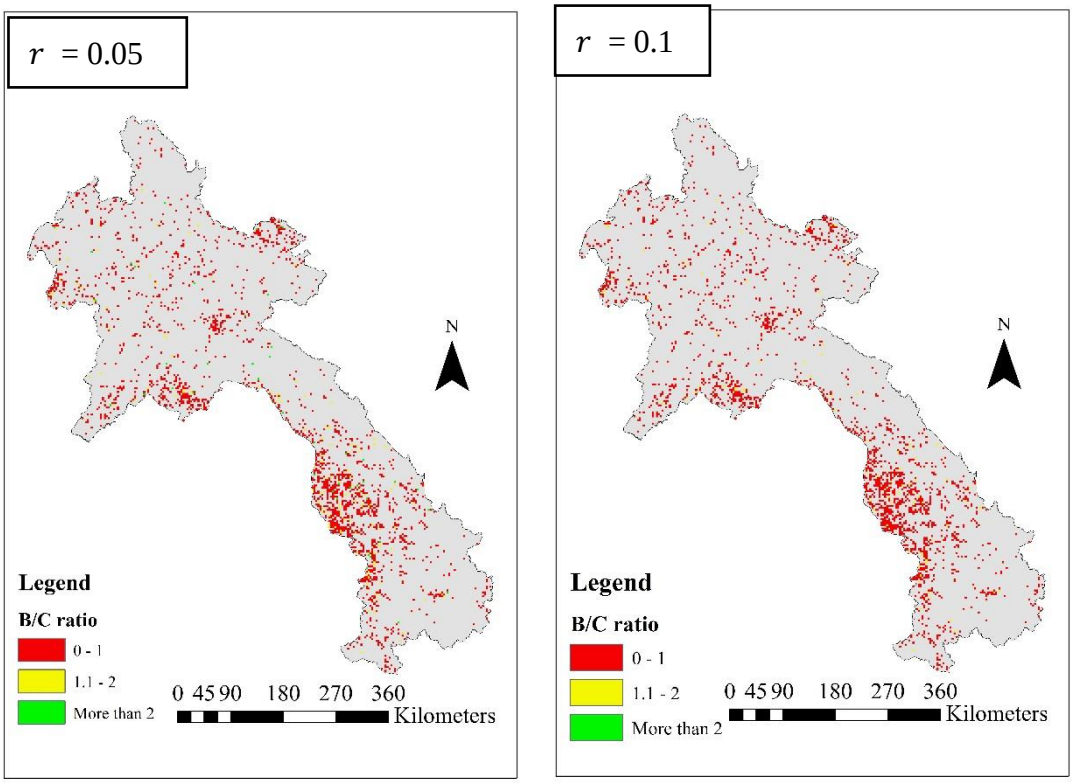

Figure 6-13 B/C ratio with discount rates (r = 0.05 and 0.1) in the case of relocation from agricultural and paddy field with RCP 4.5 scenario for the intergrated risk map

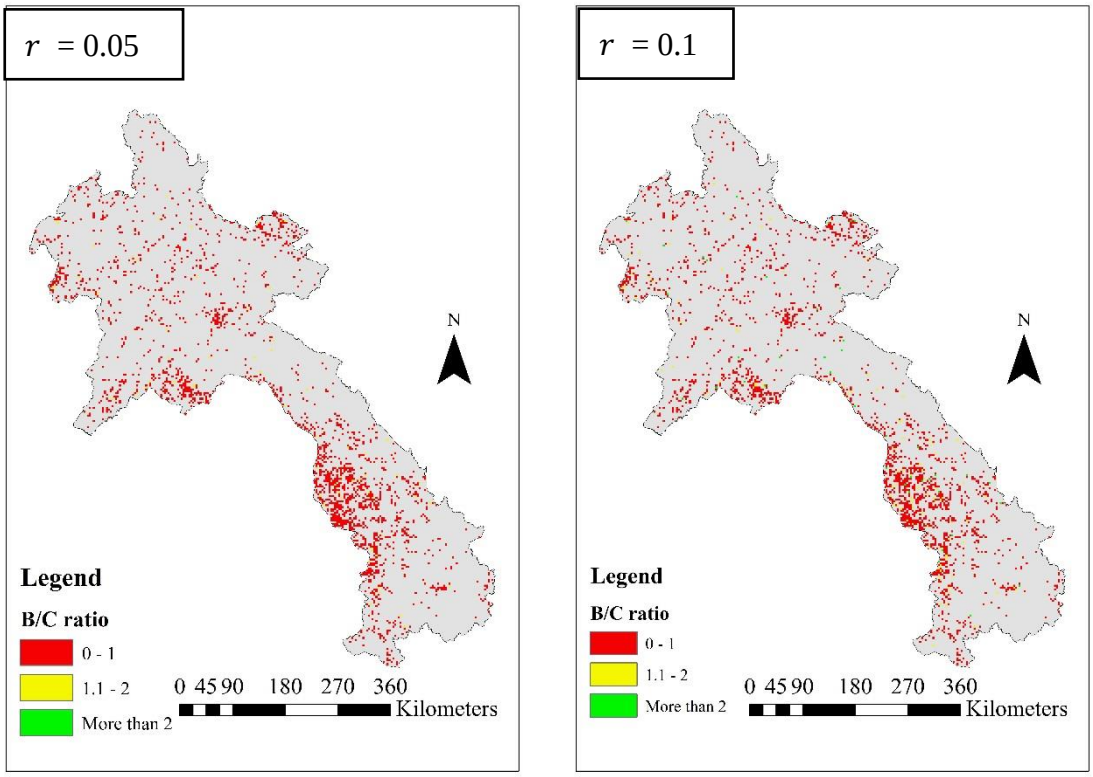

Figure 6-14 B/C ratio with discount rates (r = 0.05 and 0.1) in the case of relocation from agricultural and paddy field with RCP 8.5 scenario for the intergrated risk map

6.3 Discussion

Flood risk map have illustrated distribution of potential damage cost from risk area across the study area. It is noteworthy that most of distribution of risk area and the potential damage costs were mostly distributed in central and southern region of Lao PDR. Based on the finding, high damage cost from risk area is visible around central-southern region of Lao PDR because central region is a location of the capital of Lao PDR. Total damage cost from risk areas in each province were shows in Table 6-1. The total damage cost from risk areas of flood risk map is around 19.18 billion USD/year. If we considering by regional, central region have the highest of total damage cost (13.9 billion USD/year), southern region have the second high of total damage cost (4.4 billion USD/year) and the last is northern region (0.88 billion USD/year). The capital of Lao PDR Vientiane capital have the highest of total damage cost (10.71 billion USD/year) among all the provinces. In the southern region, Khammouan and Champasak province are one of the big province and developed area of Lao PDR. Both of the province have highest damage cost among the province in southern region. The total damage cost from risk area in Khammouan province is around 1.78 billion USD/year and the total damage cost from risk area in Champasak province is around 1.45 billion USD/year.

Table 6-1 Total damage cost from flood risk areas in each province.

Province name	Total damage cost (Billion USD/year)
Attapeu	0.02
Bokeo	0.55
Bolikhamxai	1.92
Champasak	1.45
Houaphan	0.07
Khammouan	1.78
Louang Namtha	0.04
Louang Prabang	0.07
Oudomxai	0.04
Phongsaly	0.05
Salavan	0.84
Savannakhet	0.36
Vientiane	1.18
Vientiane Capital City	10.71
Xaignabouly	0.05
Xekong	0.02
Xiangkouang	0.09
Total damage cost across the country	19.18

Land use change risk map illustrated similar of distribution to flood risk map but with higher magnitude and damage cost. Overall, the total damage cost from risk area are increase when compare land use change risk map to the flood risk map (Table 6-2). The total damage costs from risk areas of land use change risk map (22 billion USD/year) are increase around 15% when compared to total damage costs from risk areas of current flood hazard map. Similarly to flood risk map, Vientiane capital city have the highest total damage costs (12.11 billion USD/year) among all the province. The total damage cost from Vientiane capital increase around 13.1% compare to the total damage costs from Vientiane capital risk area of flood risk map (Table 6-2). Bolikhamxai and Vientiane province have the highest percentage of total damage costs increase from risk areas of land use change risk map compare to total damage costs from risk areas of current flood risk map. The total damage costs from Bolikhamxai province risk areas of land use change risk map is around 2.53 billion USD/year. It is increase around 31.5 % compare to the total damage costs from Bolikhamxai province risk areas of current flood risk map. The total damage costs from Vientiane province risk areas of land use change risk map is around 1.59 billion USD/year. It is increase around 34.3 % compare to the total damage costs from Vientiane province risk areas of current flood risk map. Even though, the Vientiane capital city have the highest total damage costs among all of the province but Bolikhamxai and Vientiance province have a significant increase of total damage costs. Therefore, government of Lao PDR need to consider these two provinces when the measurement or adaptation planning are made.

Table 6-2 Total damage cost from land use change impact to flood risk areas in each province.

Province name	Total damage cost (Billion USD/year)	Percentage increase from current flood risk map
Attapeu	0.02	8.8%
Bokeo	0.56	1.1%
Bolikhamxai	2.53	31.5%
Champasak	1.54	6.4%
Houaphan	0.08	8.7%
Khammouan	1.81	6.3%
Louang Namtha	0.04	16.4%
Louang Prabang	0.08	8.4%
Oudomxai	0.04	16.4%
Phongsaly	0.05	13.4%
Salavan	0.91	8.7%
Savannakhet	0.44	20.7%
Vientiane	1.59	34.3%
Vientiane Capital City	12.11	13.1%
Xaignabouly	0.06	11.8%
Xekong	0.02	11.7%
Xiangkouang	0.10	11.5%
Total damage cost across the country	22	

Land slide risk map shown the distribution of potential damage cost from risk area from land slide around mountainous of central and southern region. The risk area in mountainous area will cause impact to the agricultural and paddy field areas of ethic group who have livelihood near mountainous area. Total damage costs from risk areas of land slide risk map is around 13 million USD/year. Central region have highest total damage cost (11.3 million USD/year) from risk areas of land slide risk map. For the southern region, total damage cost is around 1.1 million USD/year and for the northern region is around 0.6 million USD/year. Among all of province of Lao PDR, Vientiane, Xiangkoung, Blolikhamxai and Vientiane have high mountainous area. Based on Table 6-3, Bolikhamxai province have highest total damage costs from risk area of land slide risk map (4.84 million USD/year). Vientiane province have total damage costs from risk area of landslide risk map around 3.6 million USD/year. Xiankoung province also have high total damage costs (2.66 million USD/year). These provinces have higher damage cost than other province due to the agricultural and paddy fiend in these three province area located near mountainous area. The landslide risk map can be used for developing counter measurement and adaptation method for reduce the potential of damage cost in concern area.

Table 6-3 Total damage cost from landslide risk areas in each province.

Province name	Total damage cost (Million USD/year)
Attapeu	0.55
Bokeo	0
Bolikhamxai	4.84
Champasak	0
Houaphan	0.60
Khammouan	0.54
Louang Namtha	0
Louang Prabang	0
Oudomxai	0
Phongsaly	0
Salavan	0
Savannakhet	0
Vientiane	3.60
Vientiane Capital City	0
Xaignabouly	0
Xekong	0.20
Xiangkouang	2.66
Total damage cost across the country	13

Climate change impacts to flood risk maps or future flood risk maps are represented by the flood risk map under future climate condition with 3 scenario (RCP2.6, 4.5 and 8.5) and 2 time periods (near future and far future). The flood risk area under influences of the future rainfall condition shows the increase of risk area and potential of damage cost across the country. By considering the near future period, the total damage costs of risk area from climate change impacts to flood risk map increases from 27.18 billion USD/year under the scenario of RCP 2.6 to 27.53 billion USD/year under the scenario of RCP 4.5. Figure 6-15 (d) shows the area of the damage cost increase when comparing the scenario of RCP 2.6 and RCP 4.5 Luang Namtha province has the highest increase (23.89%) of total damage costs of risk areas when comparing the future flood risk map under scenario RCP 2.6 to that under RCP 4.5 (Table 6-4). Savannakhet province also have high increase (19.88%) of total damage costs of risk areas when comparing the future risk map under scenario RCP 2.6 to the under RCP 4.5. Under the scenario of RCP 8.5 the total damage cost of risk areas from flood risk map increases to 27.94 billion USD/year. Figure 6-15 (e) shows the area of the damage cost increase when comparing the scenario of RCP 8.5 and RCP 4.5. Among others, Khammoun province has the highest increase (5%) of total damage cost from risk areas when comparing the future flood risk map under scenario RCP 4.5 and RCP 8.5 (Table 6-5). Many provinces from climate change impacts to flood risk map with near future have continuously increase of damage cost from RCP 2.6 to RCP 8.5. For instance, the total damage cost of risk area in Vientaine province increase around 2.56% comparing the total damage cost of risk area under the scenario RCP 2.6 to that under RCP 4.5 and the total damage cost of risk area in Bolikhamxai increase around 2.2% comparing the total damage cost of risk area under the scenario RCP 4.5 to that under RCP 8.5. For the far future period, total damage cost

of risk area from increases from 27.87 billion USD/year under the scenario of RCP 2.6 to 28.11 billion USD/year under the scenario of RCP 4.5. Figure 6-16 (d) shows the area of the damage cost increase when comparing the scenario of RCP 4.5 and RCP 2.6. Khammouan province has the highest increase (2.79%) of total damage costs of risk areas when comparing the future flood risk map under the scenario of RCP 2.6 and RCP 4.5 (Table 6-6). Under the scenario of RCP 8.5 the total damage costs of risk areas from future flood risk map is 28.74 billion USD/year. Figure 6-16 (e) shows the area of the damage cost increase when comparing the scenario of RCP 8.5 and RCP 4.5. Khammouan province has the highest increase (7.39%) of the total damage costs of risk areas when comparing the future flood risk map under the scenario of RCP 4.5 and RCP 8.5 (Table 6-7). The total damage costs of risk areas in most of the provinces from climate change impacts to flood risk map with far future increase continually from RCP 2.6 to RCP 8.5 such as Champasak province. The total damage costs of risk areas in Champasak province increase around 2.2% comparing the total damage costs of risk areas from future flood risk map under the scenario RCP 2.6 to that under RCP 4.5 and The total damage costs of risk areas in Champasak province increase around 5.23% comparing the total damage costs of risk areas from future flood risk map under the scenario RCP 4.5 to that under RCP 8.5. According to the results, the significantly increase of damage cost of risk areas in future flood risk map for all RCP scenarios is observed.

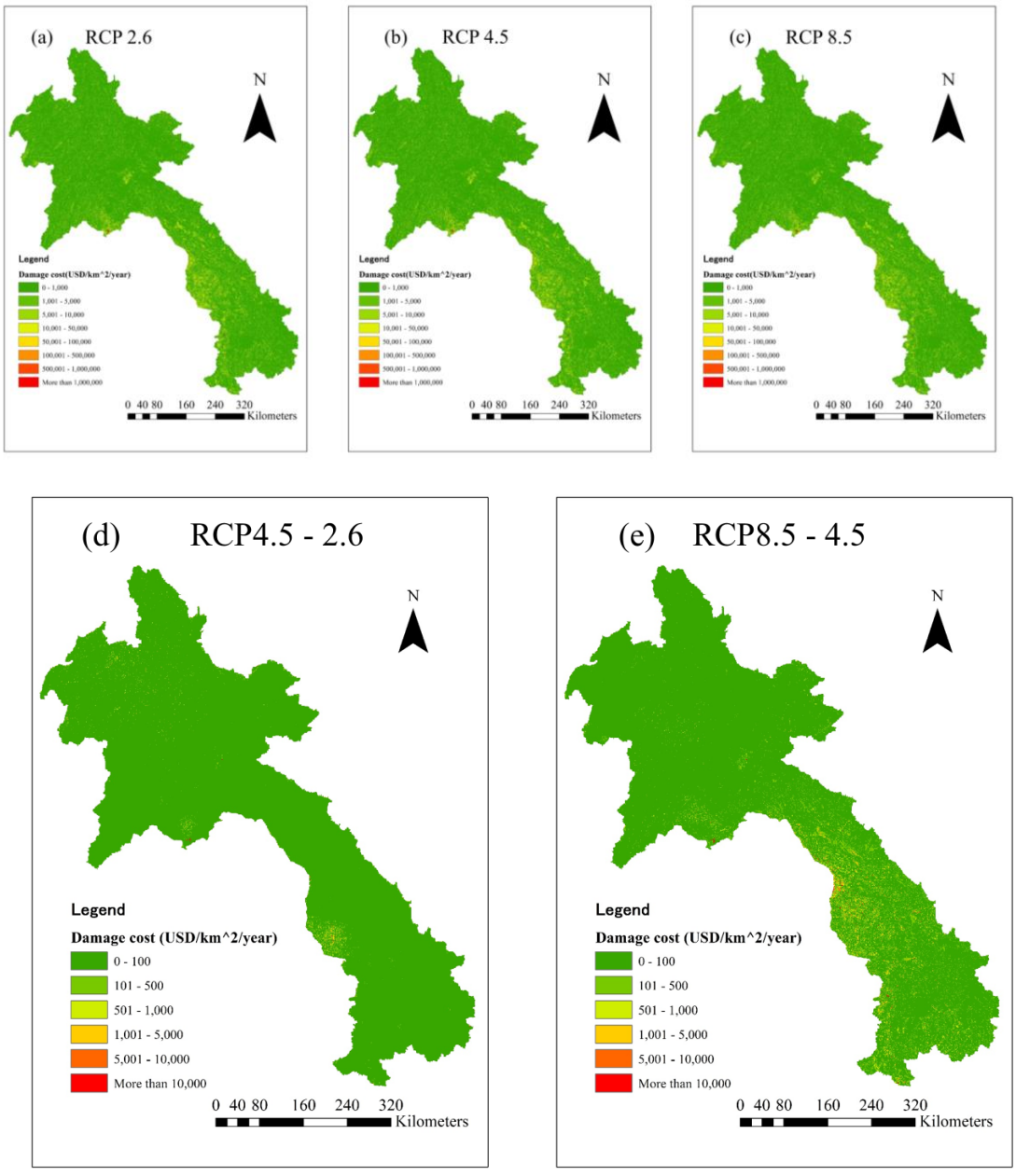

Figure 6-15 Future flood risk maps under scenario of (a) RCP 2.6, (b) RCP 4.5, (c) RCP 8.5, the difference of damage costs between (d) RCP 4.5 and RCP 2.6 scenario, and (e) RCP 8.5 and RCP 4.5 scenario during near future

Table 6-4 Total damage cost from climate change impact to flood risk map in each province and percentage of increase between RCP 4.5 and RCP 2.6 scenario during near future

Province name	Total damage cost from risk area under scenario RCP 2.6 (Billion USD/year)	Total damage cost from risk area under scenario RCP 4.5 (Billion USD/year)	Percentage increase of risk area between RCP 4.5 and 2.6
Attapeu	0.02	0.023	0.03%
Bokeo	1.33	1.333	0.37%
Bolikhamxai	2.08	2.088	0.53%
Champasak	2.30	2.301	0.20%
Houaphan	0.09	0.085	0.12%
Khammouan	2.88	2.893	0.36%
Louang Namtha	0.04	0.052	23.89%
Louang Prabang	0.09	0.089	0.13%
Oudomxai	0.04	0.042	0.06%
Phongsaly	0.05	0.052	0.07%
Salavan	1.12	1.139	1.58%
Savannakhet	0.41	0.497	19.88%
Vientiane	1.24	1.274	2.56%
Vientiane Capital City	15.32	15.496	1.16%
Xaignabouly	0.06	0.060	0.09%
Xekong	0.02	0.017	0.02%
Xiangkouang	0.09	0.087	0.12%
Total damage cost across the country	27.18	27.53	

Table 6-5 Total damage cost from climate change impact to flood risk map in each province and percentage of increase between RCP 8.5 and RCP 4.5 scenario during near future

Province name	Total damage cost from risk area under scenario RCP 4.5 (Billion USD/year)	Total damage cost from risk area under scenario RCP 8.5 (Billion USD/year)	Percentage increase of risk area between RCP 8.5 and 4.5
Attapeu	0.023	0.023	0.04%
Bokeo	1.333	1.363	2.31%
Bolikhamxai	2.088	2.164	3.61%
Champasak	2.301	2.393	3.98%
Houaphan	0.085	0.085	0.15%
Khammouan	2.893	3.037	5.00%
Louang Namtha	0.052	0.052	0.09%
Louang Prabang	0.089	0.089	0.15%
Oudomxai	0.042	0.042	0.07%
Phongsaly	0.052	0.052	0.09%
Salavan	1.139	1.162	1.97%
Savannakhet	0.497	0.501	0.86%
Vientiane	1.274	1.302	2.20%
Vientiane Capital City	15.496	15.508	0.08%
Xaignabouly	0.060	0.061	0.10%
Xekong	0.017	0.017	0.03%
Xiangkouang	0.087	0.088	0.15%
Total damage cost across the country	27.53	27.94	

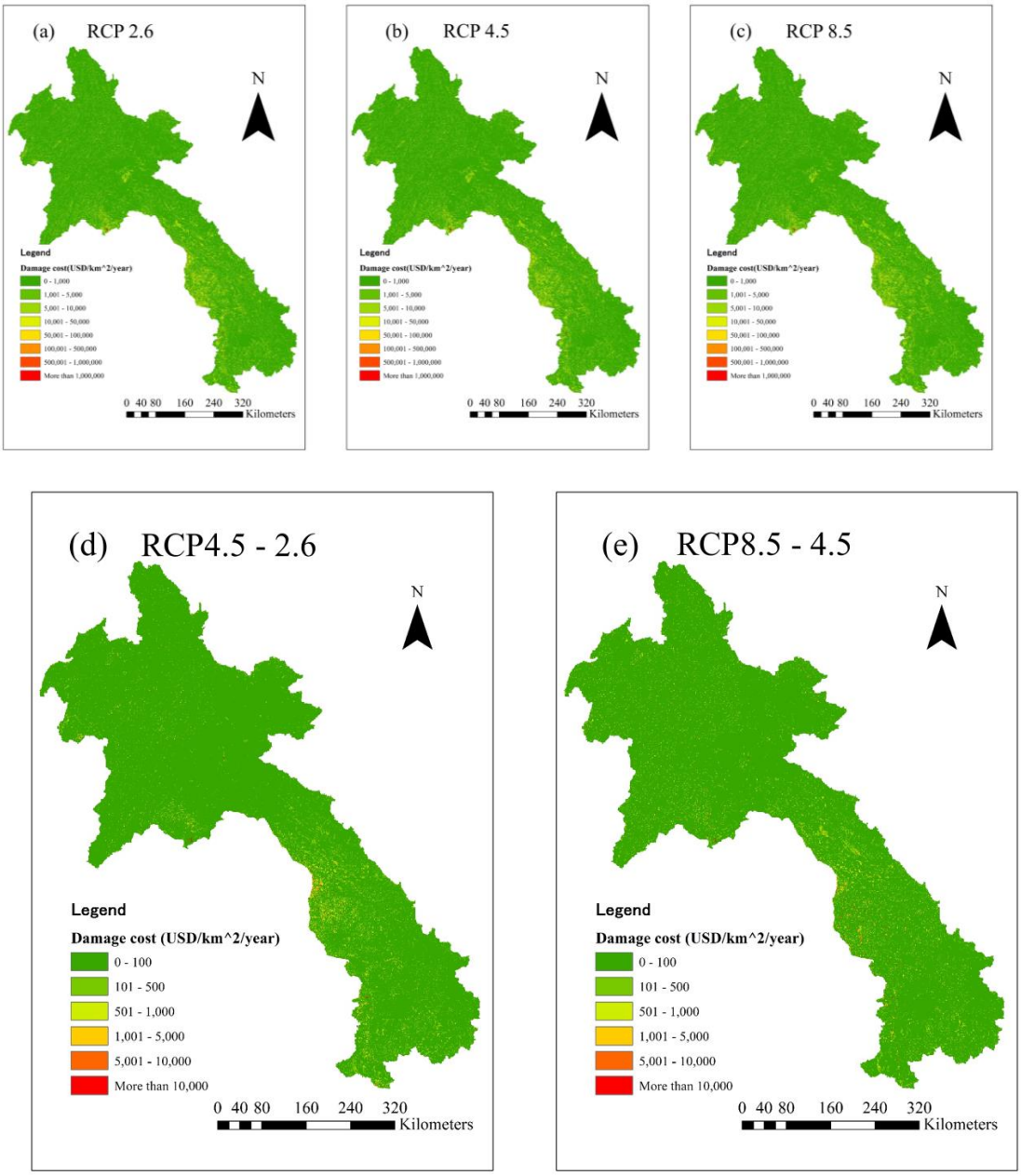

Figure 6-16 Future flood risk maps under scenario of (a) RCP 2.6, (b) RCP 4.5, (c) RCP 8.5, the difference of damage costs between (d) RCP 4.5 and RCP 2.6 scenario, and (e) RCP 8.5 and RCP 4.5 scenario during far future

Table 6-6 Total damage cost from climate change impact to flood risk map in each province and percentage of increase between RCP 4.5 and RCP 2.6 scenario during far future

Province name	Total damage cost from risk area under scenario RCP 2.6 (Billion USD/year)	Total damage cost from risk area under scenario RCP 4.5 (Billion USD/year)	Percentage increase of risk area between RCP 4.5 and 2.6
Attapeu	0.023	0.023	0.02%
Bokeo	1.358	1.375	1.26%
Bolikhamxai	2.150	2.192	1.99%
Champasak	2.376	2.428	2.20%
Houaphan	0.085	0.085	0.08%
Khammouan	3.011	3.095	2.79%
Louang Namtha	0.052	0.052	0.05%
Louang Prabang	0.089	0.089	0.08%
Oudomxai	0.042	0.042	0.04%
Phongsaly	0.052	0.052	0.05%
Salavan	1.157	1.170	1.07%
Savannakhet	0.500	0.503	0.46%
Vientiane	1.297	1.313	1.20%
Vientiane Capital City	15.512	15.525	0.08%
Xaignabouly	0.061	0.061	0.06%
Xekong	0.017	0.017	0.02%
Xiangkouang	0.088	0.088	0.08%
Total damage cost across the country	27.87	28.11	

Table 6-7 Total damage cost from climate change impact to flood risk map in each province and percentage of increase between RCP 8.5 and RCP 4.5 scenario during far future

Province name	Total damage cost from risk area under scenario RCP 4.5 (Billion USD/year)	Total damage cost from risk area under scenario RCP 8.5 (Billion USD/year)	Percentage increase of risk area between RCP 8.5 and 4.5
Attapeu	0.023	0.023	0.05%
Bokeo	1.375	1.420	3.28%
Bolikhamxai	2.192	2.307	5.23%
Champasak	2.428	2.569	5.80%
Houaphan	0.085	0.086	0.20%
Khammouan	3.095	3.323	7.39%
Louang Namtha	0.052	0.052	0.12%
Louang Prabang	0.089	0.090	0.21%
Oudomxai	0.042	0.042	0.10%
Phongsaly	0.052	0.053	0.13%
Salavan	1.170	1.202	2.79%
Savannakhet	0.503	0.509	1.20%
Vientiane	1.313	1.354	3.13%
Vientiane Capital City	15.525	15.545	0.13%
Xaignabouly	0.061	0.061	0.14%
Xekong	0.017	0.017	0.04%
Xiangkouang	0.088	0.088	0.21%
Total damage cost across the country	28.11	28.74	

Climate change impacts to landslide risk maps or future landslide risk maps are represented by the land slide risk map under future climate condition with 3 scenarios and 2 time periods. By considering the near future period, the total damage costs of risk areas from future landslide risk map is around 25 million USD/year under the scenario of RCP 2.6 and it increases to 25.9 million USD/year under the scenario of RCP 4.5. Figure 6-17 (d) shows the area of damage costs of risk areas increase when comparing the scenario of RCP 2.6 and RCP 4.5. Bolikhamxai province have highest of total damage costs from risk areas of future landslide risk map. The Bolikhamxai province's total damage costs of risk areas increases from 6.84 million USD/year under the scenario of RCP 2.6 to 6.99 million USD/year under the scenario of RCP 4.5 (Table 6-8). In addition, Xekong province have the highest percentage increase (6.82%) of total damage cost for risk area among all of province. Under the scenario of RCP 8.5 the total damage costs of risk areas increases to 26.7 million USD/year. Figure 6-17 (e) shows the damage costs of risk areas increase when comparing the scenario of RCP 8.5 and RCP 4.5. Among others, Attappeu, Houaphan and Xekong province have the highest increase of damage costs of risk areas when comparing future landslide risk map under scenario of RCP 4.5 and RCP 8.5 (Table 6-9). Many provinces from climate change impacts to landslide risk map with near future have continuously increase of total damage cost from risk area from RCP 2.6 to RCP 8.5. For example the total damage costs of risk areas in Houaphan province increase from 2.60 million USD/year under the scenario of RCP 2.6 to 2.75 million USD/year under the scenario of RCP 4.5 and increases to 2.88 million USD/year under scenario of RCP 8.5. For the far future, under scenario of RCP 2.6 the total damage costs of risk areas is 26.1 million USD/year and increases to 29 million USD/year under scenario of RCP 4.5. Figure 6-18 (d) shows the damage costs of risk areas increase when comparing the

scenario of RCP 4.5 and RCP 2.6. Comparing the increase of the damage costs of risk areas between future landslide risk map under RCP 2.6 and RCP 4.5 scenario, Xekong province has the highest increase (20.29%). That is, the total damage costs of risk areas increases from 2.38 million USD/year under RCP 2.6 scenario to 2.87 million USD/year under RCP 4.5 scenario (Table 6-10). Under the scenario of RCP 8.5, the total damage costs for the risk areas from climate change impact to landslide risk map increases to 38.37%. Figure 6-18 (e) shows the damage costs of risk areas increase when comparing the scenario of RCP 8.5 and RCP 4.5. Bolikhamxai province has the highest increase (61.49%) of total damage cost from risk area when comparing between future landslide risk map under scenario of RCP 4.5 and RCP 8.5 (Table 6-11). The total damage cost of risk area in most of the provinces from climate change impacts to landslide risk map with far future increase continually from RCP 2.6 to RCP 8.5 for example Vientiane province. The total damage costs of risk areas in Vientiane province increase from 5.78 million USD/year under scenario of RCP 2.6 to 6.26 million USD/year under the scenario RCP 4.5 and increase to 8.88 million USD /year under RCP 8.5 scenario.

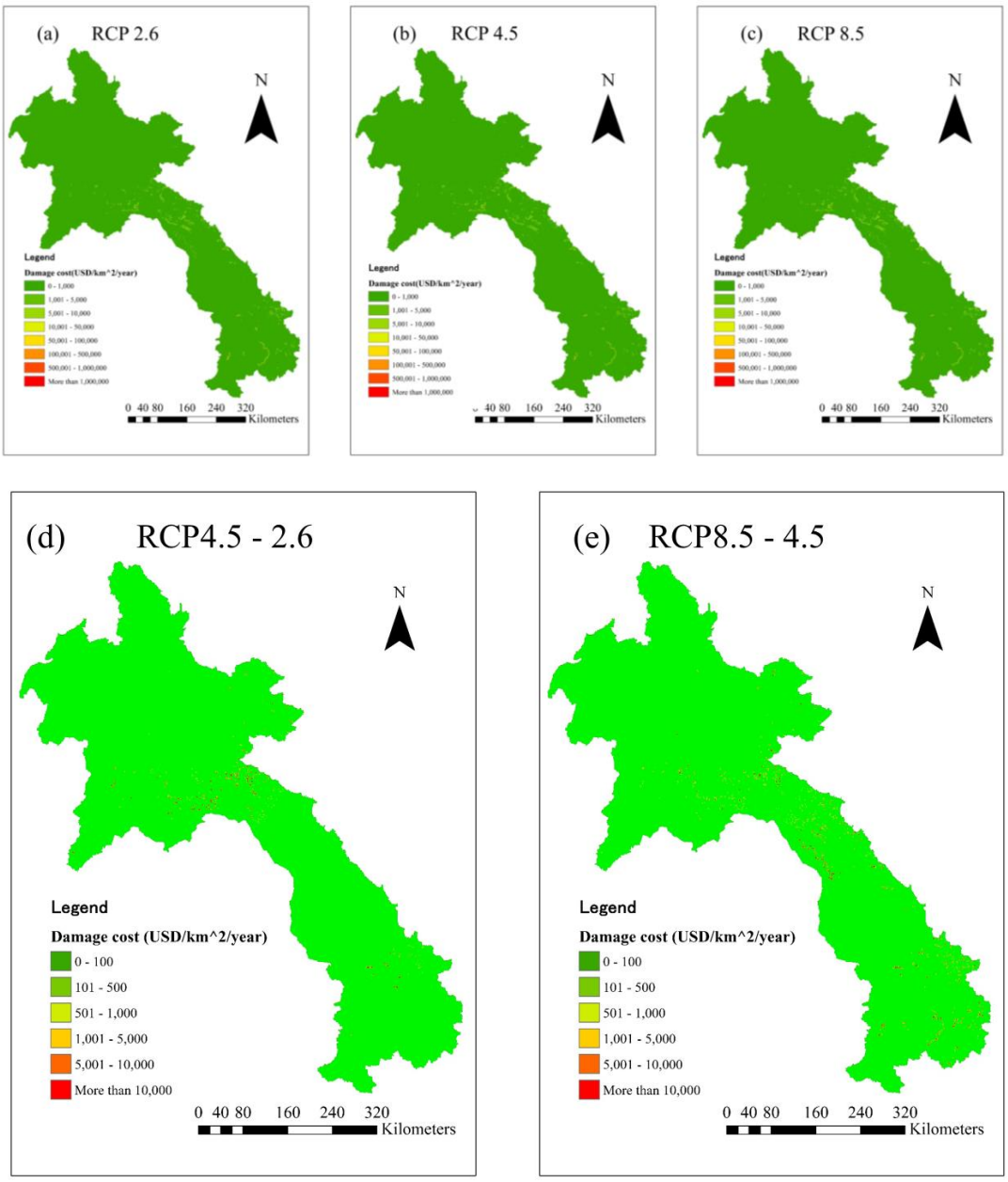

Figure 6-17 Future landslide risk maps under scenario of (a) RCP 2.6, (b) RCP 4.5, (c) RCP 8.5, the difference of damage costs between (d) RCP 4.5 and RCP 2.6 scenario, and (e) RCP 8.5 and RCP 4.5 scenario during near future

Table 6-8 Total damage cost from climate change impact to landslide risk map in each province and percentage of increase between RCP 4.5 and RCP 2.6 scenario during near future

Province name	Total damage cost from risk area under scenario RCP 2.6 (Million USD/year)	Total damage cost from risk area under scenario RCP 4.5 (Million USD/year)	Percentage increase of risk area between RCP 4.5 and 2.6
Attapeu	2.555	2.705	5.87%
Bokeo	0	0	0%
Bolikhamxai	6.840	6.990	2.19%
Champasak	0	0	0%
Houaphan	2.601	2.750	5.74%
Khammouan	0.545	0.546	0.30%
Louang Namtha	0	0	0%
Louang Prabang	0	0	0%
Oudomxai	0	0	0%
Phongsaly	0	0	0%
Salavan	0	0	0%
Savannakhet	0	0	0%
Vientiane	5.600	5.750	2.68%
Vientiane Capital City	0	0	0%
Xaignabouly	0	0	0%
Xekong	2.200	2.350	6.82%
Xiangkouang	4.660	4.810	3.22%
Total damage cost across the country	25	25.9	

Table 6-9 Total damage cost from climate change impact to landslide risk map in each province and percentage of increase between RCP 8.5 and RCP 4.5 scenario during near future

Province name	Total damage cost from risk area under scenario RCP 4.5 (Million USD/year)	Total damage cost from risk area under scenario RCP 8.5 (Million USD/year)	Percentage increase of risk area between RCP 8.5 and 4.5
Attapeu	2.705	2.838	4.91%
Bokeo	0	0	0%
Bolikhamxai	6.990	7.123	1.90%
Champasak	0	0	0%
Houaphan	2.750	2.883	4.83%
Khammouan	0.546	0.548	0.37%
Louang Namtha	0	0	0%
Louang Prabang	0	0	0%
Oudomxai	0	0	0%
Phongsaly	0	0	0%
Salavan	0	0	0%
Savannakhet	0	0	0%
Vientiane	5.750	5.883	2.31%
Vientiane Capital City	0	0	0%
Xaignabouly	0	0	0%
Xekong	2.350	2.483	5.65%
Xiangkouang	4.810	4.943	2.76%
Total damage cost across the country	25.9	26.7	

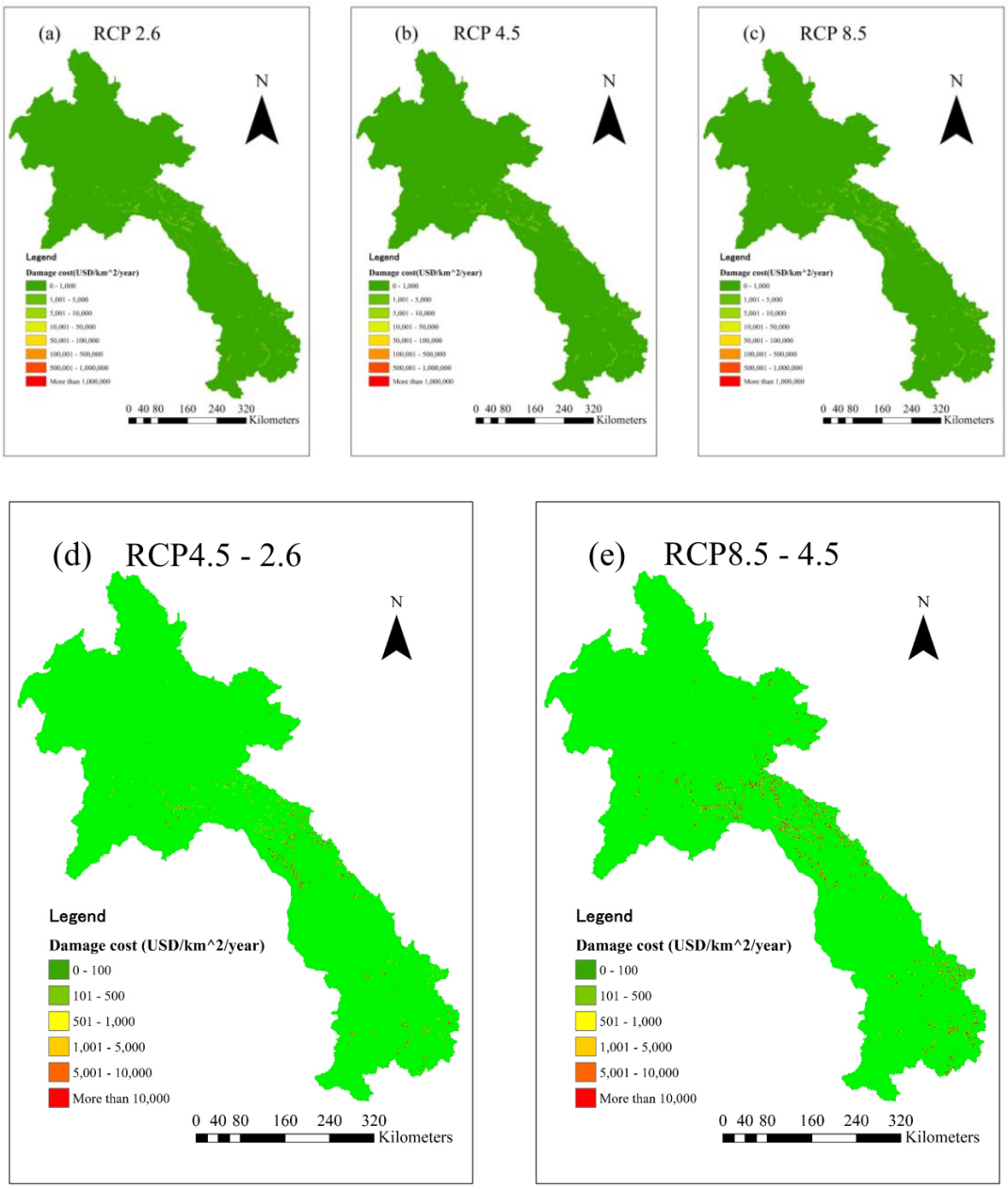

Figure 6-18 Future landslide risk maps under scenario of (a) RCP 2.6, (b) RCP 4.5, (c) RCP 8.5, the difference of damage costs between (d) RCP 4.5 and RCP 2.6 scenario, and (e) RCP 8.5 and RCP 4.5 scenario during far future

Table 6-10 Total damage cost from climate change impact to landslide risk map in each province and percentage of increase between RCP 4.5 and RCP 2.6 scenario during far future

Province name	Total damage cost from risk area under scenario RCP 2.6 (Million USD/year)	Total damage cost from risk area under scenario RCP 4.5 (Million USD/year)	Percentage increase of risk area between RCP 4.5 and 2.6
Attapeu	2.737	3.221	17.66%
Bokeo	0	0	0%
Bolikhamxai	7.022	7.506	6.88%
Champasak	0	0	0%
Houaphan	2.782	3.266	17.37%
Khammouan	0.551	0.557	1.09%
Louang Namtha	0	0	0%
Louang Prabang	0	0	0%
Oudomxai	0	0	0%
Phongsaly	0	0	0%
Salavan	0	0	0%
Savannakhet	0	0	0%
Vientiane	5.782	6.266	8.36%
Vientiane Capital City	0	0	0%
Xaignabouly	0	0	0%
Xekong	2.382	2.866	20.29%
Xiangkouang	4.842	5.321	9.88%
Total damage cost across the country	26.1	29	

Table 6-11 Total damage cost from climate change impact to landslide risk map in each province and percentage of increase between RCP 8.5 and RCP 4.5 scenario during far future

Province name	Total damage cost from risk area under scenario RCP 4.5 (Million USD/year)	Total damage cost from risk area under scenario RCP 8.5 (Million USD/year)	Percentage increase of risk area between RCP 8.5 and 4.5
Attapeu	3.221	4.636	43.95%
Bokeo	0	0	0%
Bolikhamxai	7.506	12.121	61.49%
Champasak	0	0	0%
Houaphan	3.266	4.781	46.41%
Khammouan	0.557	0.563	1.08%
Louang Namtha	0	0	0%
Louang Prabang	0	0	0%
Oudomxai	0	0	0%
Phongsaly	0	0	0%
Salavan	0	0	0%
Savannakhet	0	0	0%
Vientiane	6.266	8.881	41.74%
Vientiane Capital City	0	0	0%
Xaignabouly	0	0	0%
Xekong	2.866	4.181	45.91%
Xiangkouang	5.321	7.136	34.12%
Total damage cost across the country	29	38.7	

The integrated risk map has 6 maps, as do the integrated hazard maps. The risk in low-asset areas causes low damage costs, while the risk in high-value asset areas causes high damage costs despite the low hazard index. The integrated risk maps show that the increasing trend of damage costs is due to climate changes. For far future, the total damage costs of risk areas from integrated risk map is around 20.16 billion USD/year under the scenario of RCP 2.6 and it increases to 20.31 million USD/year under the scenario of RCP 4.5. Figure 6-19 (d) shows the increase of damage costs for risk areas when comparing the integrated risk map for near future under RCP2.6 and RCP 4.5 scenario. Loung Namta province is highly influenced by the climate change. The percentage of the total damage cost of risk areas from integrated risk map increases around 14.07% when comparing the scenario of RCP 2.6 and RCP 4.5 (Table 6-12). Figure 6-19 (e) shows the increase of damage costs for risk areas when comparing the scenario of RCP 8.5 and RCP 4.5. Among others, Attapeu, Louang Namta, Phongsalyand Xekong province have higher increase of damage costs from risk area when comparing integrated risk map under scenario RCP4.5 and RCP8.5 (Table 6-13). Overall, the damage costs of risk area in most of the provinces from integrated risk map with near future increase continually from RCP 2.6 to RCP 8.5 for instance Bolikhamxai province. The total damage costs of risk area in Savannakhet increase around 4.03% comparing the total damage costs of risk area under the scenario RCP 2.6 to that under RCP 4.5 scenario and the total damage costs of risk area in Bolikhamxai province increase around 3.29% comparing the total damage costs of risk area under the scenario RCP 4.5 to that under RCP 8.5 scenario. For far future period, Figure 6-20 (d) shows the increase of damage costs for risk areas when comparing the scenario of RCP 4.5 and RCP 2.6. Comparing the increase of damage costs for risk areas between integrated risk map under RCP 2.6 and

RCP 4.5 scenario, Xekong province has the highest percentage increase of damage cost (23.92%) (Table 6-14). Figure 6-20 (e) shows the increase of damage costs for risk areas when comparing the scenario of RCP 8.5 and RCP 4.5. Savannakhet province has the highest increase of total damage cost for risk areas (9.28%) when comparing between integrated risk map under scenario of RCP 4.5 and RCP 8.5 (Table 6-15). The total damage cost for risk areas in most of the provinces from integrated risk map with far future increase continually from RCP 2.6 to RCP 8.5for example Bolikhamxai province. The total damage costs for risk areas in Bolikhamxai province increase around 2.82% comparing the very high hazard area under the scenario RCP 2.6 to that under RCP 4.5 and the very high hazard area in Bolikhamxai province increase around 6.13% comparing the total damage costs of risk areas under the scenario RCP 4.5 to that under RCP 8.5. The same trend has been observed in the study of integrated hazard maps in Lao PDR (Phrakonkham et al., 2019). A joint report of the Multilateral Development Banks' (MDB) Climate Finance (2018) and the World Bank Disaster Risk Finance Diagnostic Note: Lao PDR (2018) included similar comments. In 2017, Lao PDR had a budget for the management of natural hazard risk of approximately 82 million USD. The budget amounted to 40 (49%), 37 (45%) and 5 million USD/year (6%), respectively, for climate change, flood and landslide risk management. In this study, the weights of each hazard from the AHP method indicate the proportion of the damage costs in the integrated risk. To compare the proportions of the damage costs and the risk management budget, it was assumed that the weights of the climate change leading to floods and landslides can be combined. A similar assumption can be considered for floods and land use changes leading to floods. Finally, it is observed that the damage costs shown in the risk maps are 55%, 44% and 5% from climate change, flood and landslide risk, respectively. The

damage costs of the integrated risk maps have similar proportions to the government budget. In addition, the government policy complies with the weight priority of the AHP method. However according to Post disaster assessment report(World bank, 2018), total damage from flood in 2018 around country was estimate to be around 371 million USD/year, which is very far from our results (26-36 billion). If we compare our estimation of total damage with World Bank, our result is overestimate around 70 times more than World Bank due to the difference in estimate of household asset. According to their report they estimate the asset value of house is around 500 USD/m^2, while in our study we estimate the asset value of house around 2597 USD/m^2. The integrated risk maps can be used in combination with other maps to demonstrate their implications. For instance, we can apply integrated risk maps together with government and private sector development plans to analyze and verify risk areas in agricultural and urban areas. These maps are applicable for the presentation of the spatial distribution of hazard areas. Adequate planning can minimize the impacts of multi-hazard risk on the expansion of agricultural and urban areas. Moreover, local authorities can use integrated risk maps in line with policies and multi-hazard risk mitigation strategies in their respective areas.

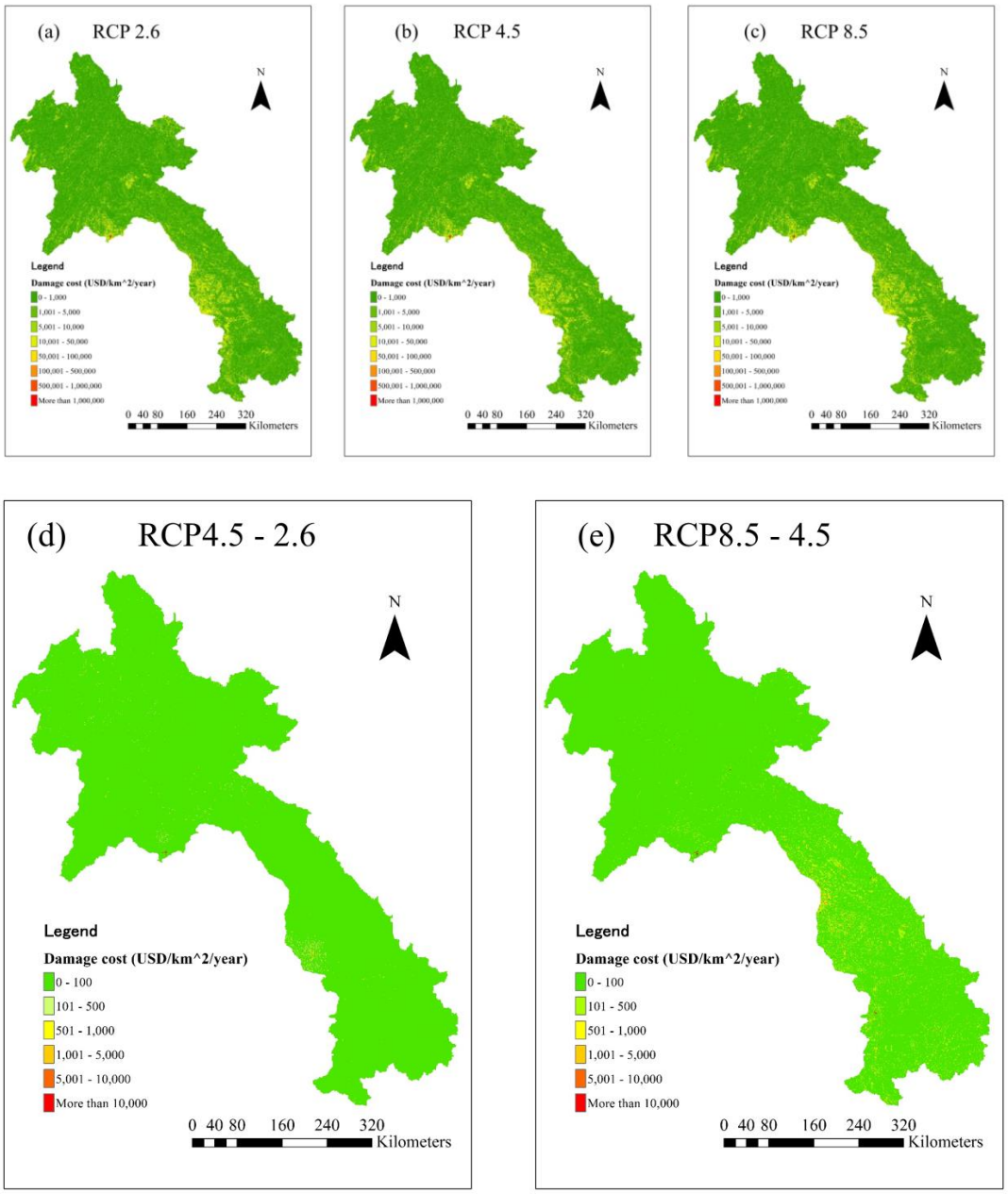

Figure 6-19 Integrated risk maps under scenario of (a) RCP 2.6, (b) RCP 4.5, (c) RCP 8.5, the difference of damage costs between (d) RCP 4.5 and RCP 2.6 scenario, and (e) RCP 8.5 and RCP 4.5 scenario during near future

Table 6-12 Total damage cost from integrated risk map in each province and percentage of increase between RCP 4.5 and RCP 2.6 scenario during near future

Province name	Total damage cost from risk area under scenario RCP 2.6 (Billion USD/year)	Total damage cost from risk area under scenario RCP 4.5 (Billion USD/year)	Percentage increase of risk area between RCP 4.5 and 2.6
Attapeu	0.015	0.016	7.41%
Bokeo	0.212	0.213	0.47%
Bolikhamxai	0.620	0.645	4.03%
Champasak	2.953	2.968	0.51%
Houaphan	0.031	0.033	6.81%
Khammouan	2.823	2.848	0.89%
Louang Namtha	0.015	0.017	14.07%
Louang Prabang	0.033	0.035	6.40%
Oudomxai	0.022	0.024	9.60%
Phongsaly	0.018	0.020	11.73%
Salavan	0.690	0.715	3.62%
Savannakhet	0.210	0.212	0.95%
Vientiane	0.046	0.048	4.59%
Vientiane Capital City	11.823	11.838	0.13%
Xaignabouly	0.031	0.033	6.81%
Xekong	0.010	0.011	11.11%
Xiangkouang	0.607	0.632	4.12%
Total damage cost across the country	20.16	20.31	

Table 6-13 Total damage cost from integrated risk map in each province and percentage of increase between RCP 8.5 and RCP 4.5 scenario during near future

Province name	Total damage cost from risk area under scenario RCP 4.5 (Billion USD/year)	Total damage cost from risk area under scenario RCP 8.5 (Billion USD/year)	Percentage increase of risk area between RCP 8.5 and 4.5
Attapeu	0.016	0.019	20.00%
Bokeo	0.213	0.224	5.28%
Bolikhamxai	0.645	0.666	3.29%
Champasak	2.968	3.000	1.05%
Houaphan	0.033	0.035	6.71%
Khammouan	2.848	2.870	0.75%
Louang Namtha	0.017	0.019	12.99%
Louang Prabang	0.035	0.037	6.33%
Oudomxai	0.024	0.026	9.22%
Phongsaly	0.020	0.022	11.05%
Salavan	0.715	0.736	2.97%
Savannakhet	0.212	0.232	9.55%
Vientiane	0.048	0.050	4.62%
Vientiane Capital City	11.838	11.850	0.10%
Xaignabouly	0.033	0.035	6.71%
Xekong	0.011	0.012	11.00%
Xiangkouang	0.632	0.653	3.36%
Total damage cost across the country	20.31	20.48	

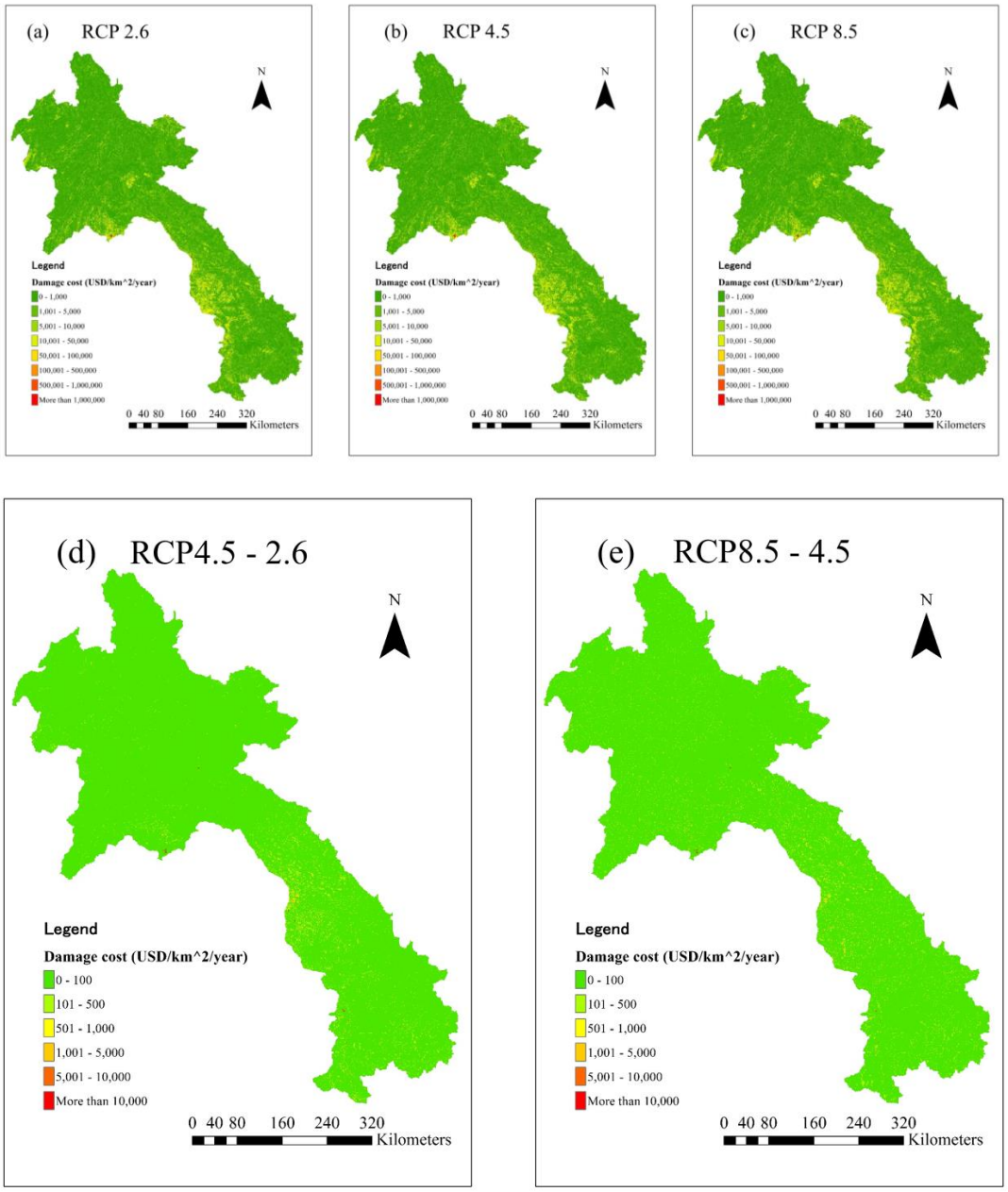

Figure 6-20 Integrated risk maps under scenario of (a) RCP 2.6, (b) RCP 4.5, (c) RCP 8.5, the difference of hazard index between (d) RCP 4.5 and RCP 2.6 scenario, and (e) RCP 8.5 and RCP 4.5 scenario during far future

Table 6-14 Total damage cost from integrated risk map in each province and percentage of increase between RCP 4.5 and RCP 2.6 scenario during far future

Province name	Total damage cost from risk area under scenario RCP 2.6 (Billion USD/year)	Total damage cost from risk area under scenario RCP 4.5 (Billion USD/year)	Percentage increase of risk area between RCP 4.5 and 2.6
Attapeu	0.017	0.020	16.91%
Bokeo	0.231	0.236	2.55%
Bolikhamxai	0.662	0.681	2.82%
Champasak	2.986	2.992	0.20%
Houaphan	0.034	0.040	17.28%
Khammouan	2.866	2.872	0.21%
Louang Namtha	0.016	0.018	12.99%
Louang Prabang	0.036	0.042	16.32%
Oudomxai	0.025	0.031	23.48%
Phongsaly	0.021	0.027	27.95%
Salavan	0.732	0.738	0.80%
Savannakhet	0.229	0.234	2.57%
Vientiane	0.048	0.054	12.23%
Vientiane Capital City	11.851	11.854	0.02%
Xaignabouly	0.034	0.040	17.28%
Xekong	0.012	0.015	23.92%
Xiangkouang	0.649	0.655	0.91%
Total damage cost across the country	20.45	20.55	

Table 6-15 Total damage cost from integrated risk map in each province and percentage of increase between RCP 8.5 and RCP 4.5 scenario during far future

Province name	Total damage cost from risk area under scenario RCP 4.5 (Billion USD/year)	Total damage cost from risk area under scenario RCP 8.5 (Billion USD/year)	Percentage increase of risk area between RCP 8.5 and 4.5
Attapeu	0.020	0.021	6.69%
Bokeo	0.236	0.250	5.82%
Bolikhamxai	0.681	0.723	6.13%
Champasak	2.992	3.031	1.33%
Houaphan	0.040	0.041	3.34%
Khammouan	2.872	2.911	1.38%
Louang Namtha	0.018	0.019	7.35%
Louang Prabang	0.042	0.043	3.18%
Oudomxai	0.031	0.032	4.31%
Phongsaly	0.027	0.028	4.95%
Salavan	0.738	0.778	5.38%
Savannakhet	0.234	0.256	9.28%
Vientiane	0.054	0.055	2.47%
Vientiane Capital City	11.854	11.876	0.18%
Xaignabouly	0.040	0.041	3.34%
Xekong	0.015	0.016	8.93%
Xiangkouang	0.655	0.695	6.07%
Total damage cost across the country	20.55	20.82	

In this study we make an assumption that total damage cost occurred from integrated risk map by 100 year return period is the total damage cost per year in our study area. This assumption is based on the record of damage and lost from historical hazard events in Lao only record events that occurred from 100 year return period (Laos national report, 2012; Management and Programme, 2011; UNDP, 2011). It is indicated that people who live around risk area are adapted and resilient to the hazard risk that occurred under extreme rainfall by 100 year return period. We made this assumption in order to calculated B/C analysis of relocation adaptation. For r = 0.05, the total percentage of relocatable areas from agricultural and paddy field from integrated risk map is around 21.89% under the scenario of RCP 2.6 and it decreases to 20.14% under the scenario of RCP 4.5. Savanakhet have highest percentage decrease of relocatable areas. The relocatable areas in integrated risk map decrease around 18.11% when comparing the scenario of RCP 2.6 and RCP 4.5 (Table 6-16). Under scenario of RCP 8.5, the relocatable area from integrated risk map decrease to 18.76%. Among all of province, Champasak, Houaphan, Savannakhet and Vientiane province have higher percentage decrease of relocatable area when comparing integrated risk map under scenario RCP4.5 and RCP8.5 (Table 6-17). Many provinces from integrated risk map decrease continually from RCP 2.6 to RCP 8.5 for instance Oudomxai province. The total relocatable area in Savannakhet decrease around 2.23% comparing the total relocatable area under the scenario RCP 2.6 to that under RCP 4.5 scenario and the relocatable area in Bolikhamxai province decrease around 2.04% comparing the total damage costs of risk area under the scenario RCP 4.5 to that under RCP 8.5 scenario. For r = 0.1, the total percentage of relocatable areas from agricultural and paddy field from integrated risk map is around 10.87% under the scenario of RCP 2.6 and it decreases to 9.73% under the scenario of RCP 4.5. Comparing the

decrease of relocatable areas between integrated risk map under RCP 2.6 and RCP 4.5 scenario, Champasak province has the highest decrease (22.59%)(Table 6-18). Under scenario of RCP 8.5, the relocatable area from integrated risk map decrease to 9%. In addition, Louang Namta, Salavan and Savannakhet province have higher percentage of decrease of relocatable areas when comparing between integrated risk map under scenario of RCP 4.5 and RCP 8.5 (Table 6-19). The relocatable area in most of the provinces from integrated hazard map decrease continually from RCP 2.6 to RCP 8.5 for example Savannakhet province. The total percentage of relocatable areas in Savannakhet province decrease around 16.35% comparing the very high hazard area under the scenario RCP 2.6 to that under RCP 4.5 and total percentage of relocatable areas in Savannakhet province decrease around 11.37% comparing the total relocatable area from integrated risk map under the scenario RCP 4.5 to that under RCP 8.5.

The main objective of this chapter is to provide integrated risk maps on the national scale. The integrated risk maps consisting of floods, landslides, land use change and climate change leading to floods and climate change leading to landslides. In this study, damage in the forest and river areas is not yet considered due to the insufficient quantity and quality of the data available in the country. Moreover, risks from other hazards, such as typhoons, earthquakes, and epidemics, have not yet been taken into account due to the lack of observation data throughout the country. The risk from all the hazards considered in this study can have a large-scale impact on the economy and agriculture, such as livestock, crops, and fisheries. Although this study provides important information about risk areas and damage costs, limitations do exist. In this study, quantile mapping methods are used to downscale the GCM data. The quantile mapping method is simple and has a nonparametric configuration. However, the quantile mapping method can entail

uncertainty in the results if the future GCMs do correlate well with the observations. The selection of the methodology for downscaling affects the reliability of the results. Our findings demonstrate that parties concerned should pay more attention to the increase in damage costs due to climate change. The integrated risk maps could be a significant tool for the government to be able to focus on sensitive areas of risk. The produced integrated risk maps could identify low-risk areas for development in the northern part of Lao PDR.

Table 6-16 Percentage of relocatable area from agricultural and paddy field in each province and percentage of decrease between RCP 2.6 and RCP4.5 scenario with discount rate (r = 0.05)

Province name	Percentage of relocatable area with RCP 2.6	Percentage of relocatable area with RCP 4.5	Percentage decrease of relocatable area between RCP 2.6 and 4.5
Attapeu	0.17%	0.17%	0.53%
Bokeo	0.13%	0.13%	0.42%
Bolikhamxai	0.72%	0.71%	2.23%
Champasak	1.40%	1.34%	4.23%
Houaphan	1.13%	1.09%	3.42%
Khammouan	0.72%	0.70%	2.22%
Louang Namtha	0.10%	0.10%	0.31%
Louang Prabang	0.31%	0.31%	0.96%
Oudomxai	0.66%	0.64%	2.02%
Phongsaly	0.29%	0.29%	0.91%
Salavan	2.69%	2.49%	7.84%
Savannakhet	6.80%	5.76%	18.11%
Vientiane	2.08%	1.96%	6.17%
Vientiane Capital City	2.47%	2.31%	7.25%
Xaignabouly	0.76%	0.74%	2.33%
Xekong	0.01%	0.01%	0.04%
Xiangkouang	1.43%	1.38%	4.32%
Total percentage of relocatable area across the country	21.89%	20.14%	

Table 6-17 Percentage of relocatable area from agricultural and paddy field in each province and percentage of decrease between RCP 4.5 and RCP 8.5 scenario with discount rate (r = 0.05)

Province name	Percentage of relocatable area with RCP 4.5	Percentage of relocatable area with RCP 8.5	Percentage decrease of relocatable area between RCP 4.5 and 8.5
Attapeu	0.17%	0.17%	0.49%
Bokeo	0.13%	0.13%	0.39%
Bolikhamxai	0.71%	0.69%	2.04%
Champasak	1.34%	1.23%	9.25%
Houaphan	1.09%	1.00%	8.71%
Khammouan	0.70%	0.69%	2.03%
Louang Namtha	0.10%	0.10%	0.29%
Louang Prabang	0.31%	0.30%	0.89%
Oudomxai	0.64%	0.61%	5.59%
Phongsaly	0.29%	0.29%	0.84%
Salavan	2.49%	2.30%	8.51%
Savannakhet	5.76%	5.24%	9.88%
Vientiane	1.96%	1.80%	9.14%
Vientiane Capital City	2.31%	2.16%	6.62%
Xaignabouly	0.74%	0.73%	2.13%
Xekong	0.01%	0.01%	0.04%
Xiangkouang	1.38%	1.30%	5.60%
Total percentage of relocatable area across the country	20.14%	18.76%	

Table 6-18 Percentage of relocatable area from agricultural and paddy field in each province and percentage of decrease between RCP 2.6 and RCP4.5 scenario with discount rate (r = 0.1)

Province name	Percentage of relocatable area with RCP 2.6	Percentage of relocation area with RCP 4.5	Percentage decrease of relocation area between RCP 2.6 and 4.5
Attapeu	0.10%	0.10%	1.16%
Bokeo	0.07%	0.07%	0.81%
Bolikhamxai	0.64%	0.62%	2.32%
Champasak	0.82%	0.67%	22.59%
Houaphan	0.60%	0.52%	17.07%
Khammouan	0.52%	0.46%	14.93%
Louang Namtha	0.09%	0.09%	1.04%
Louang Prabang	0.26%	0.25%	2.88%
Oudomxai	0.47%	0.45%	5.09%
Phongsaly	0.25%	0.24%	2.75%
Salavan	1.29%	1.14%	12.91%
Savannakhet	2.51%	2.15%	16.35%
Vientiane	1.01%	0.87%	16.50%
Vientiane Capital City	1.14%	1.11%	2.26%
Xaignabouly	0.54%	0.51%	5.83%
Xekong	0.01%	0.01%	0.15%
Xiangkouang	0.53%	0.45%	17.95%
Total percentage of relocatable area across the country	10.87%	9.73%	

Table 6-19 Percentage of relocatable area from agricultural and paddy field in each province and percentage of decrease between RCP 4.5 and RCP 8.5 scenario with discount rate (r = 0.1)

Province name	Percentage of relocatable area with RCP 4.5	Percentage of relocatable area with RCP 8.5	Percentage decrease of relocation area between RCP 4.5 and 8.5
Attapeu	0.10%	0.10%	2.32%
Bokeo	0.07%	0.07%	9.01%
Bolikhamxai	0.62%	0.58%	7.05%
Champasak	0.67%	0.63%	6.55%
Houaphan	0.52%	0.49%	5.44%
Khammouan	0.46%	0.43%	5.11%
Louang Namtha	0.09%	0.08%	11.44%
Louang Prabang	0.25%	0.24%	7.68%
Oudomxai	0.45%	0.43%	3.77%
Phongsaly	0.24%	0.23%	4.32%
Salavan	1.14%	1.02%	11.38%
Savannakhet	2.15%	1.93%	11.37%
Vientiane	0.87%	0.80%	8.40%
Vientiane Capital City	1.11%	1.02%	8.91%
Xaignabouly	0.51%	0.49%	5.09%
Xekong	0.01%	0.01%	1.78%
Xiangkouang	0.45%	0.43%	3.77%
Total percentage of relocatable area across the country	9.73%	9.00%	

CHAPTER 7: CONCLUSIONS AND RECOMMENDATIONS

This dissertation focused on the assessment of potential risk from various hazards in Lao PDR such as flood, landslide, land use change, climate change impact flood and climate change impact landslide. The study were conducted to 1) Analyse five hazard maps namely flood, landslide, land use change, climate change impact to flood and climate change impact to landslide. 2) Multi-criteria decision making AHP approach was used for integration all of mention hazard maps together. 3) Assess total damage cost of each risk map and integrated risk map.

1. In this study distributed hydrological model develop by Kashiwa et al (2010) was used to generate flood hazard map. The flood hazard map can estimate potential of hazard area through country scale. Based on the results from flood hazard map most of flood hazard areas area distributed around northern and southern part of Lao PDR. In addition, the flood hazard map can estimate flood hazards corresponding to the historical of flood disaster in Lao PDR. Following up we used probabilistic method of statistical analysis proposed by Kawagoe et al (2010) to generated landslide hazard map. According to the results, landslide hazard events were distributed mostly in southern region. In addition, the land slide hazard map was validated by compare to historical landslide events. The comparison shows the good correlation between landslide hazard map and historical events. Next we estimate the land use

change impact to flood hazard map, the results presents that the decreasing of forest area will lead to significant increase in flood hazard area. Furthermore, rainfall under different climate change scenarios were generated to estimate the impact of climate change to flood and landslide hazard map. The results indicated that rainfall intensity will increase for any future scenario and it is will have impact to the increasing of flood and landslide hazard map. In addition, we analyse an adaptation measure for reduce the damage cost from integrated risk maps.

2. This study aim to analyse multi-hazard, therefore AHP approach was used to integrated multi-hazard. AHP approach is a multi-criteria decision making. It is use to solve complex decision making by using pairwise comparison. In this study we use AHP to obtain criteria relative importance value or weight of each hazard. The weights are obtain through experts' judgment. The integrated hazard can provided spatial distribution of multi-hazard area. It is also can use by local authorities for screening potential development area or make multi-hazard mitigation strategies. This study provides an important and reliable methodology for the development of integrated hazard maps using multi-criteria decision analysis, such as the AHP.

3. Estimation of total damage costs were derived from individual risk and integrated risk maps. Risk can determined from hazard map and its negative consequence. In this study we analyse integrated risk map based on integrated hazard map and land use categories (urban, agriculture and paddy field). Based on the results among individual risk map, climate change impact to flood risk map under RCP 8.5 scenario for far future shows highest of total damage 35.56 billion USD and lowest

is landslide risk map (13 million USD). The central region is shows the highest total damage because that area is the most developed area and also the capital city of Lao PDR is located. All the integrated risk maps shows a similar distribution of risk areas. Climate change have significantly impact to the increase of total damage costs of integrated risk maps. Total damage costs of integrated risk map under RCP 2.6 scenario is 29.37 billion USD and it is increase to 29.98 billion USD under RCP 8.5. It is worth noting that, when we compare proportion weight of hazard from AHP approach with national budget proportion for management of natural hazard they shows similar proportion. Therefore, AHP approach can be used to integrated multi-hazard in our study area. Additionally, an adaptation measure was analyse for reduce the damage cost from agricultural and paddy field for integrated risk maps. The results shows that only 30 % of agricultural and paddy field areas are relocatable.

The future researches can be envisaged from this study are outlines below:

1. In this study, we consider only direct damage costs from risk maps. Indirect damage costs from various hazard risk did not include in this study yet for instance when flood or landslide hazard is occurs it can block transportation infrastructure with lead to disrupt people business, damage to water supply system leading to possible waterborne infections, food shortage and disruption of emergency response. Furthermore, when we estimate the risk from hazard we did not consider resilience of area into account. By including those factor it can show more accurate to the assessment of risk hazard map.

2. Bias correction quantile mapping downscaling method is a famous method because it is simple and non-parametric configuration. But it can affects the results of future projection. The quantile mapping method cloud minimize the error of observation and GCMs data, which is shows in root square mean error value. The quantile mapping has an instability at the highest quantiles of the correction function and the extrapolated value out of correlations function. Another limitation of this method is when the correlation between future GCMs and observation is not positively strong, quantile mapping can produce negative projection.

Reference

Adeloye, A., Nawaz, N.R. and Bellerby, T.J. (2013), "Modelling the impact of climate change on water systems and implications for decision-makers", American Society of Civil Engineers, pp. 299–326.

Aleotti, P. and Chowdhury, R. (1999), "Landslide hazard assessment: Summary review and new perspectives", *Bulletin of Engineering Geology and the Environment*, available at:https://doi.org/10.1007/s100640050066.

Baird, I.G. and Shoemaker, B. (2007), "Unsettling Experiences: Internal Resettlement and International Aid Agencies in Laos", *Development and Change*, Vol. 38 No. 5, pp. 865–888.

Di Baldassarre, G. and Montanari, A. (2009), "Uncertainty in river discharge observations: a quantitative analysis", *Hydrology and Earth System Sciences*, Vol. 13 No. 6, pp. 913–921.

Bales, J.D. and Wagner, C.R. (2009), "Sources of uncertainty in flood inundation maps", *Journal of Flood Risk Management*, Vol. 2 No. 2, pp. 139–147.

Bank of Lao PDR. (2018), *Annual Report (in Lao)*.

Bednarik, M., Magulová, B., Matys, M. and Marschalko, M. (2010), "Landslide susceptibility assessment of the Kraľovany–Liptovský Mikuláš railway case study", *Physics and Chemistry of the Earth, Parts A/B/C*, Vol. 35 No. 3–5, pp. 162–171.

Behzadian, M., Khanmohammadi Otaghsara, S., Yazdani, M. and Ignatius, J. (2012), "A state-of the-art survey of TOPSIS applications", *Expert Systems with Applications*, Vol. 39 No. 17, pp. 13051–13069.

Bell, R. and Glade, T. (2004), "Quantitative risk analysis for landslides – Examples

from Bíldudalur, NW-Iceland", *Natural Hazards and Earth System Science*, Vol. 4 No. 1, pp. 117–131.

Black, R., Bennett, S.R.G., Thomas, S.M. and Beddington, J.R. (2011), "Migration as adaptation", *Nature*, Vol. 478 No. 7370, pp. 447–449.

Boé, J., Terray, L., Habets, F. and Martin, E. (2007), "Statistical and dynamical downscaling of the Seine basin climate for hydro-meteorological studies", *International Journal of Climatology*, Vol. 27 No. 12, pp. 1643–1655.

Bouwer, L.M., Bubeck, P. and Aerts, J.C.J.H. (2010), "Changes in future flood risk due to climate and development in a Dutch polder area", *Global Environmental Change*, Vol. 20 No. 3, pp. 463–471.

Calcaterra, D., Gili, J.A. and Iovinelli, R. (1998), "Shallow landslides in deeply weathered slates of the Sierra de Collcerola (Catalonian Coastal Range, Spain)", *Engineering Geology*, available at:https://doi.org/10.1016/S0013-7952(98)00024-6.

Carpignano, A., Golia, E., Di Mauro, C., Bouchon, S. and Nordvik, J. (2009), "A methodological approach for the definition of multi‐risk maps at regional level: first application", *Journal of Risk Research*, Vol. 12 No. 3–4, pp. 513–534.

Ceballos-Silva, A. and López-Blanco, J. (2003), "Delineation of suitable areas for crops using a Multi-Criteria Evaluation approach and land use/cover mapping: a case study in Central Mexico", *Agricultural Systems*, Vol. 77 No. 2, pp. 117–136.

Ciabatta, L., Camici, S., Brocca, L., Ponziani, F., Stelluti, M., Berni, N. and Moramarco, T. (2016), "Assessing the impact of climate-change scenarios on landslide occurrence in Umbria Region, Italy", *Journal of Hydrology*, Vol. 541, pp. 285–295.

Collison, A., Wade, S., Griffiths, J. and Dehn, M. (2000), "Modelling the impact of predicted climate change on landslide frequency and magnitude in SE England", *Engineering Geology*, Vol. 55 No. 3, pp. 205–218.

Constantin, M., Bednarik, M., Jurchescu, M.C. and Vlaicu, M. (2011), "Landslide susceptibility assessment using the bivariate statistical analysis and the index of entropy in the Sibiciu Basin (Romania)", *Environmental Earth Sciences*, Vol. 63 No. 2, pp. 397–406.

Crispino, G., Gisonni, C. and Iervolino, M. (2015), "Flood hazard assessment: comparison of 1D and 2D hydraulic models", *International Journal of River Basin Management*, Vol. 13 No. 2, pp. 153–166.

Cutter, S.L., Mitchell, J.T. and Scott, M.S. (2000), "Revealing the Vulnerability of People and Places: A Case Study of Georgetown County, South Carolina", *Annals of the Association of American Geographers*, Vol. 90 No. 4, pp. 713–737.

Dai, F.C., Lee, C.F., Li, J. and Xu, Z.W. (2001), "Assessment of landslide susceptibility on the natural terrain of Lantau Island, Hong Kong", *Environmental Geology*, available at:https://doi.org/10.1007/s002540000163.

Dankers, R. and Feyen, L. (2008), "Climate change impact on flood hazard in Europe: An assessment based on high-resolution climate simulations", *Journal of Geophysical Research Atmospheres*, Vol. 113 No. 19, pp. 1–17.

Devia, G.K., Ganasri, B.P. and Dwarakish, G.S. (2015), "A Review on Hydrological Models", *Aquatic Procedia*, Vol. 4, pp. 1001–1007.

Dinh, Q., Balica, S., Popescu, I. and Jonoski, A. (2012), "Climate change impact on flood hazard, vulnerability and risk of the Long Xuyen Quadrangle in the Mekong Delta", *International Journal of River Basin Management*, Vol. 10 No. 1, pp. 103–

120.

Domeneghetti, A., Vorogushyn, S., Castellarin, A., Merz, B. and Brath, A. (2013), "Probabilistic flood hazard mapping: effects of uncertain boundary conditions", *Hydrology and Earth System Sciences*, Vol. 17 No. 8, pp. 3127–3140.

Dottori, F., Salamon, P., Bianchi, A., Alfieri, L., Hirpa, F.A. and Feyen, L. (2016), "Development and evaluation of a framework for global flood hazard mapping", *Advances in Water Resources*, Vol. 94, pp. 87–102.

Erener, A. and Düzgün, H.S.B. (2010), "Improvement of statistical landslide susceptibility mapping by using spatial and global regression methods in the case of More and Romsdal (Norway)", *Landslides*, Vol. 7 No. 1, pp. 55–68.

Fajar Januriyadi, N., Kazama, S., Riyando Moe, I. and Kure, S. (2018), "Evaluation of future flood risk in Asian megacities: a case study of Jakarta", *Hydrological Research Letters*, Vol. 12 No. 3, pp. 14–22.

Falaschi, F., Giacomelli, F., Federici, P.R., Puccinelli, A., D'Amato Avanzi, G., Pochini, A. and Ribolini, A. (2009), "Logistic regression versus artificial neural networks: landslide susceptibility evaluation in a sample area of the Serchio River valley, Italy", *Natural Hazards*, Vol. 50 No. 3, pp. 551–569.

Fang, G.H., Yang, J., Chen, Y.N. and Zammit, C. (2015), "Comparing bias correction methods in downscaling meteorological variables for a hydrologic impact study in an arid area in China", *Hydrology and Earth System Sciences*, Vol. 19 No. 6, pp. 2547–2559.

Fernández, D.S. and Lutz, M.A. (2010), "Urban flood hazard zoning in Tucumán Province, Argentina, using GIS and multicriteria decision analysis", *Engineering Geology*, Vol. 111 No. 1–4, pp. 90–98.

Fischer, G., Nachtergaele, F., Prieler, S., Velthuizen, H.T. van, Verelst, L. and Wiberg, D. (2008), *Global Agro-Ecological Zones :Model Documentation*, *Food and Agriculture Organization of the United Nations*.

Fishburn, P.C. (1967), "Additive Utilities with Incomplete Product Set: Applications to Priorities and Assignments", *Operations Research Society of America (ORSA)*, Baltimore, MD, U.S.A.

Gigović, L., Pamučar, D., Bajić, Z. and Drobnjak, S. (2017), "Application of GIS-Interval Rough AHP Methodology for Flood Hazard Mapping in Urban Areas", *Water*, Vol. 9 No. 6, p. 360.

Golian, S., Saghafian, B. and Maknoon, R. (2010), "Derivation of Probabilistic Thresholds of Spatially Distributed Rainfall for Flood Forecasting", *Water Resources Management*, Vol. 24 No. 13, pp. 3547–3559.

Greiving, S., Fleischhauer, M. and Lückenkötter, J. (2006), "A Methodology for an integrated risk assessment of spatially relevant hazards", *Journal of Environmental Planning and Management*, Vol. 49 No. 1, pp. 1–19.

Haan, C.. (1977), "Statistical methos in hydrology", *Iowa State University Press.*, Ames.

Hirabayashi, Y., Kanae, S., Emori, S., Oki, T. and Kimoto, M. (2008), "Global projections of changing risks of floods and droughts in a changing climate", *Hydrological Sciences Journal*, Vol. 53 No. 4, pp. 754–772.

Horritt, M.S. and Bates, P.D. (2001), "Predicting floodplain inundation: raster-based modelling versus the finite-element approach", *Hydrological Processes*, Vol. 15 No. 5, pp. 825–842.

Huntington, T.G. (2006), "Evidence for intensification of the global water cycle:

Review and synthesis", *Journal of Hydrology,* Vol. 319 No. 1–4, pp. 83–95.

Huynh, V.C. (2008), "Multicriteria land suitability evaluation for crops using GIS at community level in central Vietnam with case study in Thuy Bang-Thua Thien Hue province", Hanoi, Vietnam, available at: http://wgrass.media.osaka-cu.ac.jp/gisideas10/papers/124bef5dc43ccaf84f1b42bc915c.pdf (accessed 20 February 2019).

Hwang, C.L. and Yoon, K. (1981), "Multiple Attribute Decision Making: Methods and Applications.", *New York: Springer-Verlag.*

HWSD. (2012), "harmonized world soil database", available at: http://www.fao.org/soils-portal/soil-survey/soil-maps-and-databases/harmonized-world-soil-database-v12/en/.

IPCC. (2007), *Climate Change 2007 : Mitigation of Climate Change : Contribution of Working Group III to the Fourth Assessment Report of the Intergovernmental Panel on Climate Change,* Cambridge University Press.

Jongman, B., Kreibich, H., Apel, H., Barredo, J.I., Bates, P.D., Feyen, L., Gericke, A., et al. (2012), "Comparative flood damage model assessment: towards a European approach", *Natural Hazards and Earth System Sciences*, Vol. 12 No. 12, pp. 3733–3752.

Jung, S., Smith, J.J., von Haller, P.D., Dilworth, D.J., Sitko, K.A., Miller, L.R., Saleem, R.A., et al. (2013), "Global analysis of condition-specific subcellular protein distribution and abundance.", *Molecular & Cellular Proteomics : MCP*, Vol. 12 No. 5, pp. 1421–35.

Kashiwa, S., Asaoka, Y. and Kazama, A. (2010), "Flood analysis Modeling of snow melting and Estimation", the rivers Technology, pp. 289–294.

Kawagoe, S., Kazama, S. and Sarukkalige, P.R. (2010), “Probabilistic modelling of rainfall induced landslide hazard assessment”, *Hydrology and Earth System Sciences*, Vol. 14 No. 6, pp. 1047–1061.

Kazakis, N., Kougias, I. and Patsialis, T. (2015), “Assessment of flood hazard areas at a regional scale using an index-based approach and Analytical Hierarchy Process: Application in Rhodope-Evros region, Greece.”, *The Science of the Total Environment*, Vol. 538, pp. 555–63.

Kazama, S., Hyejin, K. and Sawamoto, M. (2004), “Uncertainty of morphological data for rainfall-runoff simulation”, the International Conference on sustainable Water Resources Management in the Changing Environment of the Monsoon Region 1, Colombo, Sri Lanka, pp. 400–406.

Keeney, R.L. and Raiffa, H. (1993), *Decisions with Multiple Objectives*.

Komendantova, N., Mrzyglocki, R., Mignan, A., Khazai, B., Wenzel, F., Patt, A. and Fleming, K. (2014), “Multi-hazard and multi-risk decision-support tools as a part of participatory risk governance: Feedback from civil protection stakeholders”, *International Journal of Disaster Risk Reduction*, Vol. 8, pp. 50–67.

Komori, D., Rangsiwanichpong, P., Inoue, N., Ono, K., Watanabe, S. and Kazama, S. (2018), “Distributed probability of slope failure in Thailand under climate change”, *Climate Risk Management*, Vol. 20, pp. 126–137.

Konidari, P. and Mavrakis, D. (2007), “A multi-criteria evaluation method for climate change mitigation policy instruments”, *Energy Policy*, Vol. 35 No. 12, pp. 6235–6257.

Lafon, T., Dadson, S., Buys, G. and Prudhomme, C. (2013), “Bias correction of daily precipitation simulated by a regional climate model: a comparison of methods”,

International Journal of Climatology, Vol. 33 No. 6, pp. 1367–1381.

Laos national report. (2012), *ADPC: Lao PDR National Assessment Report on Disaster Risk Reduction (2012)*, available at: http://www.adpc.net/igo/contents/publications/publications-Details.asp?pid=416#sthash.E4Y0dK6o.dpbs (accessed 20 February 2019).

Lauri, H., de Moel, H., Ward, P.J., Räsänen, T.A., Keskinen, M. and Kummu, M. (2012), "Future changes in Mekong River hydrology: impact of climate change and reservoir operation on discharge", *Hydrology and Earth System Sciences*, Vol. 16 No. 12, pp. 4603–4619.

Lee, C.T., Huang, C.C., Lee, J.F., Pan, K.L., Lin, M.L. and Dong, J.J. (2008), "Statistical approach to earthquake-induced landslide susceptibility", *Engineering Geology*, available at:https://doi.org/10.1016/j.enggeo.2008.03.004.

Li, Y., Guo, Y. and Yu, G. (2013), "An analysis of extreme flood events during the past 400years at Taihu Lake, China", *Journal of Hydrology*, Vol. 500, pp. 217–225.

Li, Z., Liu, W., Zhang, X. and Zheng, F. (2009), "Impacts of land use change and climate variability on hydrology in an agricultural catchment on the Loess Plateau of China", *Journal of Hydrology*, Vol. 377 No. 1–2, pp. 35–42.

Macklin, M.G. and Lewin, J. (2003), "River sediments, great floods and centennial-scale Holocene climate change", *Journal of Quaternary Science*, Vol. 18 No. 2, pp. 101–105.

Management, F. and Programme, M. (2011), "Annual Mekong Flood Report 2010 Flood Management and Mitigation Programme Annual Mekong Flood Report 2010", No. 1728–3248, p. 76.

Marzocchi, W., Garcia-Aristizabal, A., Gasparini, P., Mastellone, M.L. and Di Ruocco,

A. (2012), “Basic principles of multi-risk assessment: a case study in Italy”, *Natural Hazards*, Vol. 62 No. 2, pp. 551–573.

Marzocchi, W., Mastellone, M.L., Di Ruocco, A., Novelli, P., Romeo, E. and Gasparini, P. (2009), *Principles of Multi-Risk Assessment, European Commission Joint Research Centre*, available at:https://doi.org/10.2777/30886.

Mikkelsen, P.S., Adeler, O.F., Albrechtsen, H.J. and Henze, M. (1999), “Collected rainfall as a water source in Danish households - what is the potential and what are the costs?”, *Water Science and Technology*, Vol. 39 No. 5, pp. 49–56.

Ministry of agriculture and Forestry. (2018), *Agricultural Statistics Year Book*, available at: http://183.182.107.172/publication/publicationList.

Mirza, M.M.Q. (2011), “Climate change, flooding in South Asia and implications”, *Regional Environmental Change*, Vol. 11 No. SUPPL. 1, pp. 95–107.

MohanV, R. and RajT, N. (2011), “Landslide susceptibility mapping using frequency ratio method and GIS in south eastern part of Nilgiri District, Tamilnadu, India”, *International Journal of Geomatics and Geosciences*, Vol. 1 No. 4, pp. 951–961.

Moran, A., Wastl, M., Geitner, C. & Stotter, J. (2004), “A regional scale risk analysis in the community of Ólafsfjörður, Iceland”, *International Symposium InterpraeventInterpraevent*.

Moriasi D. N., Arnold J. G., Van Liew M. W., Bingner R. L., Harmel R. D. and Veith T. L. (2007), “Model Evaluation Guidelines for Systematic Quantification of Accuracy in Watershed Simulations”, *Transactions of the ASABE*, American Society of Agricultural and Biological Engineers, Vol. 50 No. 3, pp. 885–900.

El Morjani, Z.E.A., Ebener, S., Boos, J., Abdel Ghaffar, E. and Musani, A. (2007), “Modelling the spatial distribution of five natural hazards in the context of the

WHO/EMRO Atlas of Disaster Risk as a step towards the reduction of the health impact related to disasters", *International Journal of Health Geographics*, Vol. 6 No. 1, pp. 8.

Multilateral Development Banks. (2018), *2017 Joint Report on Multilateral Development Banks' Climate Finance*, Washington, D.C., available at:https://doi.org/10.18235/0001336.

Nash, J.E. and Sutcliffe, J.V. (1970), "River flow forecasting through conceptual models part I — A discussion of principles", *Journal of Hydrology*, Vol. 10 No. 3, pp. 282–290.

Ohlmacher, G.C. and Davis, J.C. (2003), "Using multiple logistic regression and GIS technology to predict landslide hazard in northeast Kansas, USA", *Engineering Geology*, Vol. 69 No. 3–4, pp. 331–343.

Ono, K., Akimoto, T., Gunawardhana, L.N., Kazama, S. and Kawagoe, S. (2011), "Distributed specific sediment yield estimations in Japan attributed to extreme-rainfall-induced slope failures under a changing climate", *Hydrology and Earth System Sciences*, Vol. 15 No. 1, pp. 197–207.

Orlowsky, B. and Seneviratne, S.I. (2012), "Global changes in extreme events: regional and seasonal dimension", *Climatic Change*, Vol. 110 No. 3–4, pp. 669–696.

Parmesan, C. and Yohe, G. (2003a), "A globally coherent fingerprint of climate change impacts across natural systems", *Nature*, Vol. 421 No. 6918, pp. 37–42.

Parmesan, C. and Yohe, G. (2003b), "A globally coherent fingerprint of climate change impacts across natural systems", *Nature*, Vol. 421 No. 6918, pp. 37–42.

Parry, J.A., Ganaie, S.A. and Sultan Bhat, M. (2018), "GIS based land suitability analysis using AHP model for urban services planning in Srinagar and Jammu

urban centers of J&K, India", *Journal of Urban Management*, Vol. 7 No. 2, pp. 46–56.

Patro, S., Chatterjee, C., Mohanty, S., Singh, R. and Raghuwanshi, N.S. (2009), "Flood inundation modeling using MIKE FLOOD and remote sensing data", *Journal of the Indian Society of Remote Sensing*, Vol. 37 No. 1, pp. 107–118.

Phrakonkham, S. (2017), *Proposing the Flood Risk Index in View of Forest and Climate Change*.

Phrakonkham, S., Kazama, S., Komori, D. and Sopha, S. (2019), "Distributed Hydrological Model for Assessing Flood Hazards in Laos", *Journal of Water Resource and Protection*, Vol. 11 No. 08, pp. 937–958.

Ponziani, F., Pandolfo, C., Stelluti, M., Berni, N., Brocca, L. and Moramarco, T. (2012), "Assessment of rainfall thresholds and soil moisture modeling for operational hydrogeological risk prevention in the Umbria region (central Italy)", *Landslides*, Vol. 9 No. 2, pp. 229–237.

Poretti, I. and De Amicis, M. (2011), "An approach for flood hazard modelling and mapping in the medium Valtellina", *Natural Hazards and Earth System Science*, Vol. 11 No. 4, pp. 1141–1151.

Pourghasemi, H.R., Mohammady, M. and Pradhan, B. (2012), "Landslide susceptibility mapping using index of entropy and conditional probability models in GIS: Safarood Basin, Iran", *CATENA*, Vol. 97, pp. 71–84.

Pourkhabbaz, H.R., Javanmardi, S. and Faraji Sabokbar, H.A. (2014), "Suitability analysis for determining potential agricultural land use by the multi-criteria decision making models SAW and VIKOR-AHP (case study: takestan-Qazvin plain)", *Journal of Agricultural Science and Technology*, Vol. 16, pp. 1005–1016.

Prakash, T. (2003), *Land Suitability Analysis for Agricultural Crops: A Fuzzy Multicriteria Decision Making Approach*, available at: https://pdfs.semanticscholar.org/0ea0/1f638e71f9e514d90ad989c5246dd0a0e5db.pdf?_ga=2.122219535.564011215.1575598334-1946236735.1571628183.

Qin, X.S., Huang, G.H., Chakma, A., Nie, X.H. and Lin, Q.G. (2008), "A MCDM-based expert system for climate-change impact assessment and adaptation planning – A case study for the Georgia Basin, Canada", *Expert Systems with Applications*, Vol. 34 No. 3, pp. 2164–2179.

Ramya, S. and Devadas, V. (2019), "Integration of GIS, AHP and TOPSIS in evaluating suitable locations for industrial development: A case of Tehri Garhwal district, Uttarakhand, India", *Journal of Cleaner Production*, Vol. 238, p. 117872.

Refice, A. and Capolongo, D. (2002), "Probabilistic modeling of uncertainties in earthquake-induced landslide hazard assessment", *Computers and Geosciences*, available at:https://doi.org/10.1016/S0098-3004(01)00104-2.

Saaty, T.L. (1994), "How to Make a Decision: The Analytic Hierarchy Process", *Interfaces*, INFORMS , Vol. 24 No. 6, pp. 19–43.

Salem, G.S.A., Kazama, S., Shahid, S. and Dey, N.C. (2018), "Groundwater-dependent irrigation costs and benefits for adaptation to global change", *Mitigation and Adaptation Strategies for Global Change*, Vol. 23 No. 6, pp. 953–979.

Sally, P., Tapsell, S., Penning-Rowsell, E. and Viavattene, C. (2008), *Title Building Models to Estimate Loss of Life for Flood Events Lead Author Sally Priest*, available at: http://www.floodsite.net/html/search_results.asp?documentType (accessed 20 February 2019).

Sendai Framework, 2015. (2015), *Sendai Framework for Disaster Risk Reduction 2015*

- *2030*, available at: https://www.unisdr.org/files/43291_sendaiframeworkfordrren.pdf (accessed 20 February 2019).

Shirole, D., Moormann, C. and Sharma, K.G. (2017), "A New Continuum Based Model for the Simulation of a Seismically Induced Large-scale Rockslide", *Procedia Engineering*, Vol. 173, pp. 1755–1762.

Sidle, R.C. and Ochiai, H. (2006), *Landslides: Processes, Prediction, and Land Use*, Vol. 18, American Geophysical Union, Washington, D. C., available at:https://doi.org/10.1029/WM018.

Stefanidis, S. and Stathis, D. (2013), "Assessment of flood hazard based on natural and anthropogenic factors using analytic hierarchy process (AHP)", *Natural Hazards*, Vol. 68 No. 2, pp. 569–585.

Sullivan-Wiley, K.A. and Short Gianotti, A.G. (2017), "Risk Perception in a Multi-Hazard Environment", *World Development*, Vol. 97, pp. 138–152.

Tate, E., Cutter, S.L. and Berry, M. (2010), "Integrated Multihazard Mapping", *Environment and Planning B: Planning and Design*, Vol. 37 No. 4, pp. 646–663.

Tehrany, M.S., Pradhan, B. and Jebur, M.N. (2013), "Spatial prediction of flood susceptible areas using rule based decision tree (DT) and a novel ensemble bivariate and multivariate statistical models in GIS", *Journal of Hydrology*, Vol. 504, pp. 69–79.

Trenberth, K.E., Dai, A., Rasmussen, R.M. and Parsons, D.B. (2003), "The Changing Character of Precipitation", *Bulletin of the American Meteorological Society*, Vol. 84 No. 9, pp. 1205–1218.

UNDP. (2011), *National Hazard Profile of Laos*.

UNDRR. (2017), “Lao PDR disaster historical”, available at: https://www.desinventar.net/DesInventar/profiletab.jsp?countrycode=lao&continue=y.

UNISDR. (2009), *The United Nations International Strategy for Disaster Reduction, UNISDR*.

van Westen, C.J., van Asch, T.W.J. and Soeters, R. (2006), “Landslide hazard and risk zonation—why is it still so difficult?”, *Bulletin of Engineering Geology and the Environment*, Vol. 65 No. 2, pp. 167–184.

Westra, S., Fowler, H.J., Evans, J.P., Alexander, L. V., Berg, P., Johnson, F., Kendon, E.J., et al. (2014), “Future changes to the intensity and frequency of short-duration extreme rainfall”, *Reviews of Geophysics*, Vol. 52 No. 3, pp. 522–555.

White, J.A. and Singham, D.I. (2012), “Slope Stability Assessment using Stochastic Rainfall Simulation”, *Procedia Computer Science*, Vol. 9, pp. 699–706.

Winsemius, H.C., Aerts, J.C.J.H., van Beek, L.P.H., Bierkens, M.F.P., Bouwman, A., Jongman, B., Kwadijk, J.C.J., et al. (2016), “Global drivers of future river flood risk”, *Nature Climate Change*, Vol. 6 No. 4, pp. 381–385.

Wipulanusat, W., Nakrod, S. and Prabnarong, P. (2009), “Multi-hazard Risk Assessment Using GIS and RS Applications : A Case Study of Pak Phanang Basin”, *Walailak Journal of Science and Technology*, available at:https://doi.org/10.2004/wjst.v6i1.76.

World bank. (2018), *Disaster Risk Finance Country Diagnostic Note: Lao PDR*, available at: https://www.rcrc-resilience-southeastasia.org/wp-content/uploads/2017/12/world_bank_et_al._2016._lao_pdr_disaster_risk_financing_draft-diagnostc-report.pdf.

World Bank. (2017), “GDP and population of Lao PDR”, available at: https://data.worldbank.org/country/lao-pdr.

Zhang, L., Wu, F., Zhang, H., Zhang, L. and Zhang, J. (2019), “Influences of internal erosion on infiltration and slope stability”, *Bulletin of Engineering Geology and the Environment*, Vol. 78 No. 3, pp. 1815–1827.